

Report Prepared by:
Alberto A. Sagüés
Juan Rossi
Randall J. Scott
José A. Peña
Tonya Simmons

**INFLUENCE OF CORROSIVE INUNDATION ON THE
CORROSION RATES OF GALVANIZED TIE STRIPS IN
MECHANICALLY STABILIZED EARTH WALLS**

**Final Report, State Job No. 99700-3531-119
WPI 0510686**

**Prof. Alberto A. Sagüés, Ph.D., P.E.
Principal Investigator
February, 1998**

Department of Civil and Environmental Engineering

**College of Engineering
University of South Florida
Tampa Florida 33620**

1. Report No. WPI 0510686		2. Government Accession No.		3. Recipient's Catalog No.	
4. Title and Subtitle INFLUENCE OF CORROSIVE INUNDATION ON THE CORROSION RATES OF GALVANIZED TIE STRIPS IN MECHANICALLY STABILIZED EARTH WALLS				5. Report Date February, 1998	
				6. Performing Organization Code	
				8. Performing Organization Report No.	
7. Author's Alberto A. Sagüés, Juan Rossi, Randall J. Scott, José A. Peña, Tonya Simmons					
9. Performing Organization Name and Address Department of Civil and Environmental Engineering University of South Florida Tampa, FL 33620				10. Work Unit No. (TRAVIS)	
				11. Contract or Grant No. B-8451	
				13. Type of Report and Period Covered Final Report March 1993 - February 1998	
12. Sponsoring Agency Name and Address Florida Department of Transportation 605 Suwannee Street Tallahassee, FL 32399-0450				14. Sponsoring Agency Code	
15. Supplementary Notes Prepared in cooperation with the U.S. Department of Transportation and the Federal Highway Administration					
16. Abstract An investigation was conducted to assess the condition in the field of the galvanized reinforcement in Florida DOT Mechanically Stabilized Earth Walls (MSEW) that were already in service. For this purpose, 10 MSEW structures were instrumented at 8 different Florida sites for corrosion measurements. In addition, soil and metal samples were retrieved from several of the sites to evaluate the electrochemical properties of the backfill and to assess the condition of the galvanized coating after several years of exposure. The investigation also evaluated in the laboratory the influence of salt water contamination and macrocell development on the durability of the galvanized coating. The reinforcement in the structures investigated was typically in good condition and the corrosion rate of galvanized elements was low. A deterioration model was formulated using the field survey input. The model projects long durability (>100 years with only 5% element failure) in the absence of episodic saltwater flooding. Laboratory tests indicated that durability may be decreased tenfold by saltwater contamination.					
17. Key Words Tie Strips, Corrosion, Mechanically Stabilized Earth Structures, Concrete, Galvanized Steel			18. Distribution Statement No restrictions. This document is available to the public through the National Technical Information Service, Springfield, VA 22161		
19. Security Classif. (of this report) Unclassified		20. Security Classif. (of this page) Unclassified		21. No. of Pages 174	22. Price

Table of Contents

CONVERSION FACTORS	i
ACKNOWLEDGMENT	ii
EXECUTIVE SUMMARY	iii
1. INTRODUCTION	1
1.1 Problem Statement	1
1.2 Objectives	3
2. TECHNIQUE	4
2.1 Field Investigation	4
2.1.1 Brickell Avenue Bridge Wall, Miami	9
2.1.2 Howard Frankland Bridge, Tampa	12
2.1.3 Pensacola Street Bridge, Tallahassee	15
2.1.4 Palm City Bridge, Stuart	17
2.1.4.1 North East Wall	18
2.1.4.2 Palm City Bridge, North West Wall	19
2.1.5 Port St. Lucie Boulevard, Port St. Lucie	22
2.1.6 State Road 200, Ocala	23
2.1.7 Acosta Bridge, Jacksonville	25
2.1.8 Veteran's Expressway, Tampa	28
2.1.9 Figures of MSE Structures	31
2.2 Laboratory Investigation Arrangement	73
2.2.1 Experimental Setup	73
2.2.2 Soil Boxes Assembly Sequence - Series 1	77
2.2.3 Soil Boxes Saturation - Series 1	77
2.2.4 Contamination of the Soil Boxes	77
2.3 Field and Laboratory Testing Methods	80
2.3.1 Soil Properties	80
2.3.2 Electrochemical Measurements	80
2.3.2.1 Corrosion Potentials	80
2.3.2.2 In Situ Resistivity Estimates	81
2.3.2.3 Polarization Resistance Measurements	83
2.3.2.4 Conversion to Apparent Corrosion Rates	87
2.3.2.5 Macrocell Currents	87
2.3.2.6 Macrocell Resistances	88
2.3.3 Analysis of Metal Samples	88
3. RESULTS	89
3.1 Field Investigation Results	89
3.1.1 Soil Properties	89
3.1.2 Electrochemical Corrosion Assessment	90
3.1.3 Correlation between Measurements	94

3.1.4 Direct Assessment	104
3.1.4.1 In Situ Visual Inspection	104
3.1.4.2 Laboratory Evaluation of Hardware	104
3.2 Laboratory Results - Series 1	110
3.2.1 Soil Physical Properties	110
3.2.2. Soil Electrochemical Properties	112
3.2.3 Electrochemical Measurements	113
3.3 Laboratory Results - Series 2	131
3.3.1 Soil Physical Properties	131
3.3.2. Soil Electrochemical Properties.	131
3.3.3. Electrochemical Measurements.	133
4.1 Laboratory Results	138
4.2 Field Investigation	143
4.2.1 Apparent Corrosion Rate Values	143
4.2.2 Applicability of the ACR Information	145
4.3 Working Estimate of Service Life	148
4.3.1 Structures Not Subject to Episodic Chloride Contamination	148
4.3.2 Structures Subject to Episodic Chloride Contamination .	153
4.3.3 Applicability of Projections	154
 5. CONCLUSIONS	 157
 REFERENCES	 160
 APPENDIX	 162

CONVERSION FACTORS, US CUSTOMARY TO METRIC UNITS

<i>Multiply</i>	<i>by</i>	<i>to obtain</i>
inch	25.4	mm
foot	0.3048	meter
square inches	645	square mm
cubic yard	0.765	cubic meter
pound/cubic yard	0.593	kg/cubic meter
gallon/cubic yard	4.95	liter/cubic meter
standard cubic feet/hour	466.67	ml/minute
ounces	28.35	gram
pound	0.454	kilogram
pound (lb)	4.448	newtons
kip (1000 lb)	4.448	kilo newton (kN)
pound/in ²	0.0069	MPa
kip/in ²	6.895	MPa
ft-kip	1.356	kN-m
in-kip	0.113	kN-m
mpy	0.0254	mm / y

ACKNOWLEDGMENT

This investigation was supported by the State of Florida Department of Transportation, and this report is prepared in cooperation with the State of Florida Department of Transportation and the U.S. Department of Transportation. The opinions, findings, and conclusions expressed here are those of the authors and not necessarily those of the Florida Department of Transportation or the U.S. Department of Transportation.

The extensive technical support and many helpful discussions provided by Rodney G. Powers, and the assistance of the Corrosion Section of the FDOT Materials Office are gratefully acknowledged.

EXECUTIVE SUMMARY

Mechanically stabilized earth (MSE) walls using steel reinforcement are an economical construction option for bridge approaches and other highway components. Over 300 highway projects using this concept existed in Florida at the beginning of this investigation. The walls typically use galvanized steel strips in contact with backfill material. Placed transversely, the strips are attached to the interior surfaces of the walls, which are themselves made of reinforced concrete panels. The main purpose of the strips is to mechanically stabilize the fill material, thus minimizing the need for additional lateral fill. The strips serve also to retain the concrete wall sides.

The FDOT-specified backfill is a graded material that must meet a minimum set of electrochemical criteria (resistivity $> 3,000$ ohm-cm; $5 < \text{pH} < 10$; soluble chloride < 100 ppm; and sulfate < 200 ppm) to avoid corrosion of the reinforcement. The criteria are intended to promote a long service life (75 years or more).

Unfortunately, saltwater flooding of wall structures may occur during hurricanes or other episodic events. These events may create extremely corrosive conditions for galvanized steel, potentially reducing the remaining service life to a small fraction of the originally intended design value. An assessment of the conditions prevalent in the State and the possible future behavior of existing structures was required to minimize the use of costly alternatives and to properly address present maintenance strategies.

The present investigation was conducted to assess (in situ) the field condition of the galvanized reinforcement in FDOT MSE walls that were already in service. For this purpose, 10 MSE structures were instrumented at 8 different Florida sites

for corrosion measurements; and soil and metal samples were retrieved from several of the sites to evaluate the electrochemical properties of the backfill and to assess the condition of the galvanized coating after several years of exposure. In addition, a laboratory investigation was conducted to evaluate the influence of salt water contamination and macrocell development on the durability of the galvanized coating.

The field investigation found that the FDOT design limits for soil pH, resistivity, chloride content, sulfate content and size distribution were met in virtually all the test locations of the structures tested. Chloride and resistivity limits were not met at only one instance in one test point (in the Palm City North West Wall) during episodic direct contact of the wall with brackish water.

Direct visual examination of the reinforcement exposed at all the structures investigated revealed generally good to very good appearance of the galvanized surfaces. Microscopic examination of galvanized hardware extracted from the oldest wall in the State (Pensacola St.) showed only localized or partial loss of the galvanized layer and negligible corrosion of the plain steel substrate. Detailed examination of a newer wall showed negligible damage of the galvanized layer.

Field measurements of Apparent Corrosion Rates (ACR) of galvanized reinforcement showed typically very low values, with an average of $\approx 1 \mu\text{m/y}$ ($\approx 0.04 \text{ mpy}$). The ACR of galvanized reinforcement did not vary significantly with age of the structure tested. The ACR of recently introduced plain steel rods had an average of $\approx 12 \mu\text{m/y}$ ($\approx 0.5 \text{ mpy}$). There was little correlation observed between the ACR of either material and the electrochemical properties of the soil in the low aggressivity range explored and there was little correlation between the corrosion

potential and the ACR for either galvanized reinforcement or plain steel.

Laboratory experiments indicated that saltwater contamination of the backfill increased the ACR of galvanized specimens and plain steel by about one order of magnitude. The contamination also resulted in the formation of a strong corrosion macrocell between galvanized reinforcement or plain steel joining regions of coarse and fine soil, as it may exist near the concrete panels. The intensity of the macrocell action was on the order of the average corrosion rate of the reinforcement. The polarity of the macrocell aggravated the corrosion of the metal in the side of the macrocell with denser soil. Resistivity measurements in the laboratory suggest that the aggressiveness of contaminated coarse backfills can decrease with time due to their drainage capacity, if fresh water is periodically added. Therefore, coarse soils may be beneficial in mitigating reinforcement corrosion after corrosion occurs if fresh water flushing (as due to rainfall) takes place.

A conservative durability model was formulated to project the percentage of elements that reach the end of their service life after a given service time of a generic MSE wall. The model input incorporated conservatively all the field evidence representative of Florida conditions obtained in this investigation. For walls not subject to episodic saltwater flooding the model projects a period of ≈ 50 years with negligible reinforcement failure, and $\approx 5\%$ failure after 100 years. For a wall with a saltwater flood at year zero, the model projects failure development 10 times earlier.

1. INTRODUCTION

1.1 Problem Statement

Mechanically stabilized earth (MSE) walls using steel reinforcement are an economical construction option for bridge approaches and other highway components. Over 300 highway projects using this concept existed in Florida at the beginning of this investigation. The walls use galvanized steel (rolled, ASTM A-36 or A-572 Grade 65, galvanized per ASTM A-123) reinforcing strips, tie strips and fasteners, which are in contact with backfill material. The strips are typically of rectangular cross section (0.4 cm x 5 cm) and several meters in length. Placed transversely, the strips are attached to the interior surfaces of the walls, which are themselves made of reinforced concrete slab elements. Hundreds of strips, placed at various heights, may be used in a given wall. The main purpose of the strips is to mechanically stabilize the fill material, thus minimizing the need for additional lateral fill. The strips serve also to retain the concrete wall sides. Because of the load conditions and soil mechanics involved, maximum tensile stresses in the strips tend to develop away from the point of anchoring to the wall sides, at a distance determined by the elevation position of the strip.

The FDOT-specified backfill is a graded material that must meet a minimum set of electrochemical criteria (resistivity > 3,000 ohm-cm; $5 < \text{pH} < 10$; soluble chloride < 100 ppm; and sulfate < 200 ppm) to avoid corrosion of the reinforcement. The criteria, set forth in Item 528-2.7 of the FDOT Structures Design Manual [1] are intended to promote a long service life (75 years or more, based on an expected

corrosion rate of less than 1/2 mpy), following from the present knowledge of the anticipated corrosion mechanisms [2]. The water used during construction to achieve optimum compaction moisture is required to meet the same requirements as the soil; the use of saltwater is explicitly excluded (Item 528-3, Ref. [1]).

Unfortunately, until recently, the design guidelines did not consider changes in the electrochemical properties of the fill material which might result from environmental service conditions. Saltwater flooding of wall structures during hurricane Andrew brought to attention the periodic occurrence of substantial chloride-ion contamination of the backfill. These events may represent extremely corrosive conditions for galvanized steel [3-5], potentially reducing the remaining service life to a small fraction of the originally intended design value. Preliminary experiments at the Corrosion Laboratory of the Materials Office of the FDOT [3] confirmed that temporary exposure of an ideal soil (silica sand) to simulated salt water could result in a very high residual chloride content and consequent resistivity reduction (from over 100 Kohm-cm to only 110 ohm-cm) after draining and drying. Under those conditions, corrosion rates of galvanized steel in soil can reach 10 mpy [4-6]. The possibility of a large increase in the rate of deterioration above the expected design value has caused enough concern to result in an interim design restriction for new FDOT projects [7], whereby steel reinforcement is not to be used for retaining walls below elevations subject to a 100 year flood of water classified as extremely aggressive. The restriction imposes a cost burden since more expensive alternatives (cast-in-place walls, proprietary Techwalls or hybrid design [7]) could become necessary. An assessment of the conditions prevalent in the

State, the possible future behavior of existing structures, and refinement guidelines for future service was required to minimize the use of costly alternatives and to properly address present maintenance strategies.

1.2 Objectives

Pursuant to the problem statement, an investigation was conducted with the following objectives:

Objective 1: To assess (in situ) the field condition of the galvanized reinforcement in FDOT MSEW structures that were already in service. For this purpose, 10 MSEW structures were instrumented at 8 different Florida sites for corrosion measurements. In addition, soil and metal samples were retrieved from several of the sites to evaluate the electrochemical properties of the backfill and to assess the condition of the galvanized coating after several years of exposure. This objective is addressed in the Field Investigation sections.

Objective 2: To evaluate the influence of salt water contamination and macrocell development on the durability of the galvanized coating. For this purpose, an experimental setup consisting of soil test boxes containing galvanized and plain steel specimens was prepared. Some of the boxes were contaminated with artificial sea water while others served as controls. The tests were continuously monitored for several months. This objective is addressed in the Laboratory Investigation sections.

2. TECHNIQUE

2.1 Field Investigation Arrangement

Ten MSE walls throughout Florida were instrumented to enable the execution of electrochemical measurements on galvanized strips located in the MSE structures (Table 2-1). Among the criteria used to choose the sites were the age, surrounding environment, and location of the structure. Structures of varying service lives and environmental exposure were chosen, as indicated by the "Rationale" in Table 2-1. Figure 2-1 is a map of Florida showing the sites selected for instrumentation.

In the following sub-sections (2.1.1 to 2.1.8) each site is described with respect to its location and environment; and the criteria for which it was selected for testing is mentioned. An elevation view of each structure is also provided showing the location of the panels (Brickell site) or panel sets (all other structures). A description of a typical panel set and other instrumentation features are explained below.

Panel Sets. A panel set is two vertically continuous instrumented panels and is used for all sites, except Brickell, where the instrumented panels are not vertically continuous but are located in two different rows (the instrumented rows are either adjacent or separated by a non-instrumented row). This layout was used to avoid continuity between working and counter electrodes, since the tie strips (or mesh in the Howard Frankland site) will short the upper and lower reinforcing strips (or mesh) within each panel if they touch each other. Panel sets are located by numbering the rows with respect to the abutment wall or some other specified point

of reference. To indicate the row (numbered as just described) in which the panel set exists, an "R" (for row) precedes the panel set number. For example, panel sets R3 and R5 are the instrumented panel sets in rows 3 and 5 as numbered from the reference point. The electric contact positions are located for each panel set by using the corresponding figures in section 2.1.9. The figures show also the elevation of the contacts with respect to ground level.

Table 2-1. Field Installations.

Structure #	Site and Location	# of Test Clusters ¹	Age (years) ²	Regime and Rationale
1A	Brickell Ave. Northwest Wall, Miami	2	New	Costal, Possible Inundation
1B	Brickell Ave. Southeast Wall, Miami	2	New	Costal, Possible Inundation
2	Howard Frankland Bridge, Tampa	4	3	Costal, Possible Inundation
3	Pensacola Ave., Tallahassee	4	17	Land, Oldest in State, Distress Observed
4A	Palm City Bridge, Northeast Wall, Stuart	4	5	Costal, Possible Inundation
4B	Palm City Bridge, Northwest Wall, Stuart	2	5	Costal, Tidal Saltwater Aggressive Regime
5	Port St. Lucie Blvd., St. Lucie	2	4	Costal, Tidal Saltwater Aggressive Regime
6	State Rd. 200, Ocala	2	13	Land, Old, Long Term Baseline
7	Acosta Bridge, Jacksonville	2	7	Costal, Non-Spec. Backfill
8	Veterans Expressway, Tampa	2	2	Land, Representative of Present Practice

1. A test cluster consists typically of electrical connections to two close but electrically independent reinforcing strips and a reference electrode. A buried plain steel bar is usually included in the cluster. The electrical connections are externally accessible.

2. Age of the structure at the time of the first visit.

Connections to Reinforcement. In each panel set (except Brickell), holes were drilled in the top and bottom panels to accommodate electrical connections. All panel sets have 2 connections to the reinforcement (all galvanized strips except for wire mesh in the Howard Frankland site). One connection is made in the top panel to the reinforcement attached to that panel, and one to the reinforcement in the bottom panel. The drilled holes for the reinforcement contacts are typically 10 cm (4 in.) in diameter.

Titanium Reference Electrodes and Steel Bars. Each panel set has connection to an activated titanium reference electrode [8] which is usually placed at an intermediate elevation. Each structure has at least one panel set that also contains a plain steel bar as an additional test element. The bare steel specimens were made using a 3 m long N^o 4 plain steel rebar (~13 mm diameter) connected to a 6 mm stainless steel rod by threading. The mill scale present on the rebar surface was mechanically removed by steel brushing. In all panel sets with a steel bar, the bar shares the same hole (also 10 cm or 4 in. in diameter) as the activated titanium reference electrode. For panels without steel bars, a 5.1-cm (2 in.) hole was drilled for the activated titanium reference electrode.

Zn Alloy Strips. At two sites, Jacksonville and Veteran's Expressway, strips coated with an 85-15% Zn-Al alloy were inserted into the soil for durability and corrosion resistance testing in a service condition. These novel strips were supplied by Groupe TAI (LePecq, France).

Connection Details. In the following sub-sections for each site (except Brickell), a table of the connection details is given. Each table (Tables 2-3 to 2-10), lists the date of installation and the hole designation for each panel set. Holes are designated by a capital letter (for example A,B,C) as also shown in the figure of the corresponding panel set (see section 2.1.9). For each hole, the test element or elements (ie. galvanized strip, steel bar, Ti reference electrode, and/or Zn alloy strip) are identified. The last two columns of these tables briefly describe the internal and external connections. For Brickell, Figures 2-7 to 2-10 show the position of the electrodes and the configuration of the contact boxes.

Repair of Holes after Instrumentation. Typically, once contacts, electrodes and bars were installed, the holes were filled with clean silica sand with an average resistivity above 30000 ohm-cm; and all panels were repaired with mortar. However, this does not apply to the Brickell site. Also, at the Howard Frankland site, clean silica sand was used in two of the panel sets and soil from the site was used for the remaining two panel sets (see Section 2.1.2).

Instrumented Reinforcement Dimensions and Exposed Areas. Table 2-2 summarizes the dimensions of the test elements (galvanized strips, wire mesh, and plain steel bars) and exposed areas for all structures examined.

Table 2-2. Dimensions of test elements and exposed areas for instrumented sites.

Site		Reinforcing Strips: Position or Panel Set		Length (m)	Width (cm)	Thickness (cm)	Area Exposed to Soil (cm ²)	
Brickell Ave., Miami	Southeast wall	Regular strips	Top	4.6	5.0	0.4	4938	
			Bottom	6.1	7.5	1.5	10970	
	Northwest wall	Extra strips	Top	3.1	5.0	0.4	3348	
			Bottom	3.1	7.5	1.5	5580	
Pensacola Ave., Tallahassee		R17		6.1	8.0	0.3	10120	
		R23		6.1	8.0	0.3	10120	
		R44		6.1	8.0	0.3	10120	
		R62		6.1	8.0	0.3	10120	
Palm City Bridge, Northeast Wall, Stuart		R1		6.7	5.0	0.4	7242	
		R5		6.7	5.0	0.4	7242	
		R14		6.7	5.0	0.4	7242	
		R28		6.7	5.0	0.4	7242	
Palm City Bridge, Northwest Wall, Stuart		R3		5.5	5.0	0.4	5929	
		R5		5.5	5.0	0.4	5929	
Port Saint Lucie Blvd., Port Saint Lucie		R3		4.3	5.0	0.4	4613	
		R7		4.9	5.0	0.4	5271	
State Rd. 200, Ocala		R6		4.3	6.0	0.5	5553	
		R25		5.2	4.0	0.5	4667	
Acosta Bridge,* Jacksonville		R9		5.0	5.0	0.4	5404	
		R21		5.0	5.0	0.4	5404	
Veterans Expressway,* Tampa		R16		6.0	5.0	0.4	6484	
		R23		6.0	5.0	0.4	6484	
Howard Frankland Bridge, Tampa		Longitudinal Wires			Transversal Wires			Mesh
		Length (m)	Dia. (cm)	Area (cm ²)	Length (m)	Dia. (cm)	Area (cm ²)	Total Area Exposed to Soil (cm ²)
		3.7	0.95	5458	0.91	0.95	3002	8460
Steel Bars								
		Length (m)		Dia. (cm)		Area Exposed to Soil (cm ²)		
Port St. Lucie Blvd.		2.5		1.3		993		
All Other Sites		3.1		1.3		1216		

* Length was estimated based on the height of the reinforcement compared to other structures.

2.1.1 Brickell Avenue Bridge Wall, Miami

This structure is located near 444 Brickell Avenue, Miami. The bridge spans south to north, crossing the Miami River which flows East to West. The steel structure that crosses the Miami River is supported by two abutment walls, which also sustain the reinforced earth. The Miami River carries salt water at this location.

The Miami bridge walls were chosen because they were under construction, offering the unique opportunity of full instrumentation (including provision for macrocell tests) during construction. Therefore, complete monitoring of the new site from the start was possible.

Two different structures (walls) were selected: the Southeast (SE) wall and the Northwest (NW) wall. Each wall contains instrumented panels at two different levels corresponding to the top and bottom layers of soil reinforcement. External contact boxes were placed at each level. Figure 2-2 is an elevation view for the SE and NW walls showing the approximate distance (to the nearest meter) from the abutment wall for each contact box or pair of boxes (box sets) in the chosen panels. The instrumented panels in the SE wall have only one contact box each. There are two contact boxes (side by side) on each of the two instrumented panels for the NW wall.

Panel Details and Reinforcement Positions: Views of a typical panel are shown in Figure 2-3. The separation between tie strips (Figure 2-3) varies in practice as much as 7.6 cm. Figure 2-4 is an elevation view in which the position and length of the reinforcing strips are detailed. Notice the difference in the length

of the reinforcement of the top and bottom layers. This variation was designed to account for the soil pressure profile over the concrete wall. The cross sectional area of the reinforcement also changes from 2 cm² (top) to 11.25 cm².

Details of Contacts, Test Elements and Electrodes. As previously mentioned, two structures were selected for instrumentation and placement of specimens. Figures 2-5 and 2-6 are elevation views of the instrumented panels for the NW and SE walls respectively, showing the height of the contact boxes above ground level. The NW wall installation consisted of two contact-box sets at different heights (Figure 2-5). Figure 2-6 also shows the straight hole for external reference electrode placement. This hole is located directly above the bottom box and is the only hole for external electrode placement at the Brickell site.

Each set of test points included connections to two of the regular reinforcing strips, connection to an extra reinforcing strip (divided into back strip and front strip) placed specially for this investigation, and connections to four specially constructed titanium reference electrodes (see Figure 2-7). The NW-wall installation was similar to the SE wall, but with the addition of a bare steel rod (prepared as discussed in section 2.1) divided into a front and back portion (see Figure 2-8). The contact details in Figure 2-7 are identical for the top and bottom boxes; the details in Figure 2-8 are identical for the top and bottom box sets. All connections to reinforcement were made in pairs to prevent possible failure. Titanium reference electrodes were placed close to their corresponding working electrodes (regular reinforcing strips, extra reinforcing strips and bare steel rods) in order to minimize solution resistances when performing corrosion measurements on both front and back specimens.

For both walls, a three character nomenclature was used for the reference electrodes: the first character indicates the electrode position parallel to the wall (L=left, M=middle, and R=right); the second indicates the electrode type (R=reference) and the third refers to the electrode position perpendicular to the wall (B=back and F=front). On the SE wall two characters were used for the extra strips to indicate position (back or front) and contact number (1 or 2) and one character for the regular strips (left or right). On the NW wall, three characters were used to designate the test elements: the first indicates the element type (S=plain steel and G=galvanized) and the other two designate the element position and number, respectively as in the SE wall.

All electrodes cables were passed to the outside through a one-inch hole drilled in the center of the panel. Each cable was soldered to a brass screw which was later placed into a Plexiglas panel inside a box made with a PVC fitting, a PVC bushing and two Plexiglas discs. A PVC cap sealed the box. The entire setup was attached to the concrete wall using galvanized concrete screws. Front and back elements (extra strips and plain steel rebars) were electrically connected (jumped) after assembly. Details of contact boxes are shown in Figures 2-9 and 2-10.

The jumpers indicated in Figures 2-9 and 2-10 were made using a solid copper wire (1 mm in diameter) fixed in place by brass nuts, which can be easily removed using a nut driver. All contacts are redundant which simplify macrocell measurements since one of the contacts can be removed and an instrument can be plugged while the other contact is still in place (which is necessary when measuring macrocell currents and instant-off potentials).

The distribution of contacts in those boxes corresponding to the NW wall (Figure 2-10) was designed so that independent measurements could be performed in the galvanized strips and in the plain steel rebar specimens without a connection between the right and left boxes.

2.1.2 Howard Frankland Bridge, Tampa

The Howard Frankland Bridge crosses Tampa Bay connecting Tampa to St. Petersburg (I-275). The MSE wall that was instrumented is located at the NE side of the bridge (I-275 Southbound side) and was 5 years old at the time of instrumentation. This structure was selected due to its high potential for chloride-ion contamination (Tampa Bay water contains ~12,000 ppm Cl⁻ and the wall is placed at ~10 m from the waterfront with a lowest elevation of ~2m above high tide).

Four panel sets were instrumented: panel sets R7 and R15 on 11/6/95 and R11 and R17 on 12/13/95.

Panel Details and Reinforcement Position. In this wall, galvanized 6W11 mesh (wire diameter = 9.5 mm) is used as reinforcement (instead of strips). Figure 2-11 is a top view of the wall showing the reinforcement layout. Figure 2-12 is a front view of a typical panel showing the position of the reinforcing mesh. There was no electric continuity between the reinforcement at different elevations.

The instrumented panel sets (in rows 7, 11, 15 and 17) were labeled in accordance to their position with respect to the abutment wall, as shown in Figure 2-13. Panels 7 and 15 contain contacts to a Ti reference electrode and the mesh

reinforcement; panels 11 and 17 also include connections to plain steel rods. Both types of panels are shown in Figures 2-14 and 2-15, where positions of the contacts, reference electrodes, steel specimens and reinforcement are detailed. To reach the mesh through the concrete panel without damage to the reinforcement, a 10-cm diameter core hole was made for each mesh row, as shown in Figures 2-14 and 2-15. These holes were drilled 10 cm above the reinforcement center line allowing for contact placement.

Details of Contacts, Test Elements and Electrodes. The attachment between the contacts and the mesh was made using a mechanical connection consisting of a Zn alloy grounding clamp attached to a 6-mm diameter austenitic stainless steel rod. To compensate for the distance between the reinforcement position and the core hole center, the stainless steel rods used for external contacts were elbow-bent.

The activated titanium reference electrodes were made with an activated titanium rod threaded into a 6 mm diameter stainless steel rod. The joint was placed inside a PVC pipe and filled with a metallographic mount epoxy, as shown in Figure 2-16. The reference electrodes and plain steel specimens were inserted into the drilled holes as discussed in section 2.1 (see Figure 2-17). Table 2-3 lists the connection details.

Once contacts, electrodes and bars were installed, the holes were filled with clean silica sand with an average resistivity above 30,000 ohm-cm (panels 11 and 17). The holes made in panels 7 and 15 were filled with soil collected from the site with an average resistivity of 1000 ohm-cm since no silica sand was available at the

time. In all cases, the panels were repaired with mortar. The stainless steel rods protrude from the mortar for external instrumentation contacts.

Table 2-3. Connection Details for the Howard Frankland Bridge, Tampa.

Panel Set	Date Installed	Hole	Test Element	Internal Connection	External Contact
R7 & R15	11/6/95	A	top galvanized steel mesh	zinc alloy grounding clamp	stainless steel rod
		B	activated titanium reference	stainless steel rod	stainless steel rod in a PVC fitting
		C	bottom galvanized steel mesh	zinc alloy grounding clamp	stainless steel rod
R11 & R17	12/13/95	D	top galvanized steel mesh	zinc alloy grounding clamp	stainless steel rod
		E	activated titanium reference	stainless steel rod	stainless steel rod in a PVC fitting
			plain steel	stainless steel rod	stainless steel rod
		F	bottom galvanized steel mesh	zinc alloy grounding clamp	stainless steel rod

2.1.3 Pensacola Street Bridge, Tallahassee

This structure supports Pensacola Street and is located directly east of Stadium Drive on the Florida State University campus (between the university and the Doak Campbell Stadium). A front view of the wall is shown in Figure 2-18. Using this figure, the instrumented panel sets can be located by either counting panel rows or by measuring the distance from the tunnel or Stadium Drive.

This site was selected because it is the oldest MSEW structure in the state (in service for 17 years at the time of the first visit). Also, the wall suffered a partial collapse at one location with associated soil movement. The structure is not near a chloride source so it serves as a good reference for comparison to sites that are exposed to Cl⁻ contamination.

Four panel sets were instrumented: R17 and R62 on 1/12/96 and R23 and R44 on 1/19/96.

Panel Details and Reinforcement Position. In this wall, the reinforcement consisted of galvanized steel strips (80 mm wide x 3 mm thick x 6.1 m long). Figure 2-19 shows the typical wall panel layout. Unlike the other structures investigated, the top and bottom reinforcement layers of each panel are connected by a tie strip.

Details of Contacts, Test Elements and Electrodes. Panel sets R17 and R23 have contacts to the upper and lower reinforcing strips, a plain steel rebar and an activated titanium reference electrode. Panels R44 and R62 have contacts to the upper and lower reinforcing strips and an activated titanium reference electrode (no plain steel rebar). See Figures 2-20 to 2-22 for the elevations (above ground

level) of the contacts, reference electrodes, steel bars and reinforcement. Both activated titanium reference electrodes and plain steel bars have the same dimensions and features as the ones used in the Howard Frankland Bridge (Figures 2-16 and 2-17). To reach the galvanized strips through the concrete panel without damage to the reinforcement, a 10 cm diameter core hole was made for each strip row (Figures 2-20 to 2-22). These holes were drilled 10 cm above the reinforcement center line allowing for contact placement. On panel sets R17 and R23, a second 10 cm hole was made in the bottom panel to place both the plain steel rebar and the Ti reference electrode (Figure 2-20). The plain steel elements were prepared as discussed in section 2.1. The attachment between the contacts and the strip was made using a mechanical connection consisting of a custom austenitic stainless steel clamp attached to a 6 mm diameter austenitic stainless steel rod. To compensate for the difference between reinforcement position and the hole center, the stainless steel rods were elbow-bent as in the Howard Frankland site. Table 2-4 lists the connection details.

Table 2-4. Connection Details for the Pensacola Street Bridge MSE wall.

Panel Set	Date Installed	Hole	Test Element	Internal Connection	External Connection
R17 & R23	R17 (1/12/96)	A	top galvanized steel strips	stainless steel clamp	stainless steel rod
		B	bottom galvanized steel strips	stainless steel clamp	stainless steel rod
	R23 (1/19/96)	C	plain steel	stainless steel rod	stainless steel rod
			activated titanium reference	stainless steel rod	stainless steel rod in a PVC fitting
R44 & R62	R44 (1/19/96)	D	top galvanized steel strips	stainless steel clamp	stainless steel rod
		E	activated titanium reference	stainless steel rod	stainless steel rod in a PVC fitting
	R62 (1/12/96)	F	bottom galvanized steel strips	stainless steel clamp	stainless steel rod

2.1.4 Palm City Bridge, Stuart

This structure is located at State Road 714 in Stuart and crosses the Saint Lucie River in the east-west direction. The bridge and wall had been in service for 5 years at the time of the first visit. The Saint Lucie River has brackish water containing up to 10,000 ppm Cl⁻. The Northeast (NE) wall (see section 2.1.4.1) was located on a grass field approximately 1.6 meters above the normal high tide level. Unlike the Northwest (NW) wall (see section 2.1.4.2), the NE wall is not regularly flooded.

2.1.4.1 North East Wall

The general layout of the structure is shown in Figure 2-23. Four panel sets were instrumented on 5/2/96. Panel sets are numbered according to their position from the abutment wall that limits with the river shore, as shown in Figure 2-24.

Panel Details and Reinforcement Position. The reinforcement consisted of galvanized steel strips (50 mm wide x 4 mm thick). The length of the strips was 6.1 m for panel sets R1 and R5; and 4.3 m for R14 and R28. Figure 2-25 shows the dimensions of a typical panel for the Palm City site. Figures 2-26 and 2-27 detail the elevation (from ground level) of the contacts, reference electrodes, and plain steel specimens. The reference electrodes and plain steel rebars have the same dimensions and features as in the MSE walls of the Howard Frankland Bridge and the Pensacola Street Bridge (Figures 2-16 and 2-17).

Details of Contacts, Test Elements and Electrodes. All panel sets had contacts to the upper and lower reinforcing strips and an activated titanium reference electrode and two of the panel sets also contained a plain steel rebar each. The contact type and procedure for installation was the same as in Pensacola Street (Tallahassee). The plain steel bars were prepared as discussed in section 2.1. Table 2-5 lists the connection details for the Northeast wall.

Table 2-5. Connection Details for the Palm City Northeast MSE wall in Stuart.

Panel Set	Date Installed	Hole	Test Element	Internal Connection	External Connection
R1 & R14	5/2/96	A	top galvanized steel strip	stainless steel clamp	stainless steel rod
		B	bottom galvanized steel strip	stainless steel clamp	stainless steel rod
		C	plain steel	stainless steel rod	stainless steel rod
			activated titanium reference	stainless steel rod	stainless steel rod (with red cap) in a PVC fitting
R5 & R28	5/2/96	D	top galvanized steel strip	stainless steel clamp	stainless steel rod
		E	bottom galvanized steel strip	stainless steel clamp	stainless steel rod
		F	activated titanium reference	stainless steel rod	stainless steel rod (with red cap) in a PVC fitting

2.1.4.2 Palm City Bridge, North West Wall

The Northwest wall was of special interest because here, the Port St. Lucie River is in direct contact with the MSE structure. During high tide, the water level can flood the lower portion of the wall up to approximately 0.5 m (measured from the ground).

Panel Details and Reinforcement Position. The typical panel dimensions of the NW wall were the same as the NE wall (Figure 2-25). The galvanized steel strips were 50 mm wide x 4 mm thick x 5.5 m long for the instrumented panel sets.

Electrical connections were installed in two panel sets (R3 and R5) on 7/30/96. The location of the panel sets is shown in Figure 2-28.

Details of Contacts, Test Elements and Electrodes. In each panel set, there were electrical connections made to two galvanized strips (one strip from the top panel , and one from the bottom panel) as in the other structures. In addition, an extra galvanized strip in the top panel of R3 (hole B) was also instrumented. Holes B, C, AA, E, and D have connections to galvanized strips (see Figures 2-29 and 2-30). The plain steel rebars and activated titanium reference electrodes were prepared and placed in the drilled holes as discussed in section 2.1. It is estimated that during high tide, the water level usually covers Holes A, AA, and D. Table 2-6 lists the connection details for the Northwest wall.

Abnormal electrochemical measurements indicated faulty connections in holes A and D; therefore, the connections were inspected on 9/9/96. It was found that in hole A, the plain steel was in contact with the bottom galvanized strip (in hole AA) so the rebar was removed. A new hole (G) was drilled in the wall and a new steel rebar was inserted into the soil. In hole D, it was determined that the clamp was not connected to the strip. The connection was re-established by replacing the stainless steel clamp with a galvanized clamp.

Table 2-6. Connection Details for the Palm City Northwest MSE wall in Stuart.

Panel Set	Date Installed	Hole	Element	Internal Connection	External Connection
R3	7/30/96	AA	bottom galvanized steel strip	stainless steel clamp	stainless steel rod
		A*	no element	-	-
		B*	galvanized steel strip	stainless steel clamp	stainless steel rod
		C	top galvanized steel strip	stainless steel clamp	stainless steel rod
	activated titanium reference		stainless steel rod	stainless steel rod	
	9/9/96	G	plain steel	stainless steel rod	stainless steel rod
H*		galvanized steel strip	no connection	-	
R5	7/30/96	D	bottom galvanized steel strip	galvanized clamp	white copper wire
		E	top galvanized steel strip	stainless steel clamp	stainless steel rod
		F	plain steel	stainless steel rod	stainless steel rod
			activated titanium reference	stainless steel rod	stainless steel rod

* Defective connection; should not be used.

2.1.5 Port St. Lucie Boulevard, Port St. Lucie

This site was chosen because a portion of the of the structure is in the flood plain of the Port St. Lucie river, which is approximately 100 yards from the wall.

Panel Details and Reinforcement Position. Electrical connections were installed in two panel sets of the southeast side of Port St. Lucie Blvd. (crossing over the Port St. Lucie River) on 11/19/96. The panel sets that were selected (R7 and R3) are in the flood plain. Figure 2-31 is an elevation view of the MSE structure showing the location of the panel sets. The panel dimensions for this structure are the same as the Tallahassee wall (see Figure 2-19); however, the tie strips are not connected; they are configured like the Palm City site (see side view of Figure 2-25). The galvanized strips used in this wall are 50mm wide x 4 mm thick. The length of the strips is 4.3 m for R3 and 4.9 m for R7.

Details of Contacts, Test Elements and Electrodes. The elevations of the contacts is shown in Figures 2-32 and 2-33. In each panel set, there were electrical connections to two galvanized strips (one each for the top and bottom panels). There were two plain steel bars (prepared as discussed in section 2.1) introduced into the soil, one in the bottom panel of R3 and one in the bottom panel of R7. The activated titanium reference electrodes were similar to Figure 2-16 with the exception that a copper wire (with green insulation) was used instead of a stainless steel rod. A small hole was drilled in the titanium rod, the copper wire was inserted and then the titanium rod was crimped to secure the connection. Table 2-7 lists the connection details for the Port St. Lucie site.

Table 2-7. Connection details for the Port St. Lucie MSE wall.

Panel Set	Date Installed	Hole	Test Element	Internal Connection	External Connection
R7	11/19/96	A	top galvanized steel strip	galvanized clamp	copper wire in a PVC fitting
		B	plain steel	stainless steel rod	stainless steel rod in a PVC fitting
			activated titanium reference	copper wire	copper wire (green)
		C	bottom galvanized steel strip	galvanized clamp	copper wire in a PVC fitting
R3	11/19/96	D	top galvanized steel strip	galvanized clamp	copper wire in a PVC fitting
		E	plain steel	stainless steel rod	stainless steel rod in a PVC fitting
			activated titanium reference	copper wire	copper wire (green)
		F	bottom galvanized steel strip	galvanized clamp	copper wire in a PVC fitting

2.1.6 State Road 200, Ocala

This structure was chosen because it is one of the oldest MSE structures in the state of Florida (built in 1983). The structure is surrounded by an undeveloped field and there are no bodies of water at this site.

Panel Details and Reinforcement Position. The panel dimensions for this structure are the same as the Tallahassee wall (see Figure 2-19); however, the tie strips are not connected; they are configured like the Palm City site (see side view

of Figure 2-25). Electrical connections were installed on 1/15/97 in two panel sets of the northwest side of the State Road 200 bridge (that crosses over train tracks). The location of the panel sets (R6 and R25) are shown in Figure 2-34 and Figures 2-35 and 2-36 shows the elevation of the holes for the contacts. The galvanized strips for R6 are 60 mm wide x 5 mm thick x 4.3 m long and for R25 the dimensions are 40 mm wide x 5 mm thick x 5.2 m long.

Details of Contacts, Test Elements and Electrodes. In the each set of panels, electrical connections were made two galvanized specimens. One galvanized strip was located on the upper panel and one strip on the bottom panel. Galvanized clamps and copper wire were used to make the connections.

For both panel sets, a plain steel specimen and an activated titanium reference electrode was placed in the top panel of each set. The steel specimen was prepared and placed in the same drilled hole as the activated titanium reference electrode as discussed in section 2.1. The connections to reference electrodes were made with copper wire as in the Port Saint Lucie site. Table 2-8 lists the connection details for the Ocala site.

Table 2-8. Connection details for the Ocala MSE wall.

Panel Set	Date Installed	Hole	Test Element	Internal Connection	External Connection
R6	1/15/97	A	top galvanized steel strip	galvanized clamp	copper wire (white) in a PVC fitting
		B	plain steel	stainless steel rod	copper wire (white) in a PVC fitting
			activated titanium reference	copper wire	copper wire (green) in a PVC fitting
		C	bottom galvanized steel strip	galvanized clamp	copper wire (white) in a PVC fitting
R25	1/15/97	D	top galvanized steel strip	galvanized clamp	copper wire (white) in a PVC fitting
		E	plain steel	stainless steel rod	copper wire (white) in a PVC fitting
			Ti reference	copper wire	copper wire (green) in a PVC fitting
		F	bottom galvanized steel strip	galvanized clamp	copper wire (white) in a PVC fitting

2.1.7 Acosta Bridge, Jacksonville

This site is located on the SW side of the Acosta Bridge in Jacksonville and is approximately 100 yards from the St. John's River which contains brackish water. The structure is wall number 9 (according to drawings prepared for the FDOT). The bottom of the structure is at a low elevation and organic residue from standing water

lines the wall to a height of about 0.3 meters. It was concluded that the periodically standing water found near the wall was due to drainage of rain and excess water, rather than flooding of the river. This site also initially had areas of aggressive backfill; however the backfill was since replaced. Starting at a distance of approximately 3 meters from the wall soil is mounded, creating a slope that increases to a height of about 3 meters at the wall. The mound may be to prevent flooding from the river in extremely high tidal situations.

Panel Details and Reinforcement Position. Electrical connections were installed at two panel sets located in rows 9 and 21 on 4/8/97. Figure 2-37 is an elevation view of the wall showing the location of the instrumented panels. The panel dimensions for this structure are the same as the Tallahassee wall (see Figure 2-19); however, the tie strips are not connected; they are configured like the Palm City site (see side view of Figure 2-25). The exact dimensions of the strips were not known; therefore, a surface area of 5,000 cm² was assumed for calculating corrosion rates.

Details of Contacts, Test Elements and Electrodes. In the each panel set, connections were made to two galvanized strips, one strip from the upper panel and one from the lower panel. Figures 2-38 and 2-39 show the elevations of the holes for the contacts. Two plain steel bars (prepared as described in section 2.1) were introduced into the soil. One in the bottom panel of R9 and one in the top panel of R21. There were also two activated titanium reference electrodes (with wire connections) placed in the soil. One reference electrode was placed in the top panel of R9, and one in the top panel of R21. Table 2-9 gives the details of the connections for this site.

In addition, there was an extra instrumented galvanized strip introduced into the soil in the top panel of R9. This strip was coated with 15-85% Al-Zn and was approximately 0.6 m in length. This coating is new to the industry and is still in the experimental stages. The durability and corrosion resistance of the coating will be tested in a service condition and compared to the coating for the existing strips.

Table 2-9. Connection details for the Jacksonville MSE wall.

Panel Set	Date Installed	Hole	Test Element	Internal Connection	External Connection
R9	4/8/97	A	top galvanized steel strip	galvanized clamp	copper wire (white) in a PVC fitting
		B	bottom galvanized steel strip	galvanized clamp	copper wire (white) in a PVC fitting
		C	top 85-15% Zn-Al strip	Zn-Al strip	copper wire (white) in a PVC fitting
		D	plain steel	stainless steel rod	copper wire (white) in a PVC fitting
			activated titanium reference	copper wire	copper wire (green) in a PVC fitting
R21	4/8/97	E	top galvanized steel strip	galvanized clamp	copper wire (white) in a PVC fitting
		F	bottom galvanized steel strip	galvanized clamp	copper wire (white) in a PVC fitting
		G	plain steel	stainless steel rod	copper wire (white) in a PVC fitting
			activated titanium reference	copper wire	copper wire (green) in a PVC fitting

2.1.8 Veteran's Expressway, Tampa

The Veteran's Expressway is one of the newest structures in the state of Florida (constructed in 1994). The wall that was instrumented is located on the NW side of the intersection of Veteran's Expressway and Gunn Highway. During the service life (to date) of the roadway, drainage problems have been observed during heavy rains; however, there are no signs of flooding or possible seawater contamination.

Panel Details and Reinforcement Position. The panel dimensions for this structure are the same as the Tallahassee wall (see Figure 2-19); however, the tie strips are not connected; they are configured like the Palm City site (see side view of Figure 2-25). Two panel sets (R16 and R23) on the northwest side of the overpass were instrumented. Figure 2-40 is an elevation view of the wall showing the location of the panel sets and Figures 2-41 and 2-42 show the elevation of the contacts above ground level. The exact dimensions of the strips were not known; therefore, a surface area of 5,000 cm² was assumed for calculating corrosion rates.

Details of Contacts, Test Elements and Electrodes. There were two connections made to working galvanized strips at each panel set, one connection to a galvanized strip in a top panel and one in the bottom panel. A plain steel rebar (prepared as described in section 2.1), and two activated titanium references were introduced into the soil structure. The plain steel rebar was placed in the top panel of R16. An electrical connection to the plain steel rebar was made using a stainless steel rod instead of copper wire to insure a more durable connection. Table 10 gives

the connection details for the site.

As in the Jacksonville site, two new galvanized strips coated with the 15-85% Zn-Al alloy were introduced into the soil. The dimensions of these strips were 5.6 mm x 0.41 mm and 1.9 m long. To accommodate a successful placement in the soil, approximately 0.2 m was cut from the strip introduced in R16 (leaving a length of 1.7 m). The strips were placed in the bottom panel for each panel set. A galvanized clamp was used to make the electrical connection to the new strips. Table 2-10 lists the connection details for the Veteran's expressway.

Table 2-10. Connection details for the Veteran's Expressway MSE wall.

Panel Set	Date Installed	Hole	Test Element	Internal Connection	External Connection
R16	6/4/97	A	top galvanized steel strip	galvanized clamp	copper wire (white) in a PVC fitting
		B	plain steel	stainless steel rod	copper wire (white) in a PVC fitting
			activated titanium reference	copper wire	copper wire (green) in a PVC fitting
		C	bottom galvanized steel strip	galvanized clamp	copper wire (white) in a PVC fitting
		D	bottom 85-15% Zn-Al strip	Zn-Al strip	copper wire (green) in a PVC fitting
R23	6/4/97	E	top galvanized steel strip	galvanized clamp	copper wire (white) in a PVC fitting
		F	plain steel	stainless steel rod	copper wire (white) in a PVC fitting
			activated titanium reference	copper wire	copper wire (green) in a PVC fitting
		G	bottom galvanized steel strip	galvanized clamp	copper wire (green) in a PVC fitting
		H	bottom 85-15% Zn-Al strip	Zn-Al strip	copper wire (green) in a PVC fitting

2.1.9 Figures of MSE Structures

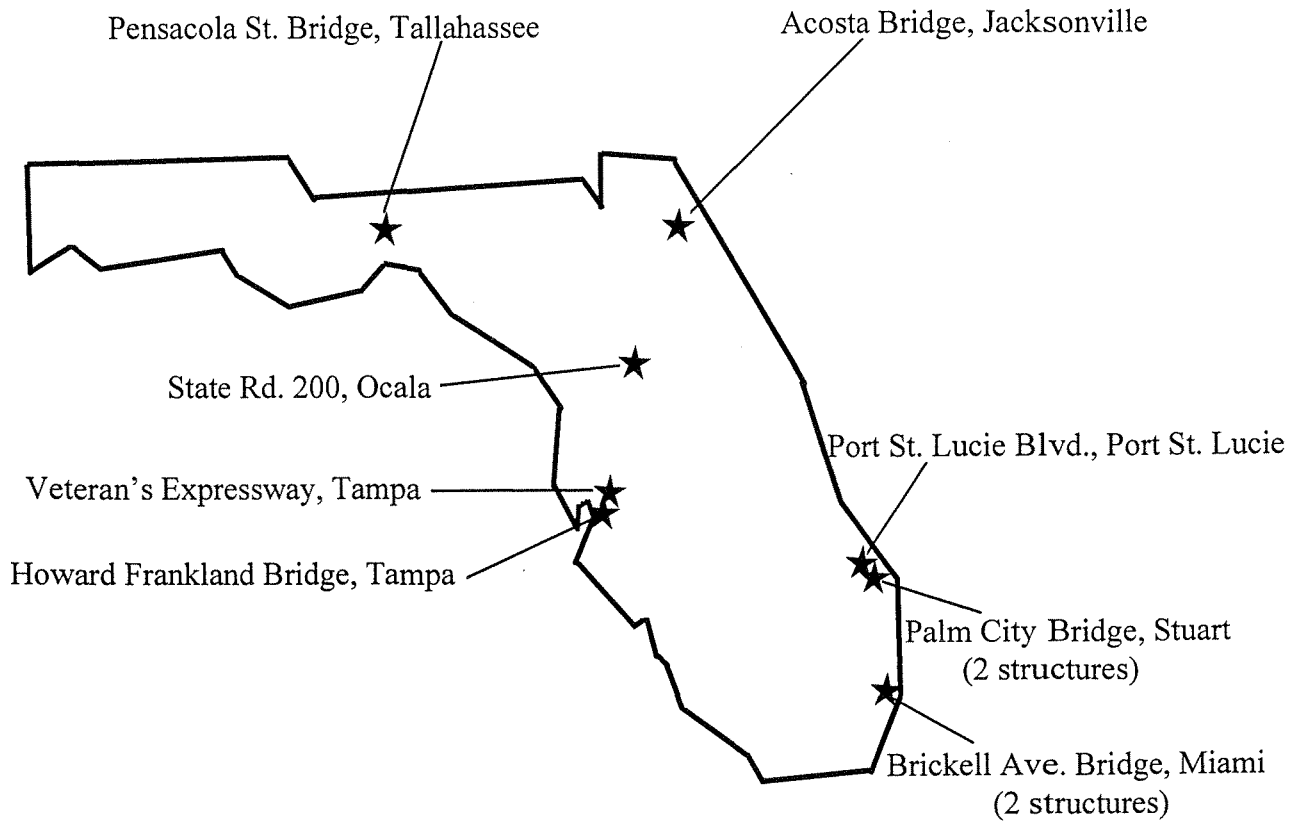


Figure 2-1. Sites selected for instrumentation.

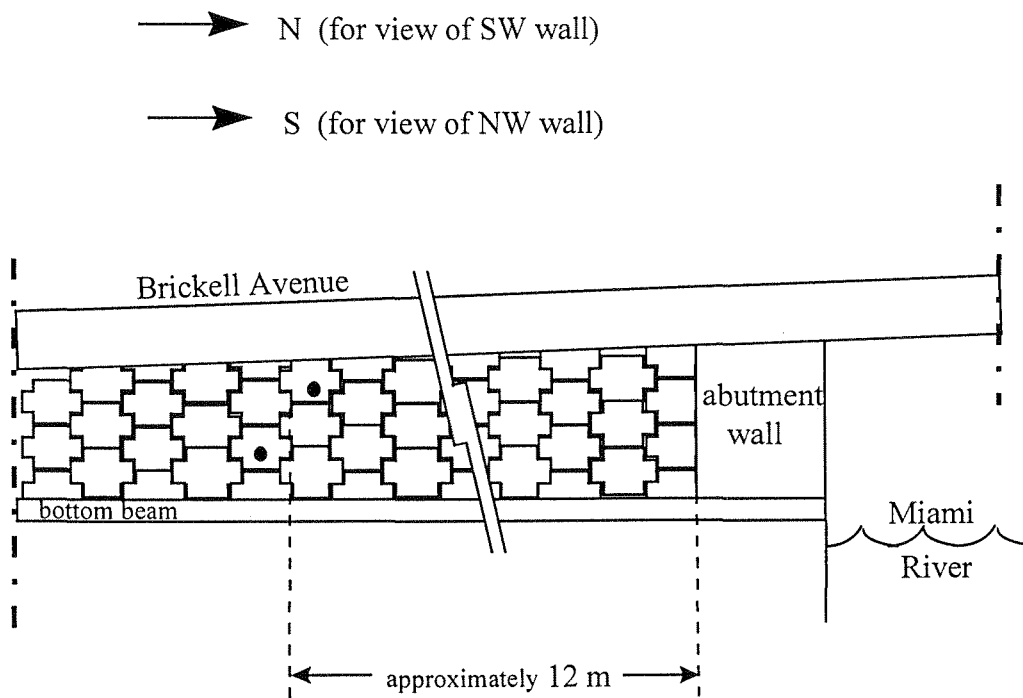


Figure 2-2. Elevation view of the SE and NW walls by the Brickell Ave. Bridge showing the approximate distance (from the abutment wall) of instrumented panels and contact boxes (single boxes is SE wall; side-by-side box sets in NW wall).

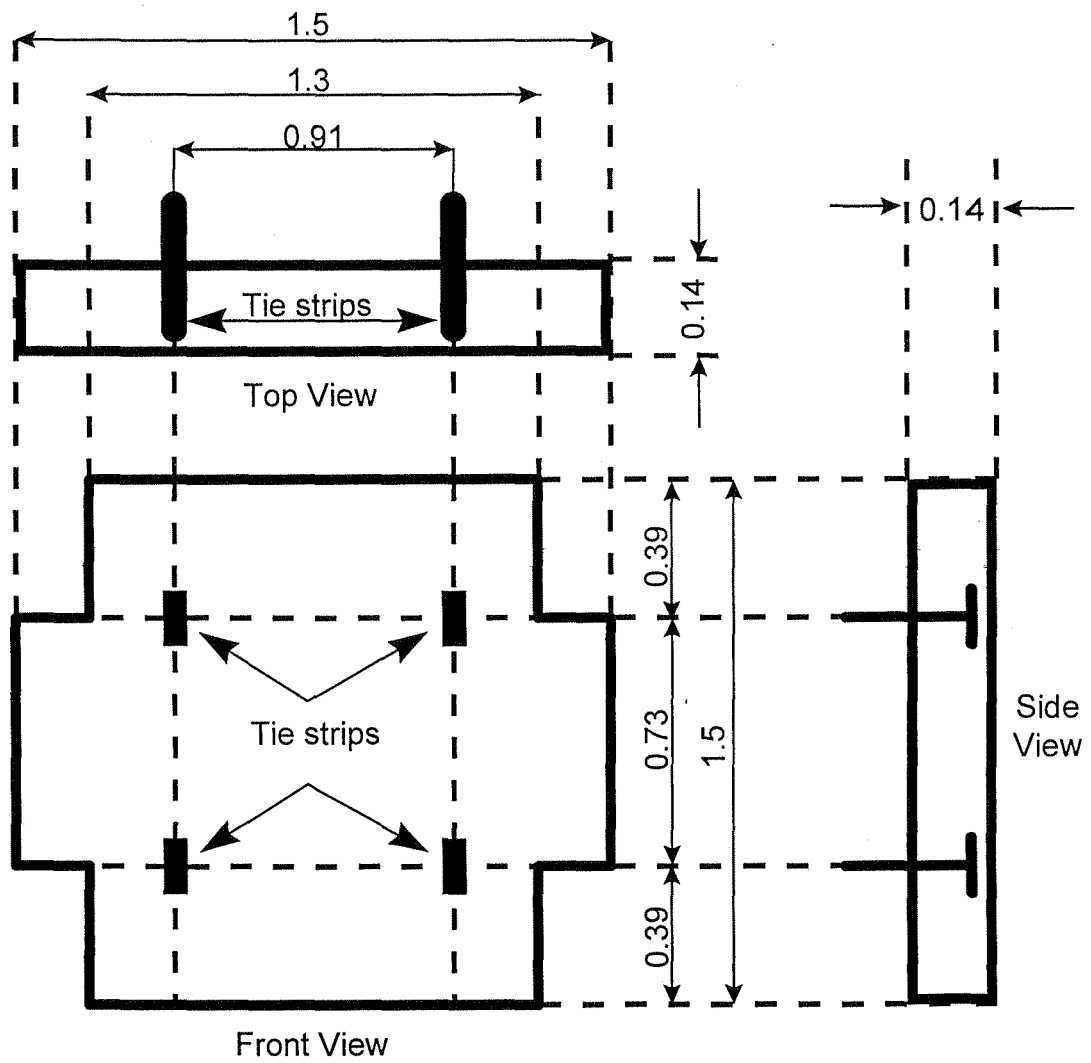


Figure 2-3. Detail of a typical concrete panel for the Brickell Ave. MSE wall. All dimensions are in meters.

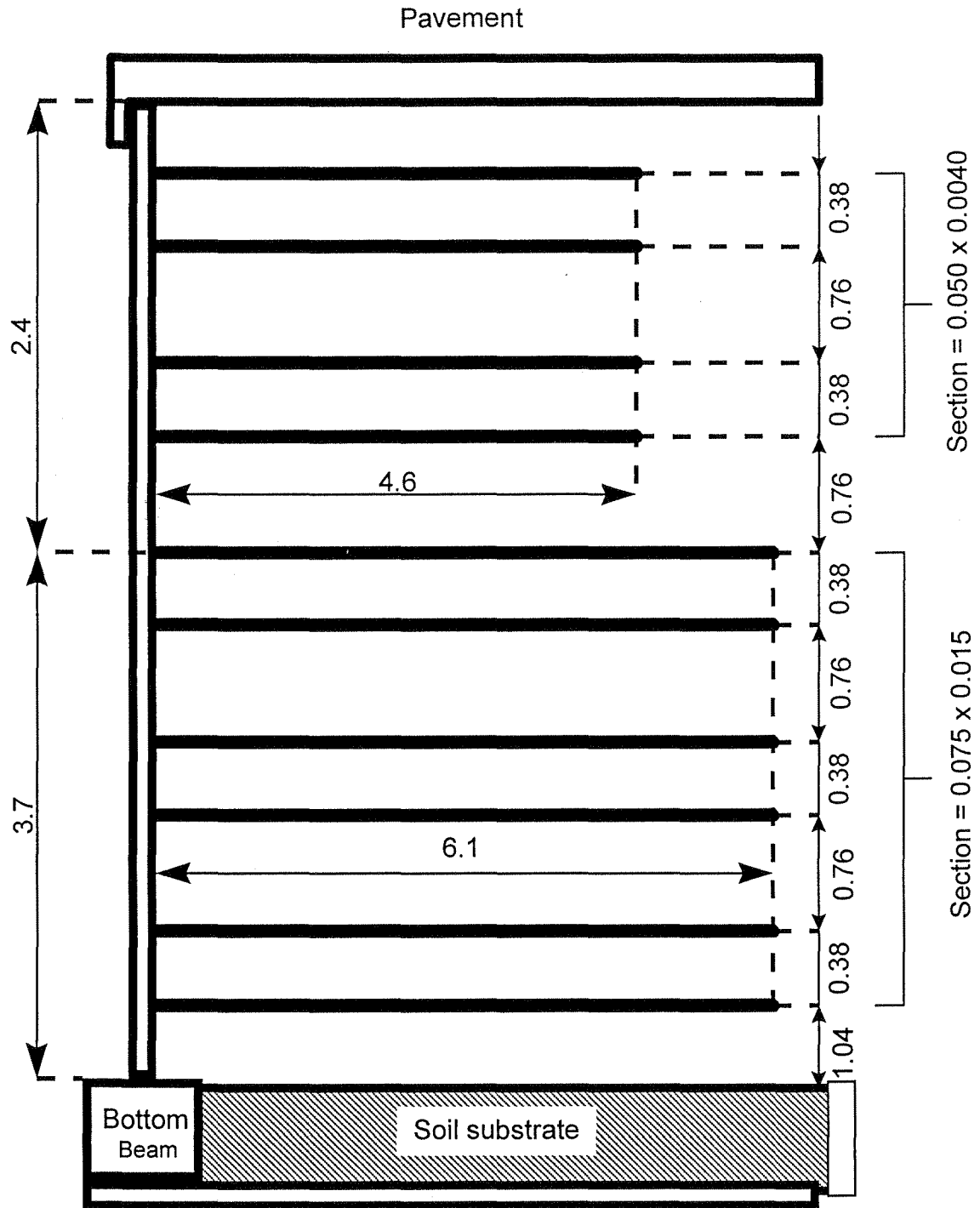


Figure 2-4. Elevation view of the Brickell Ave. MSE wall showing different strip lengths as a function of height. All dimensions are in meters.

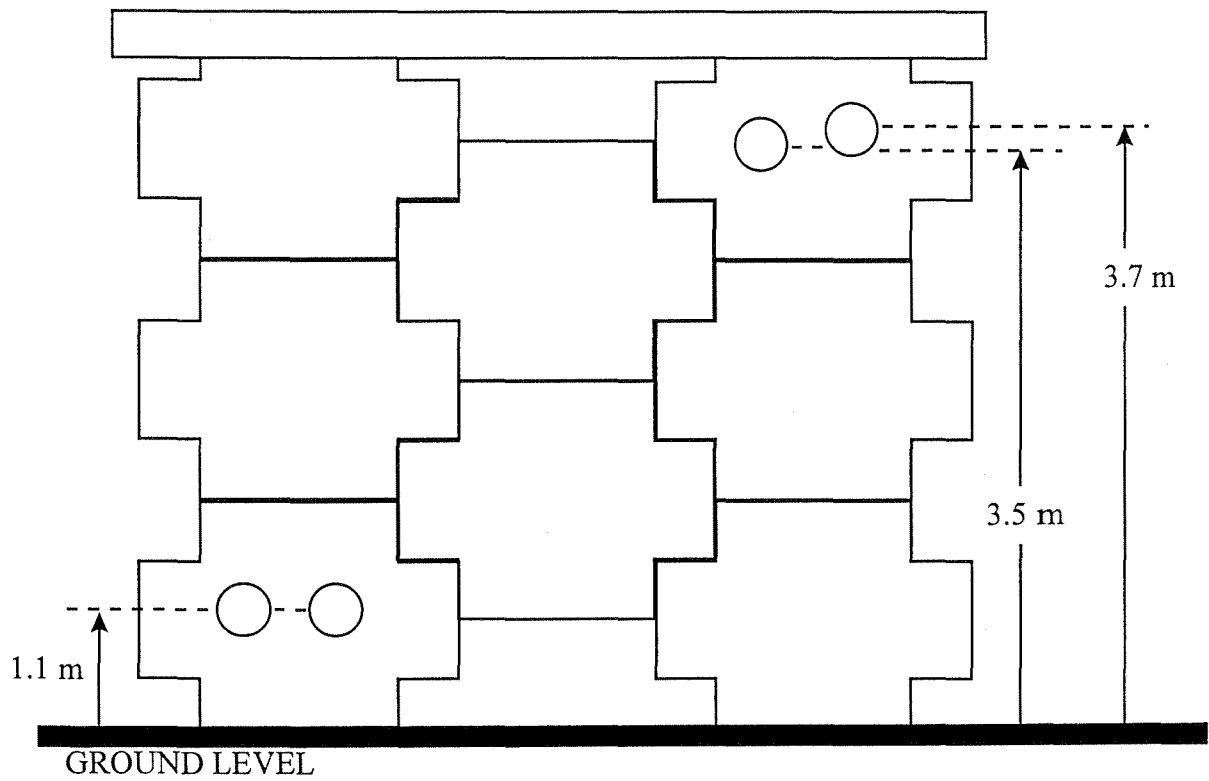


Figure 2-5. Elevation of contact boxes for the NW wall of the Brickell Ave. site.

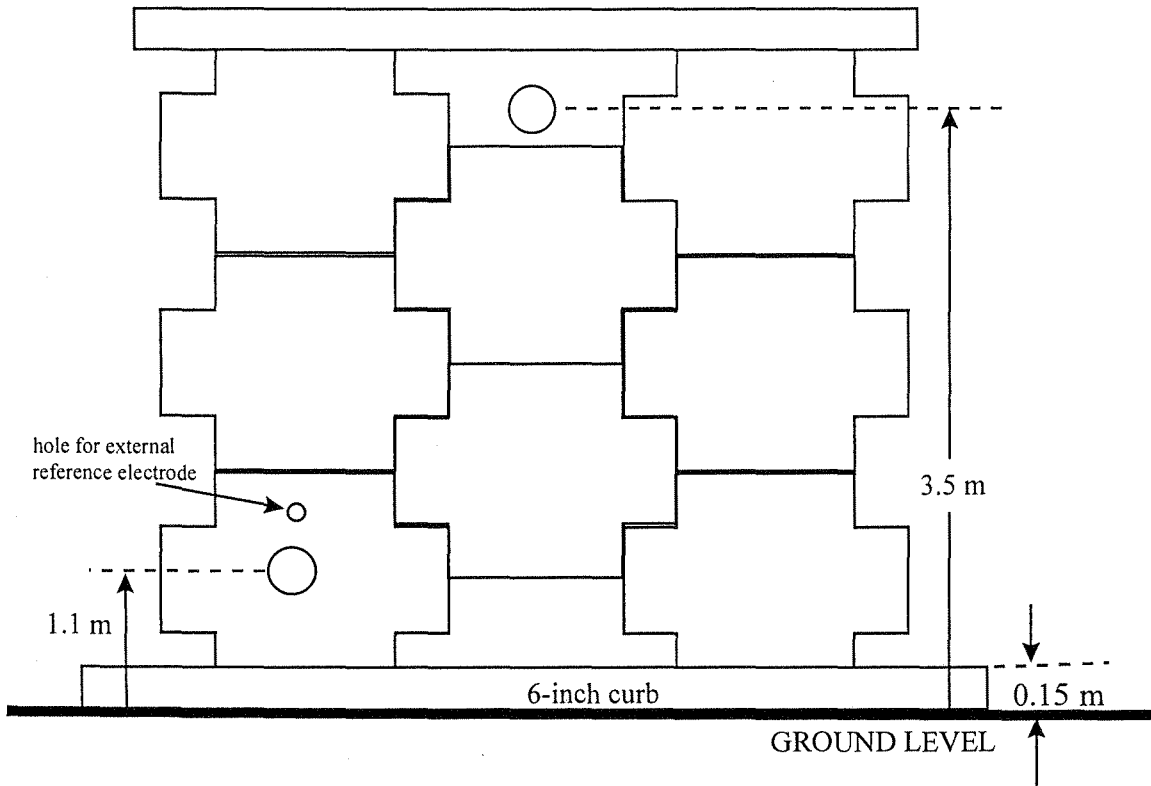


Figure 2-6. Elevation of contact boxes for the SE wall of the Brickell Ave. site.

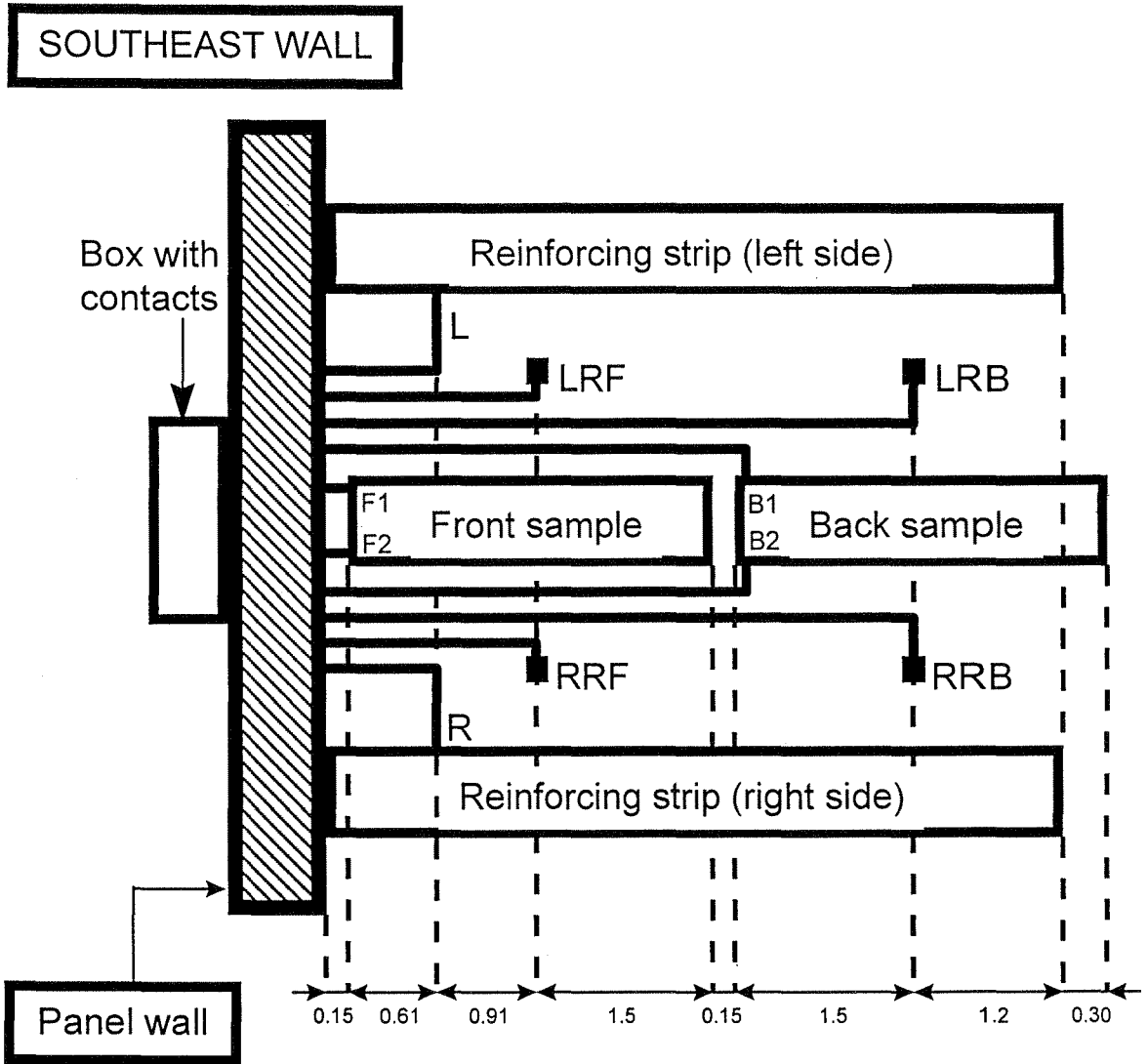


Figure 2-7. Top view of the Brickell SE wall installation showing the position of the electrodes; the configuration of the contacts is identical for top and bottom boxes. All dimensions are in meters.

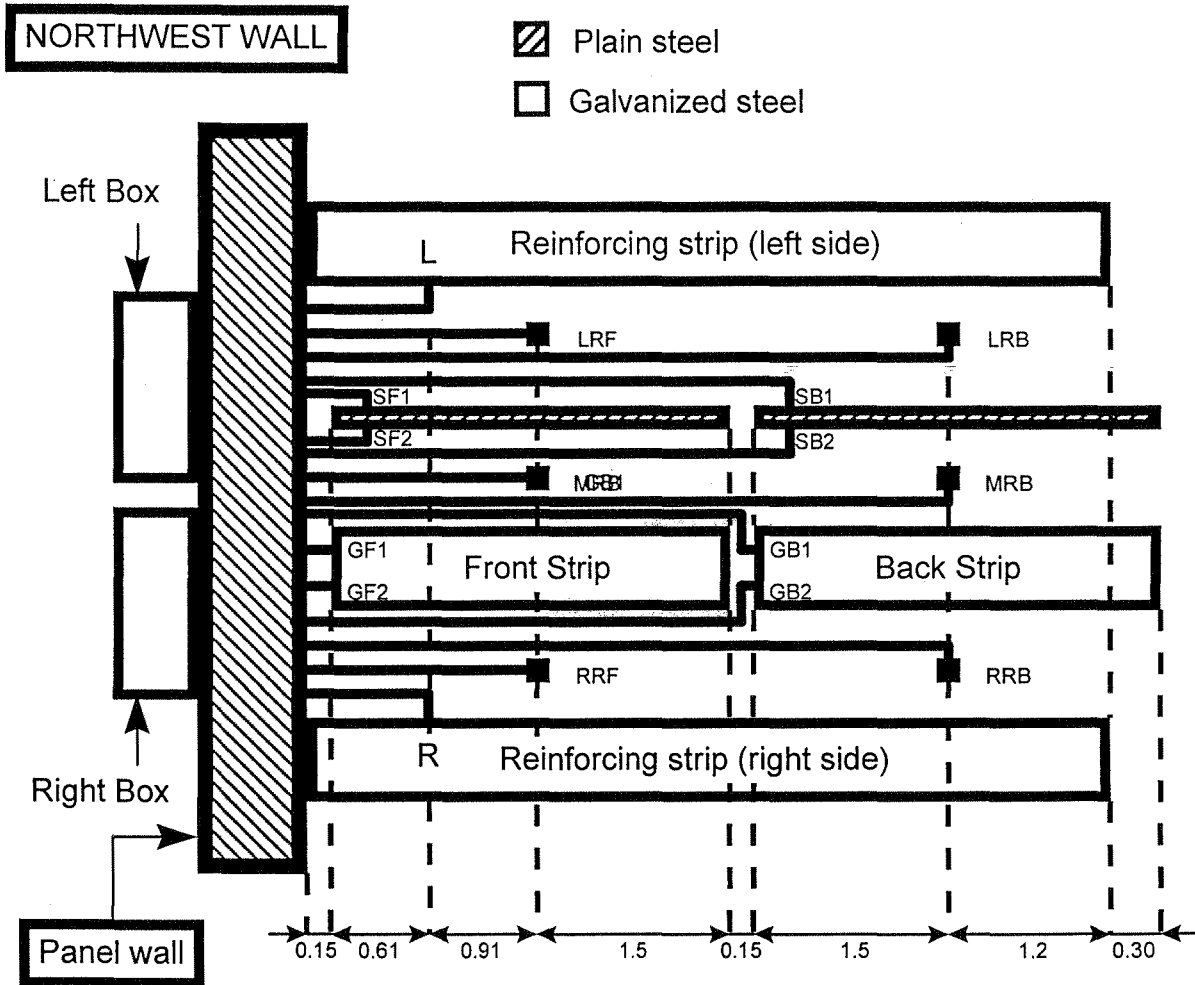


Figure 2-8. Top view of the Brickell NW wall installation showing the positions of the electrodes; the configuration of contacts is identical for top and bottom box sets. All dimensions are in meters.

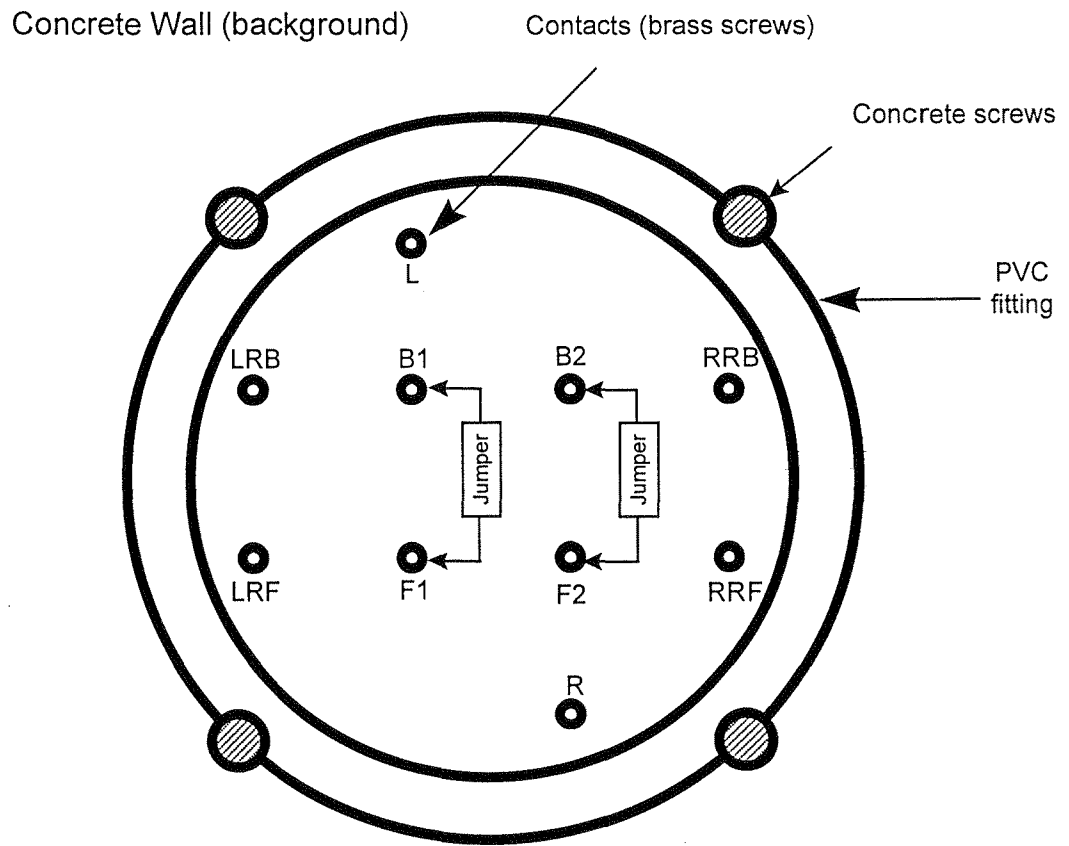


Figure 2-9. Front view of the contact box for the Brickell SE wall (top and bottom boxes are identical).

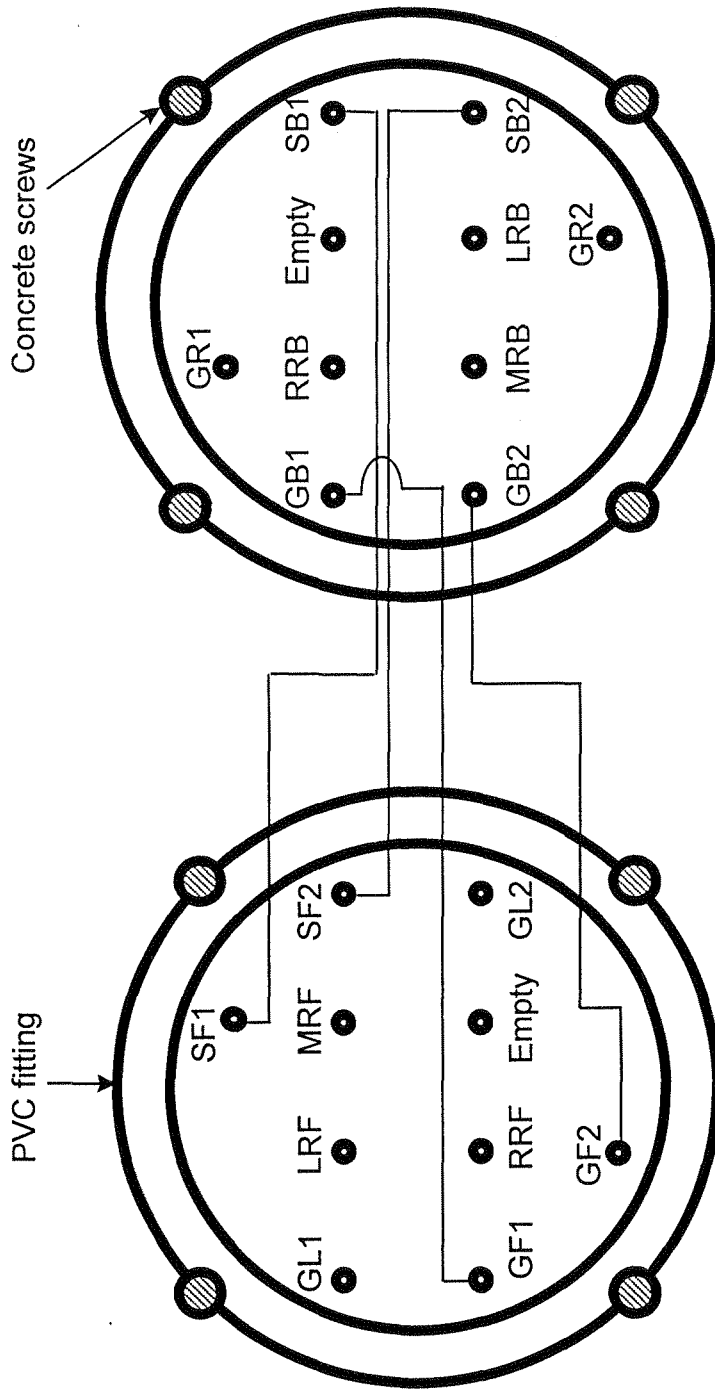


Figure 2-10. Front view of a typical contact box set for the Brickell NW wall, showing jumper connection. The box set shown is the same for the top and bottom panels.

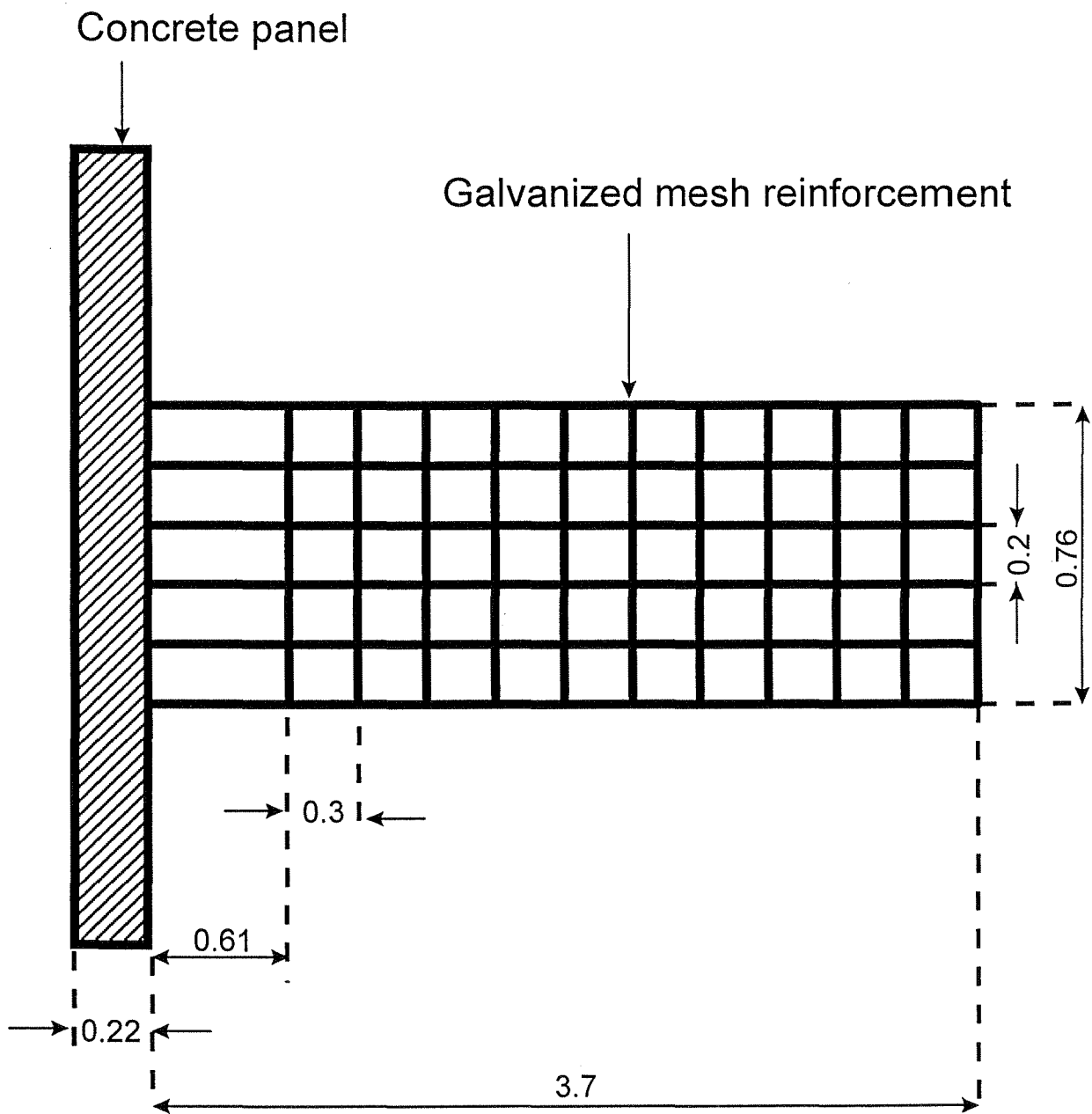


Figure 2-11. Top view of the Howard Frankland MSE wall showing the reinforcement layout (not to scale). The mesh dimensions (in meters) were obtained from shop drawings (State Project No. 15190-3479), courtesy of VSL corporation.

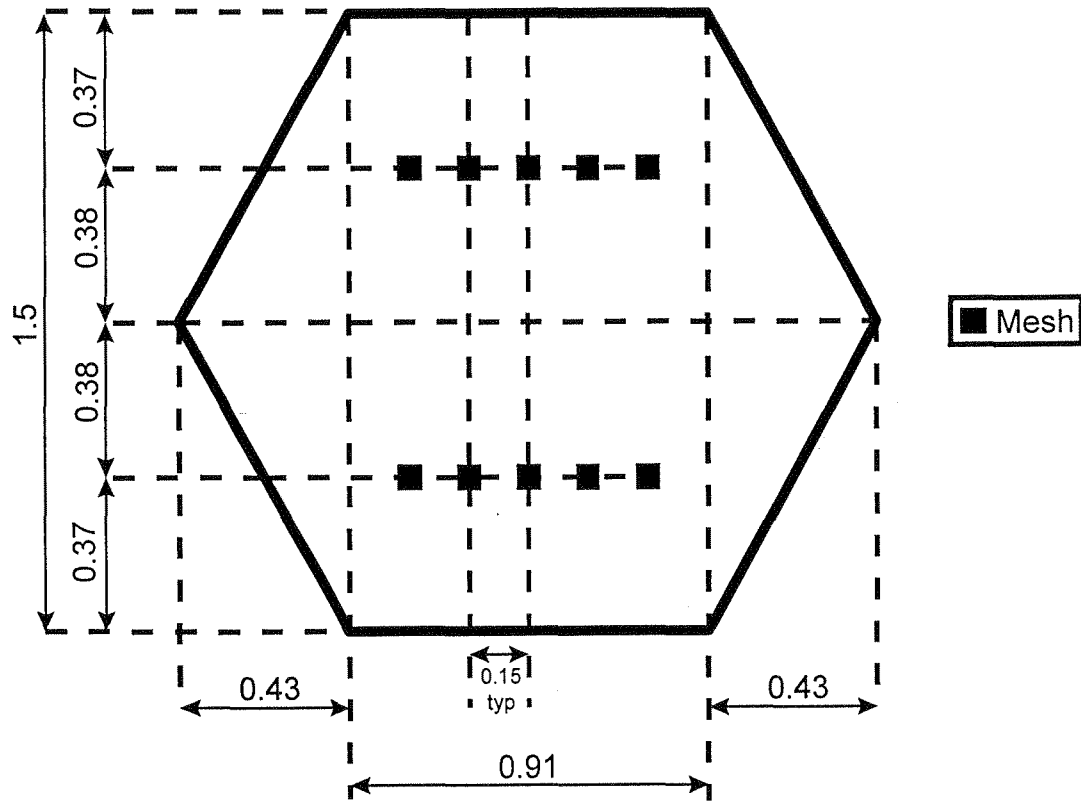


Figure 2-12. Layout of a typical panel for the Howard Frankland MSE wall showing position and spacing of the mesh reinforcement. The panel dimensions were obtained from shop drawings (State Project No. 15190-3479, 01/05/90), courtesy of VSL Corporation.

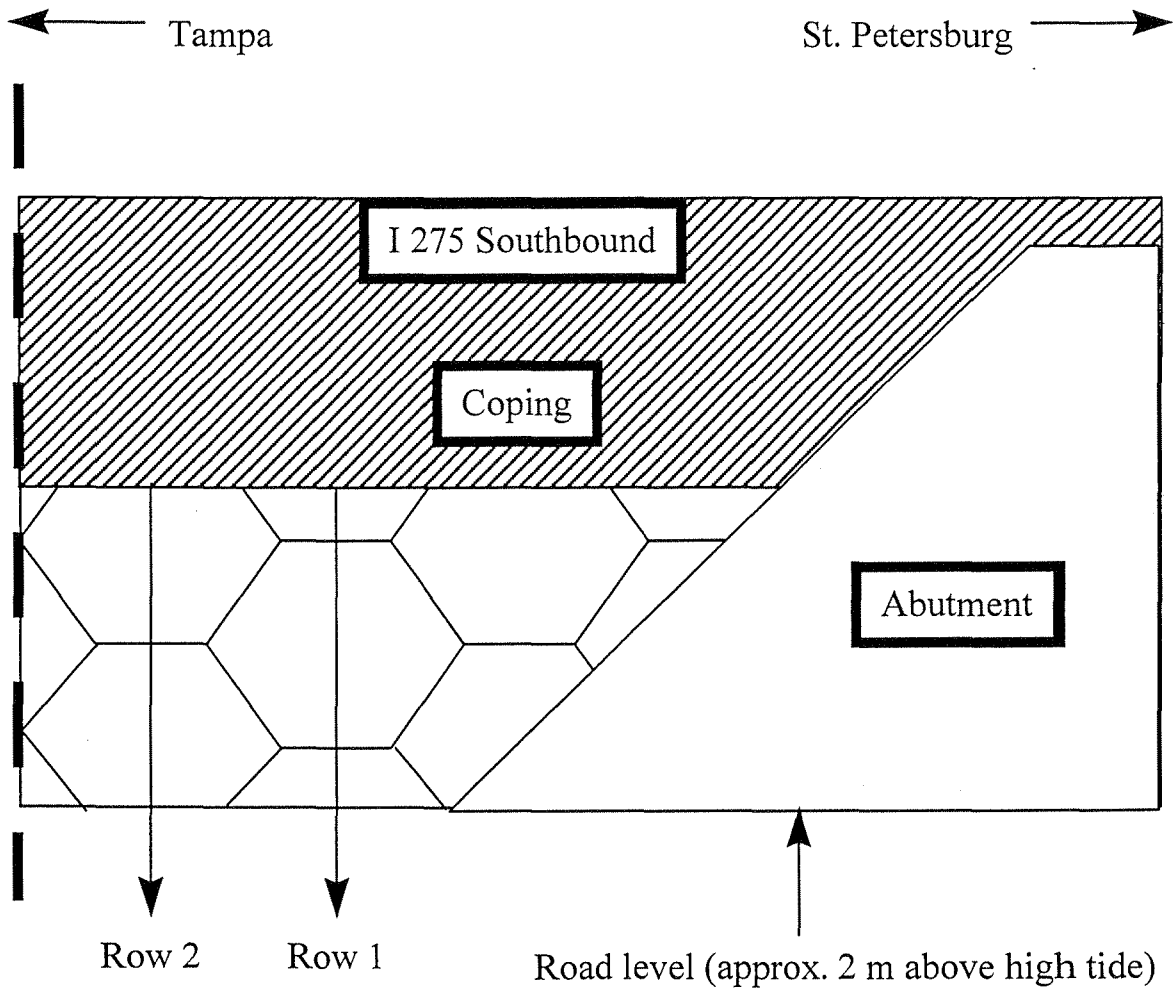


Figure 2-13. Front view of the Howard Frankland MSE wall showing panel nomenclature.

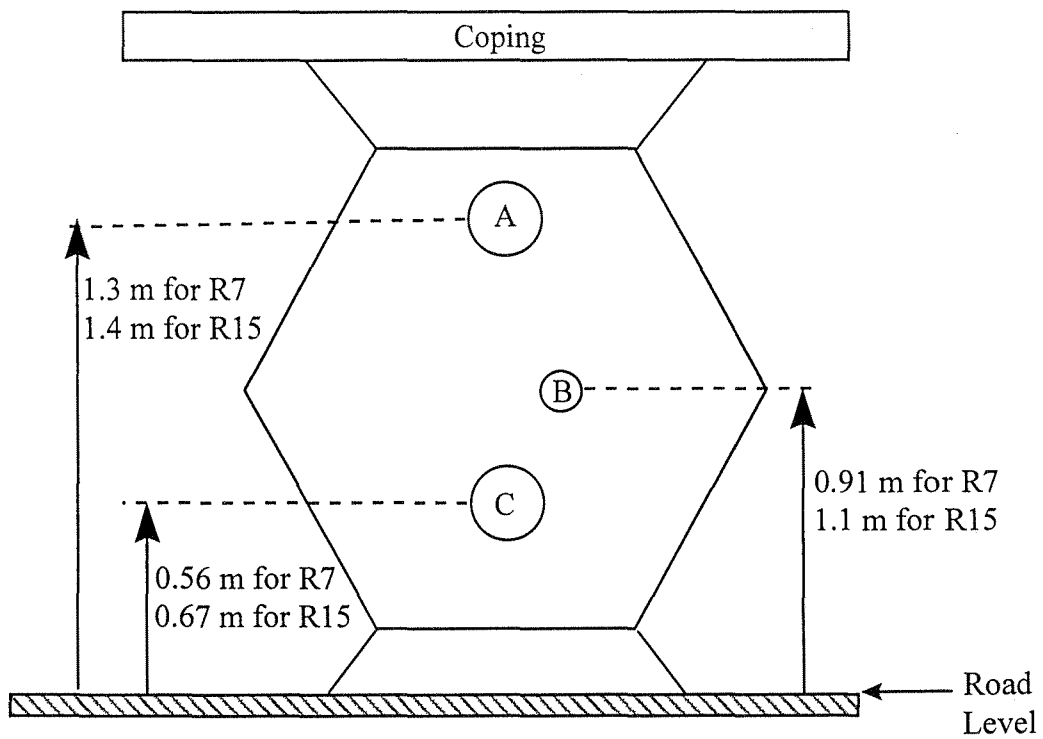


Figure 2-14. Elevation of the contacts for the Howard Frankland MSE wall; see Table 2-3 for contact and electrode details. This figure corresponds to panel sets R7 and R15.

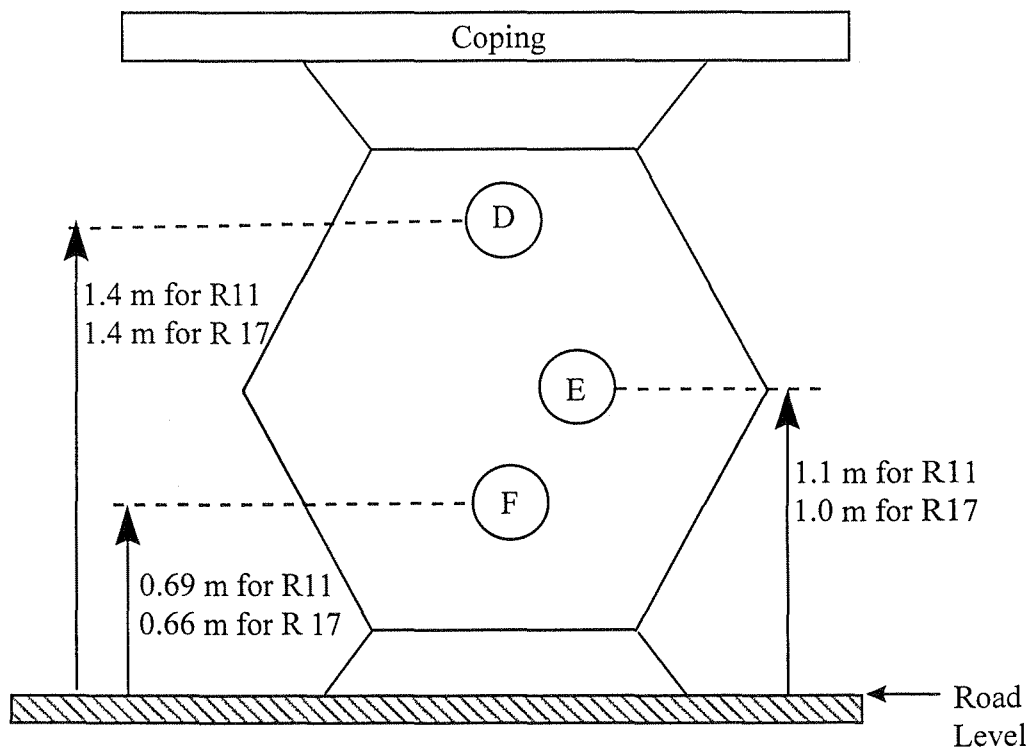


Figure 2-15. Elevation of the contacts for the Howard Frankland MSE wall; see Table 2-3 for contact and electrode details. This figure corresponds to panel sets R11 and R17.

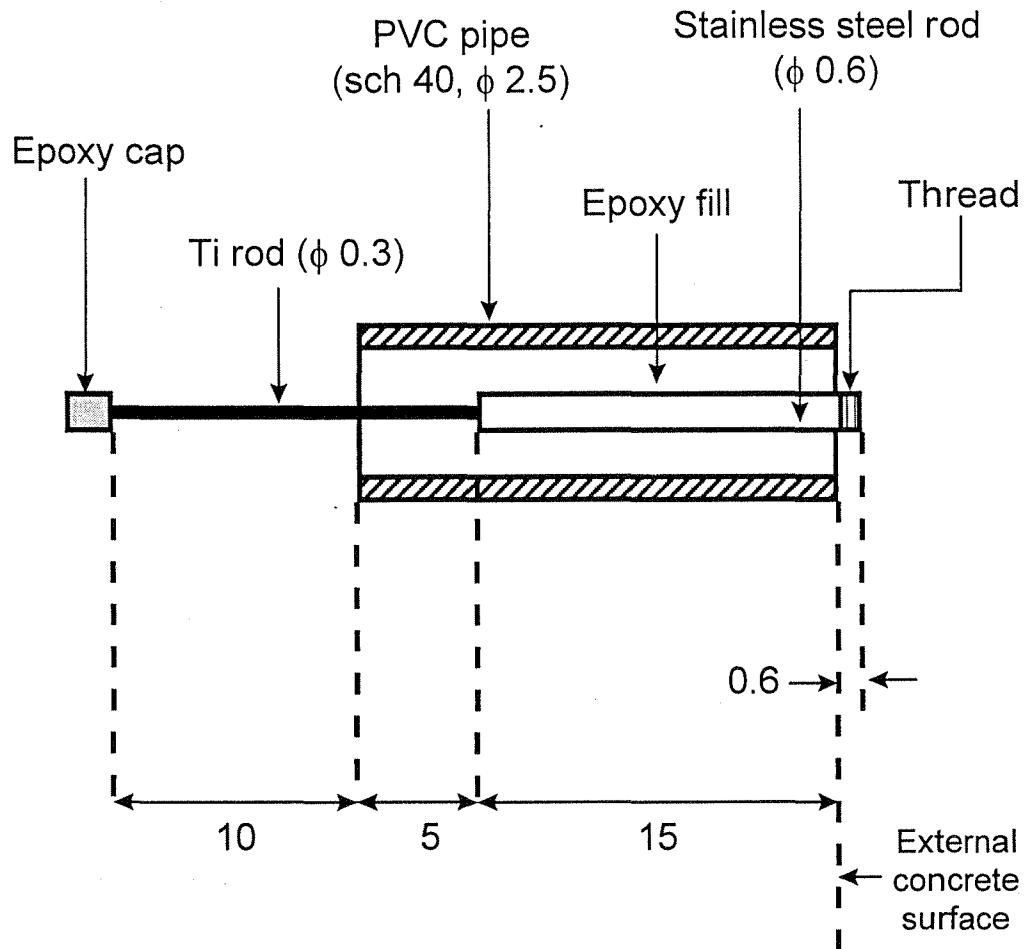


Figure 2-16. Details of the activated titanium reference electrode for the Howard Frankland MSE wall; all dimensions shown are in centimeters.

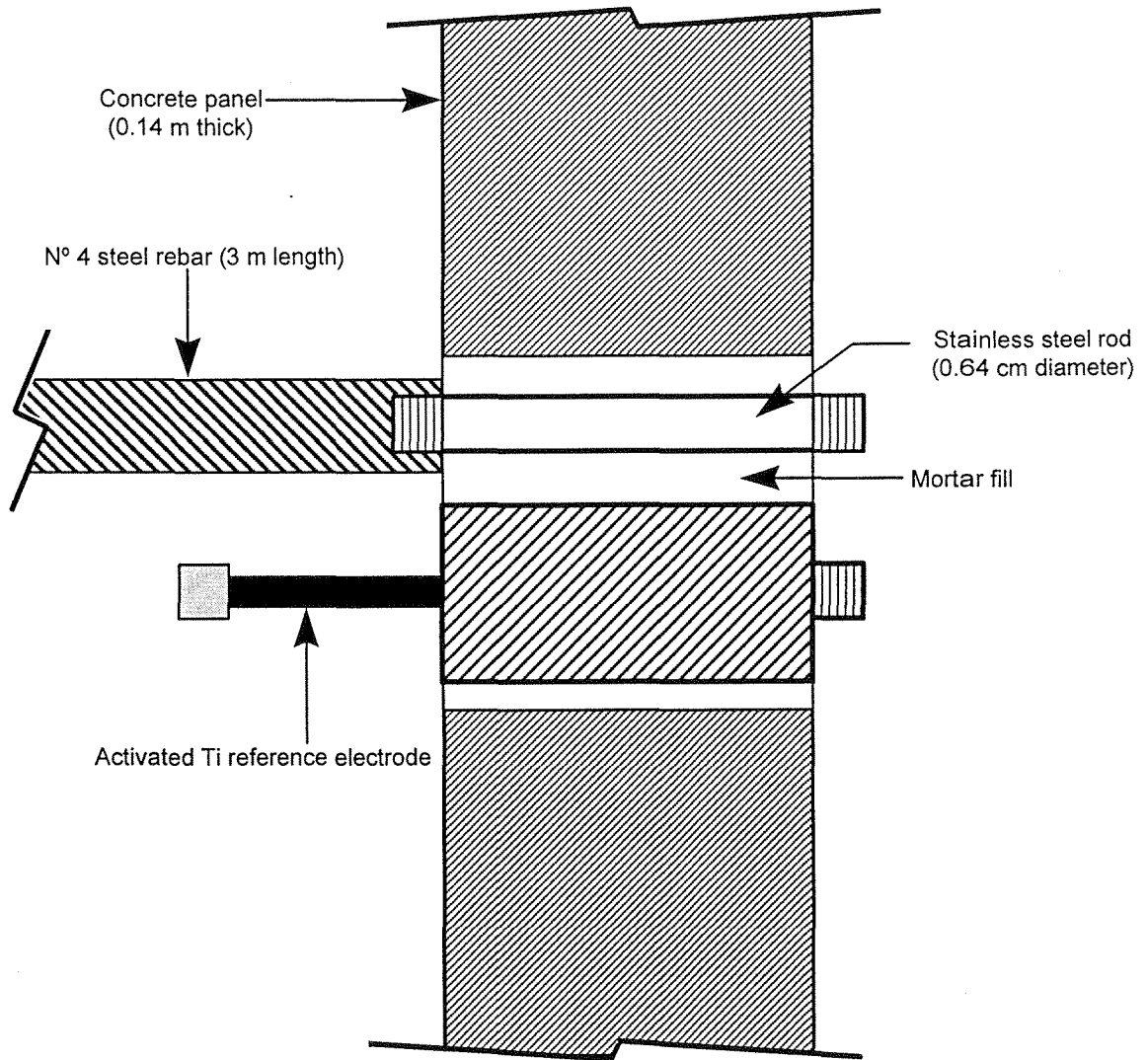


Figure 2-17. Details of the steel rod and titanium reference electrode placed at panels 11 and 17 of the Howard Frankland site (not to scale).

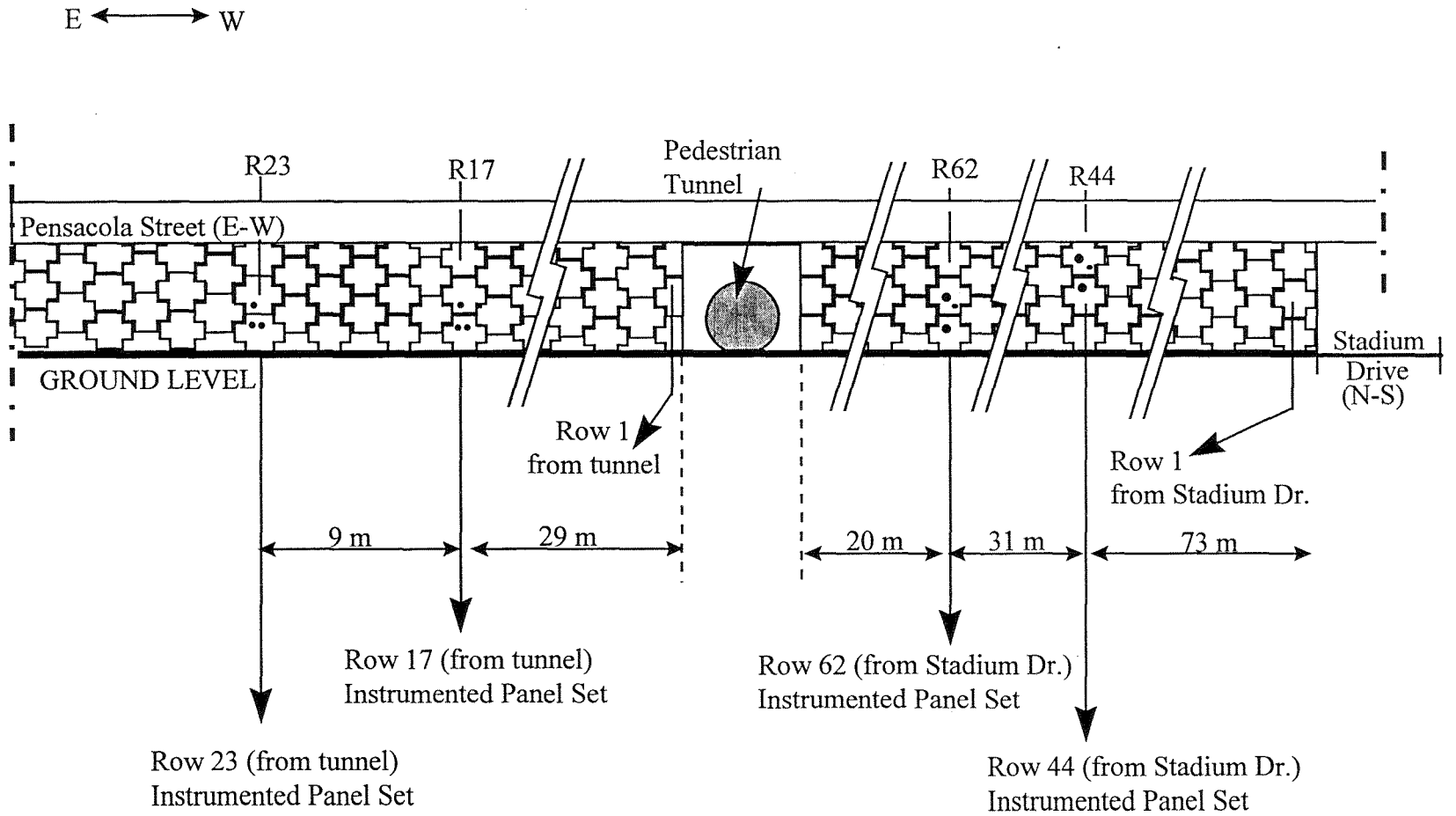


Figure 2-18. Elevation view (as seen from the north) of the Tallahassee MSE wall showing the location of the instrumented panels according to panel number (and distance) from the tunnel (for R17 and R23) and from Stadium Dr. (for R44 and R62).

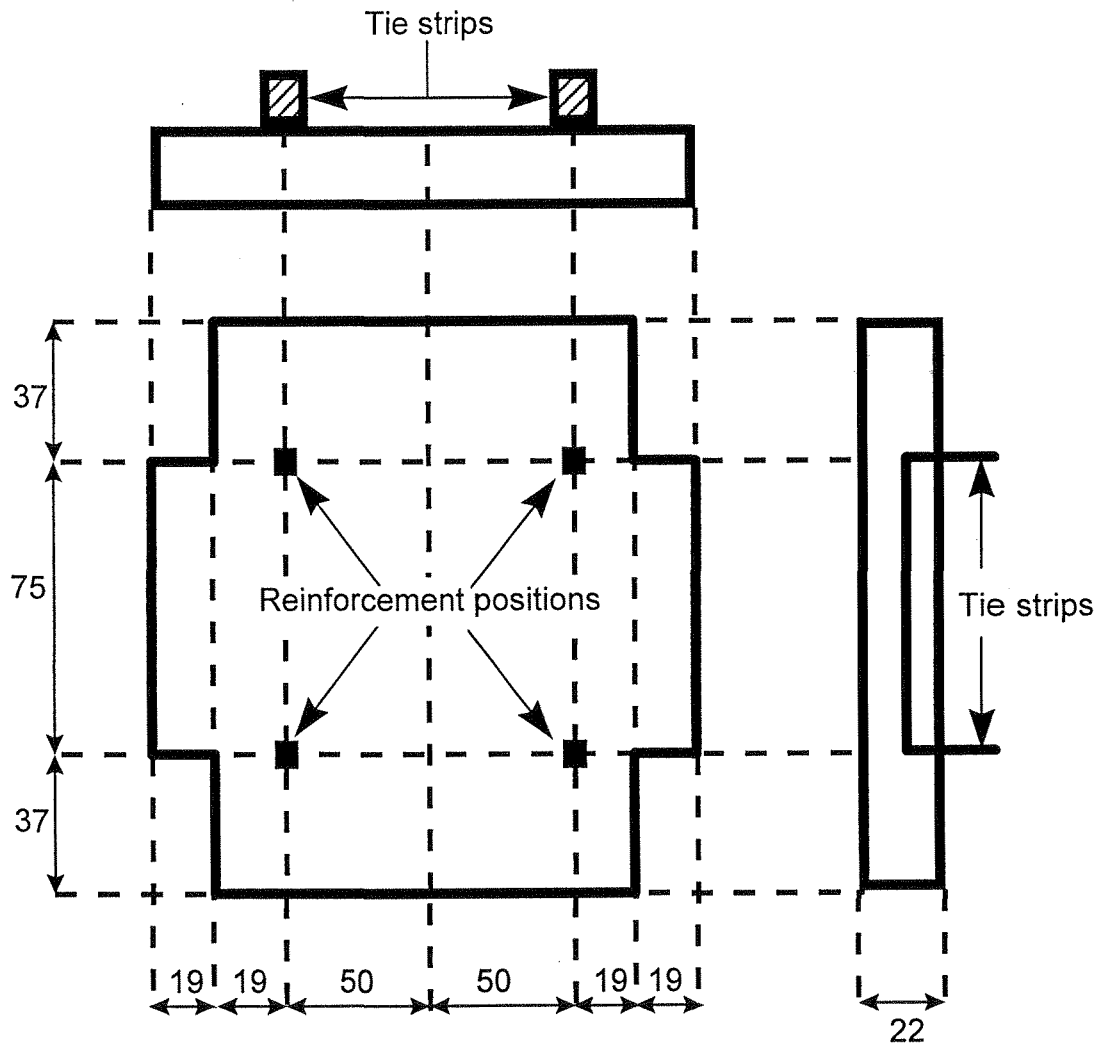


Figure 2-19. Layout of a typical panel showing reinforcement positions. Panel dimensions (shown in centimeters) were obtained from shop drawings (State Project No. 55090-3514), courtesy of The Reinforced Earth Co.

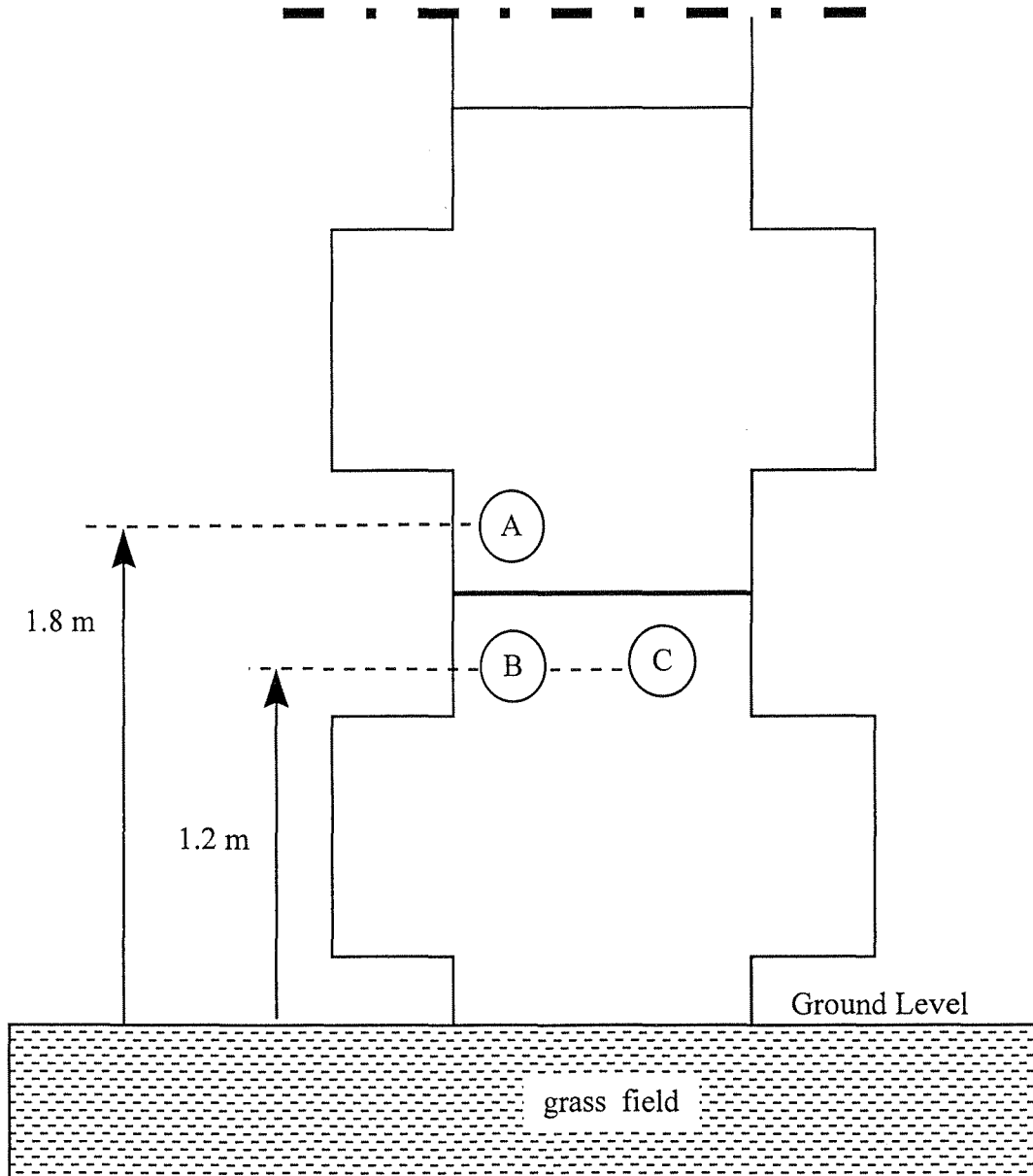


Figure 2-20. Elevation of the contacts from ground level for panels R17 and R23 of the Tallahassee MSE wall. See Table 2-4 for contact and electrode details.

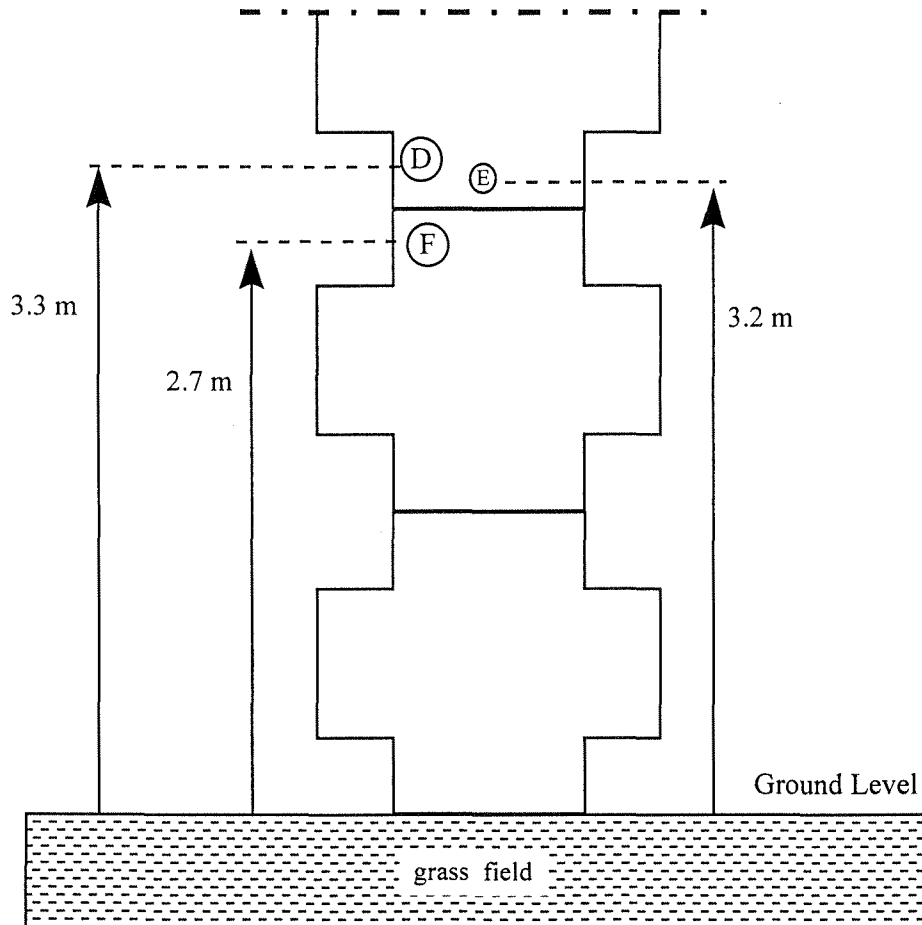


Figure 2-21. Elevation of the contacts from ground level for panel R44 of the Tallahassee MSE wall. See Table 2-4 for contact and electrode details.

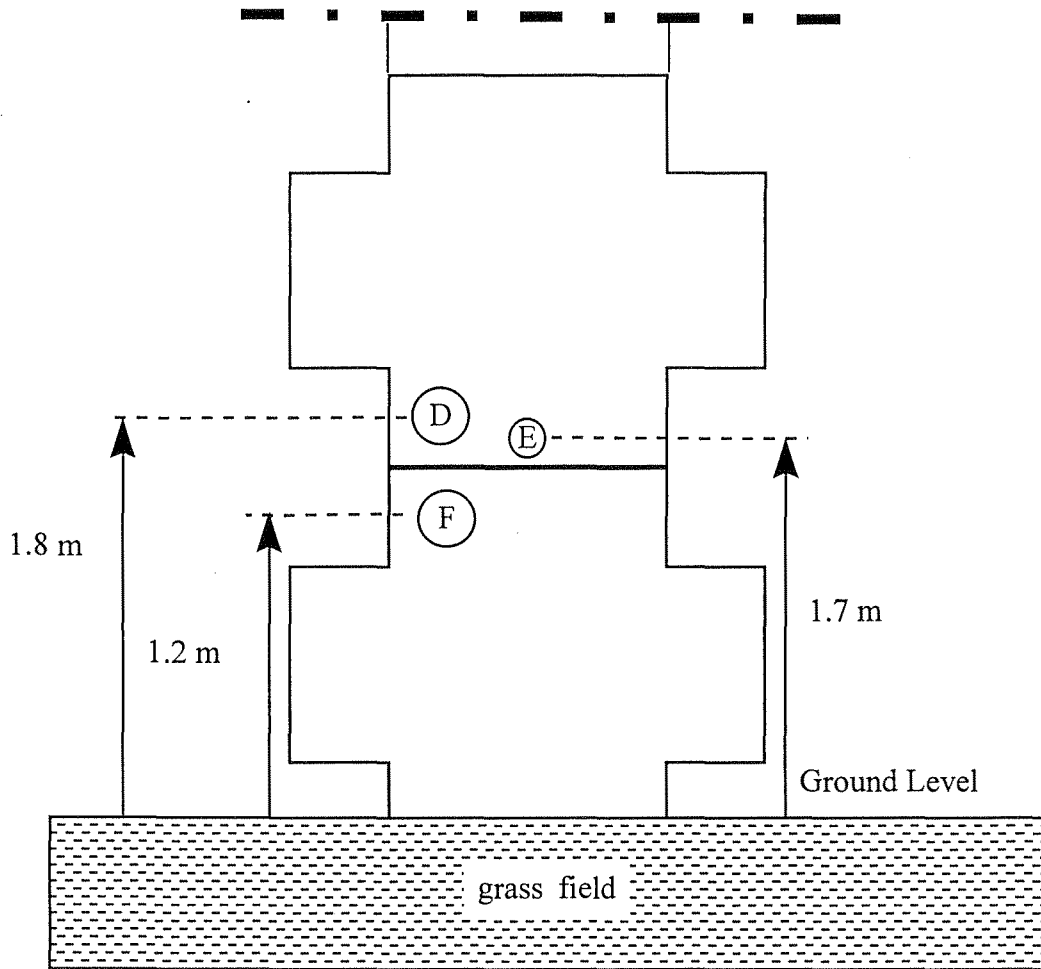


Figure 2-22. Elevation of the contacts from ground level for panel R62 of the Tallahassee MSE wall. See Table 2-4 for contact and electrode details.

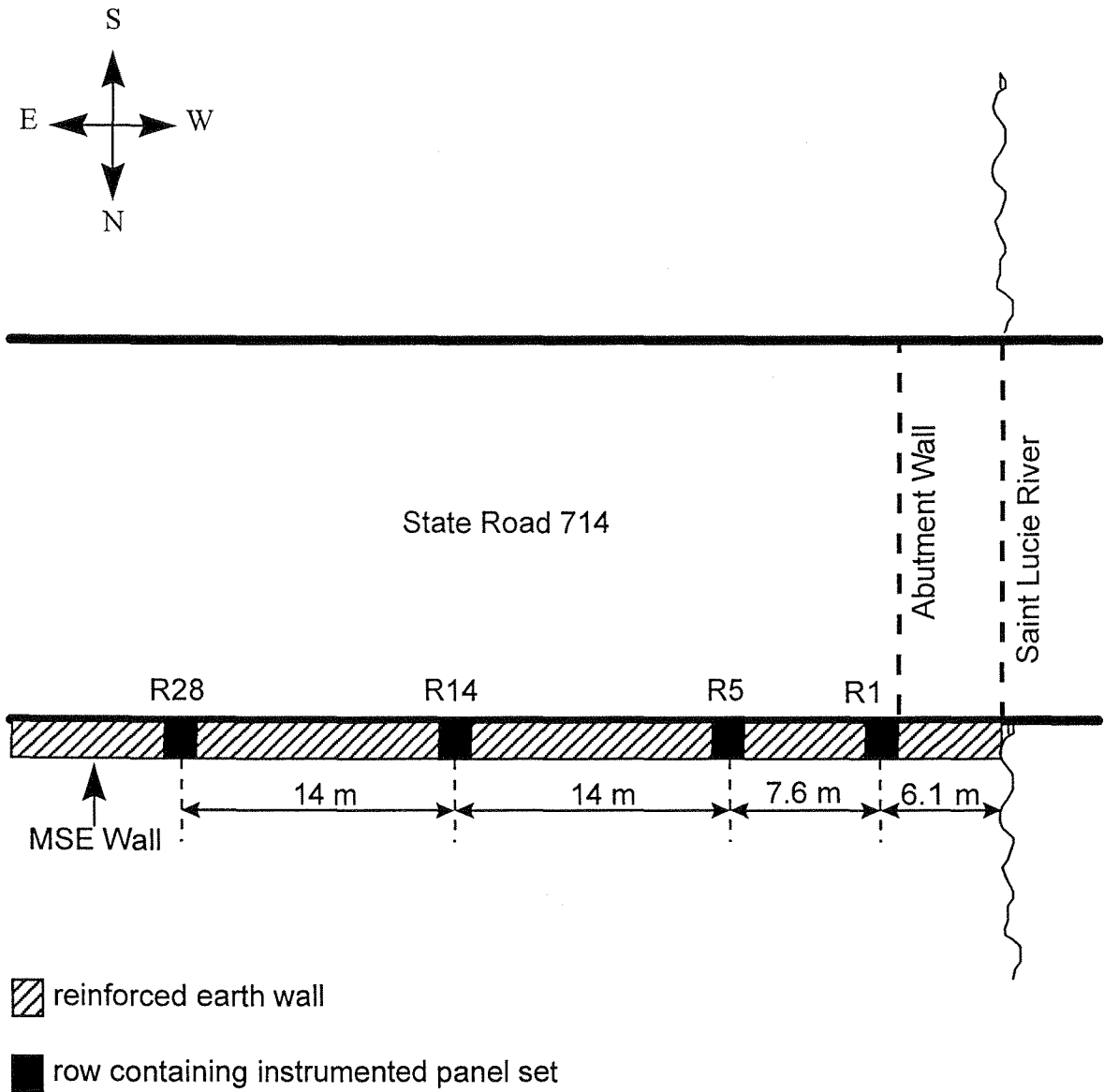


Figure 2-23. Plan view of Palm City Bridge in Stuart showing the location (not to scale) of the instrumented panel sets on the Northeast wall.

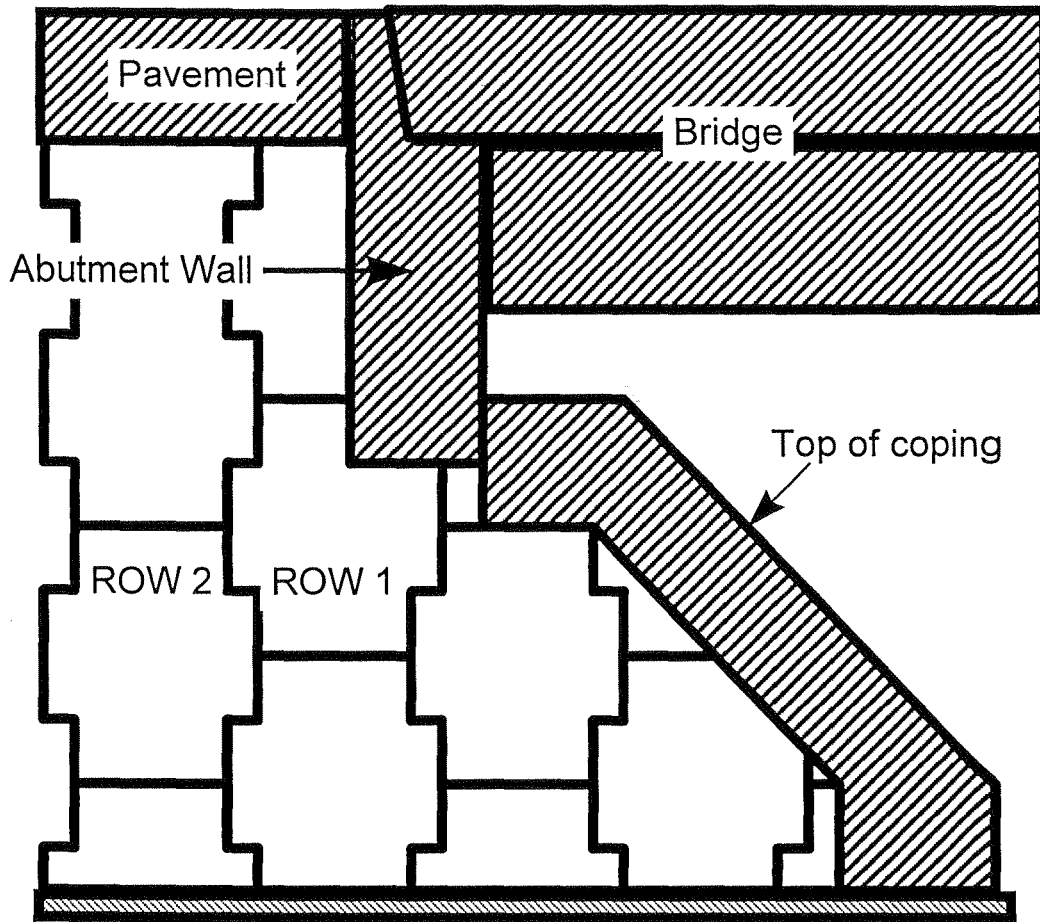


Figure 2-24. Palm City Northeast wall showing the nomenclature for row numbering starting from the abutment wall.

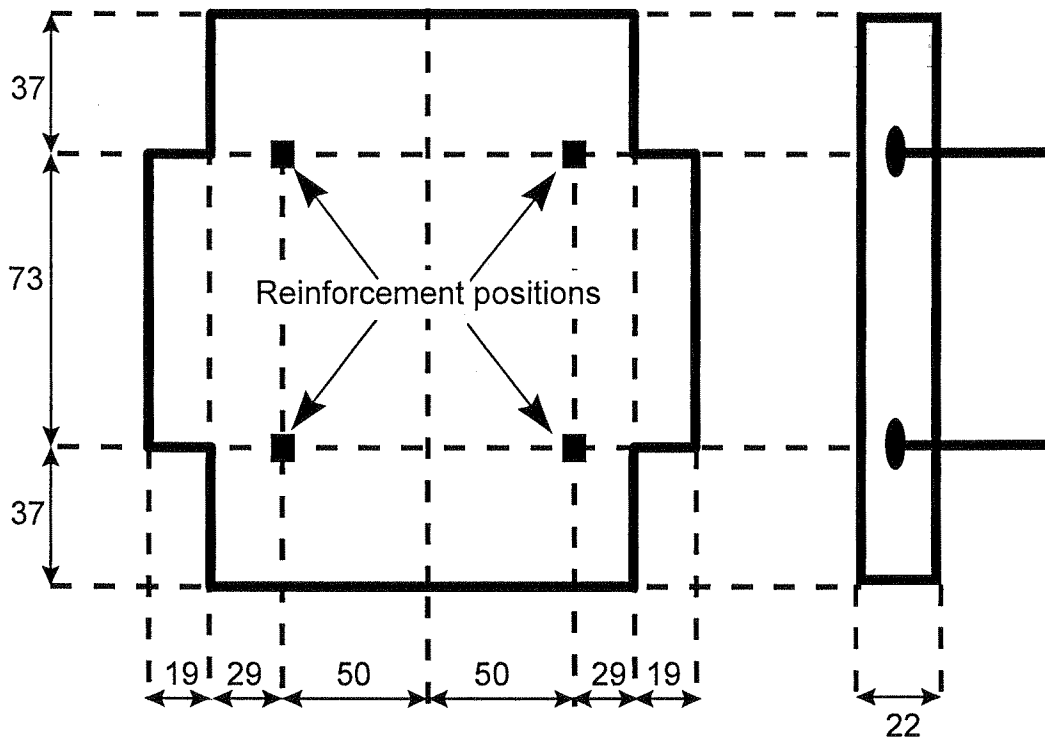


Figure 2-25. Layout (not to scale) of a typical panel for the Palm City site showing the position and dimensions (in centimeters) of the reinforcement. Panel dimensions were obtained from shop drawings (State Project No. 89090-3515), courtesy of The Reinforced Earth Co.

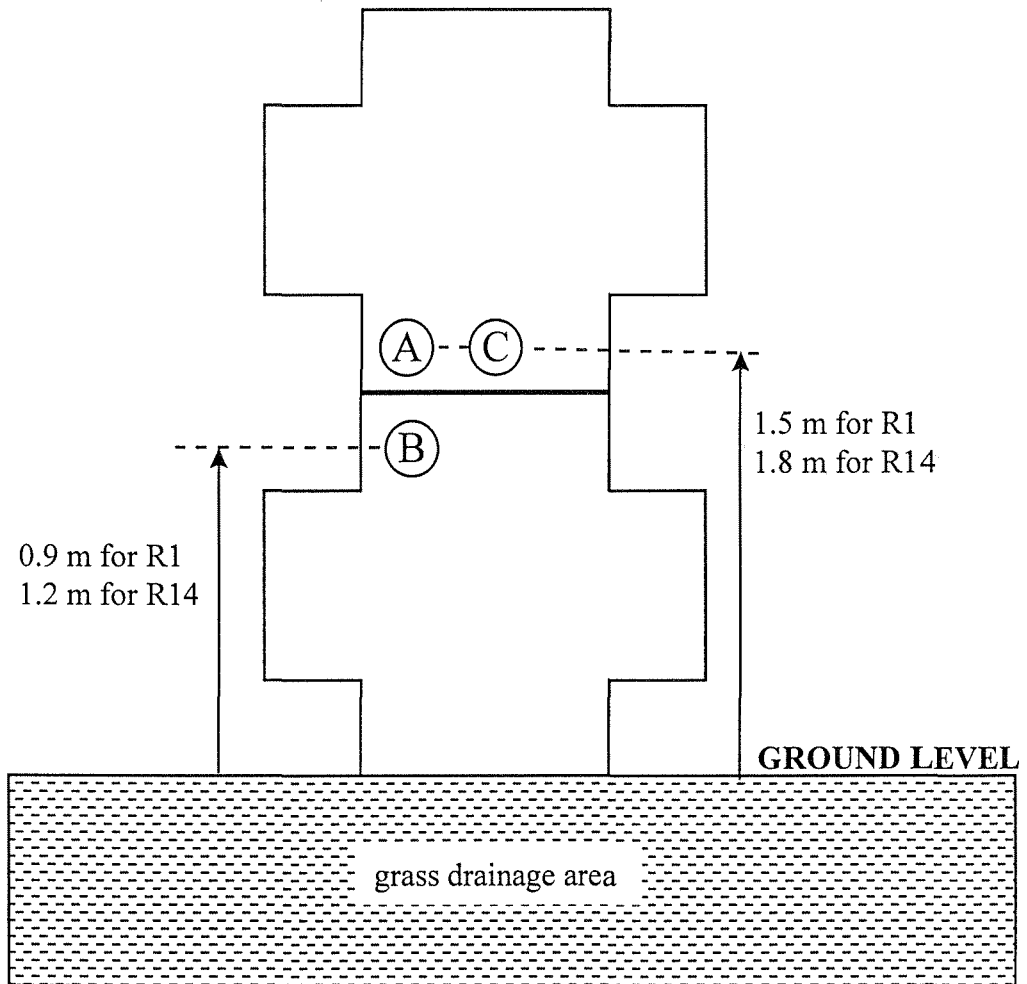


Figure 2-26. Position of the contacts for panel sets R1 and R14 of the Palm City Northeast MSE wall. See Table 2-5 for contact and electrode details.

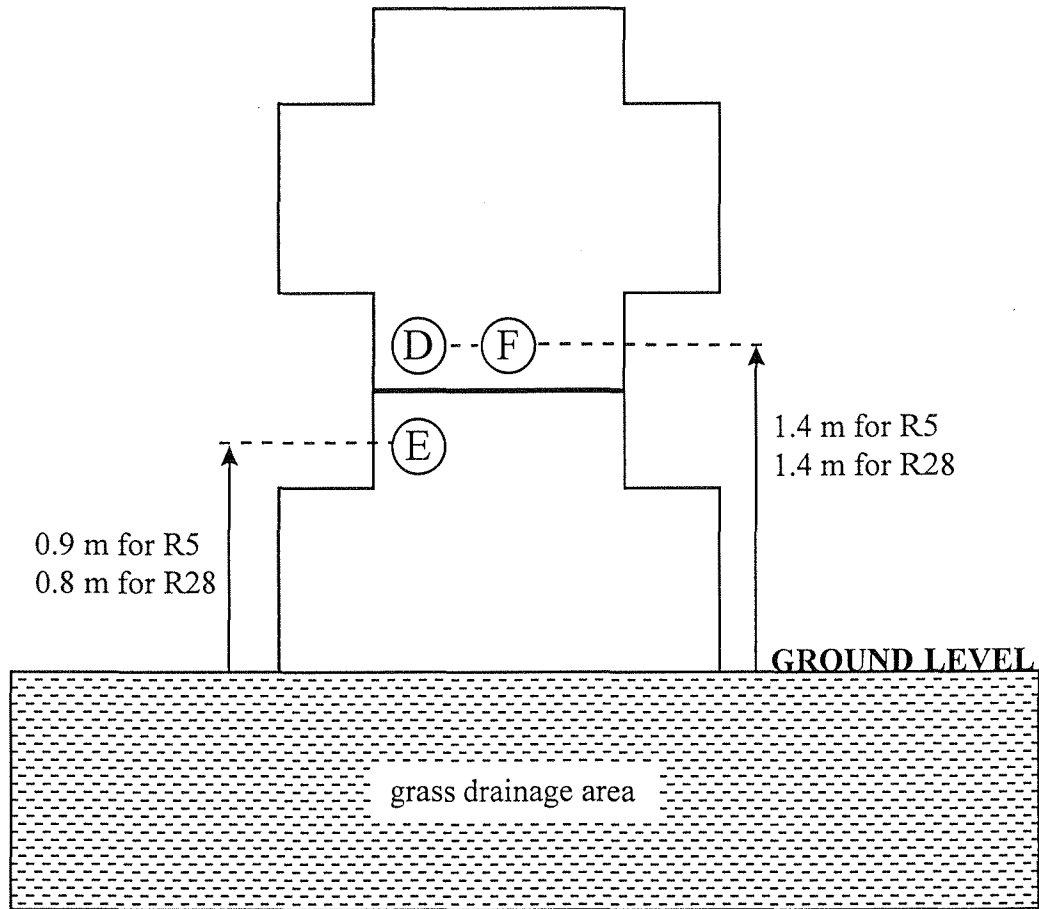


Figure 2-27. Position of the contacts for panel sets R5 and R28 of the Palm City Northeast MSE wall. See Table 2-5 for contact and electrode details.

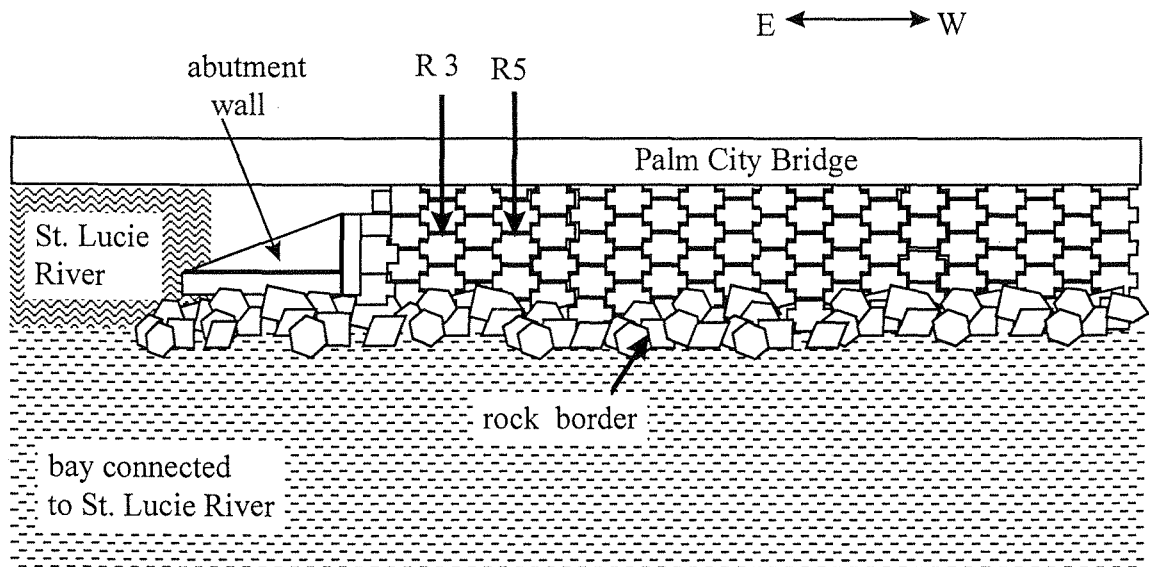


Figure 2-28. Palm City Northwest wall (elevation view as seen from the North) indicating the location of instrumented panel sets R3 and R5. Rows are numbered starting from the abutment wall.

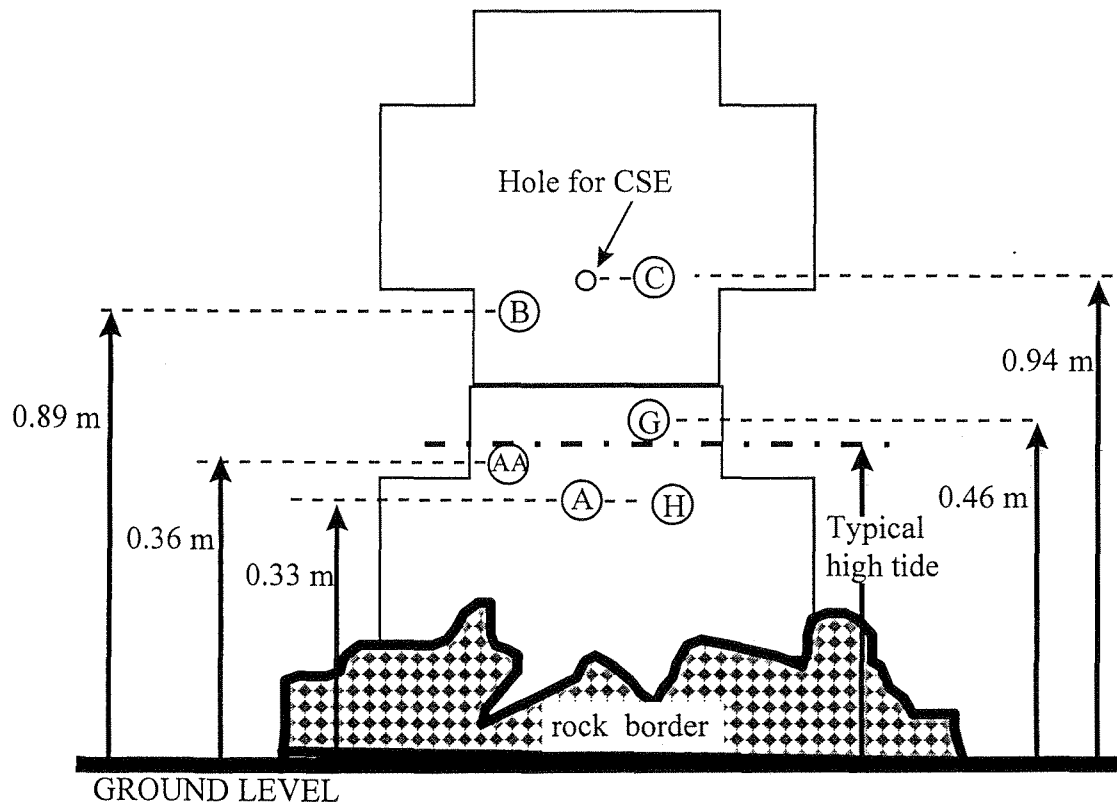


Figure 2-29. Position of the contacts for panel set R3 of the Palm City Northwest MSE wall. See Table 2-6 for contact and electrode details.

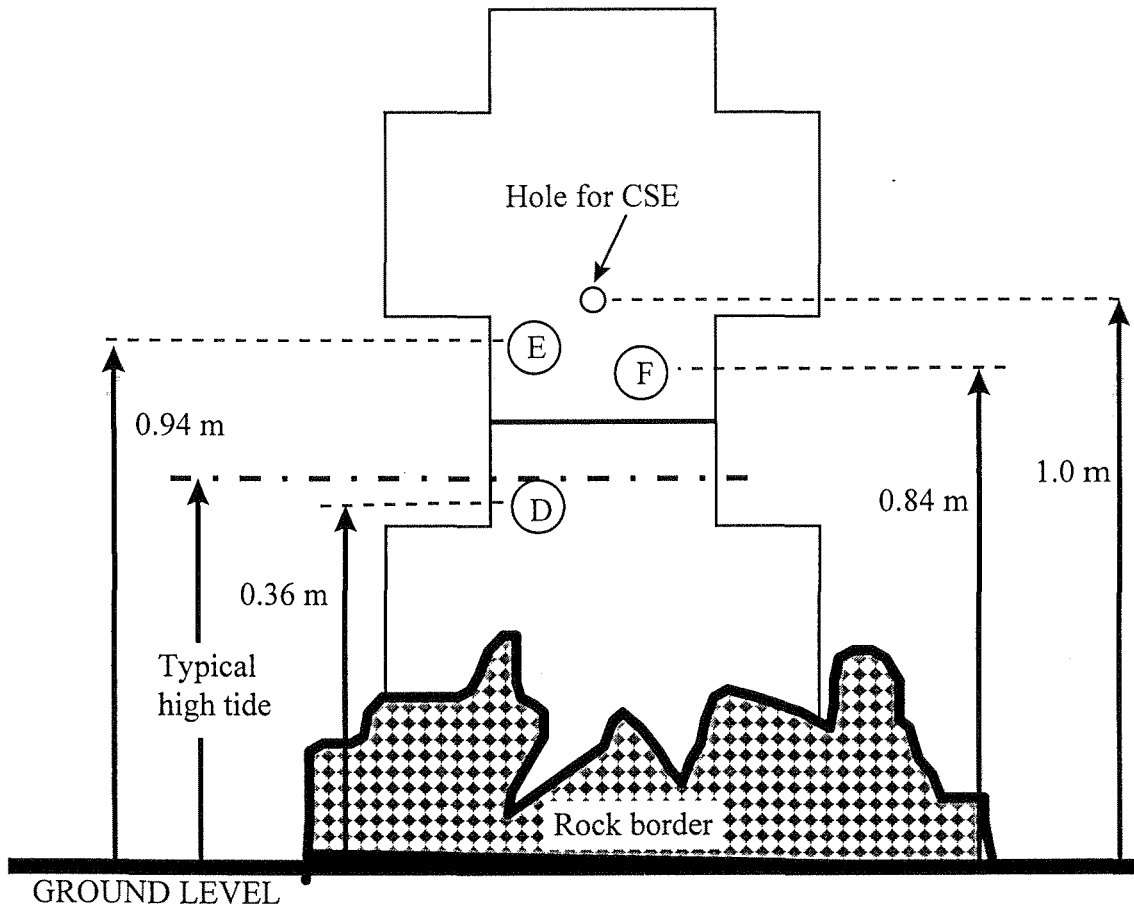


Figure 2-30. Position of the contacts for panel set R5 of the Palm City Northwest MSE wall. See Table 2-6 for contact and electrode details.

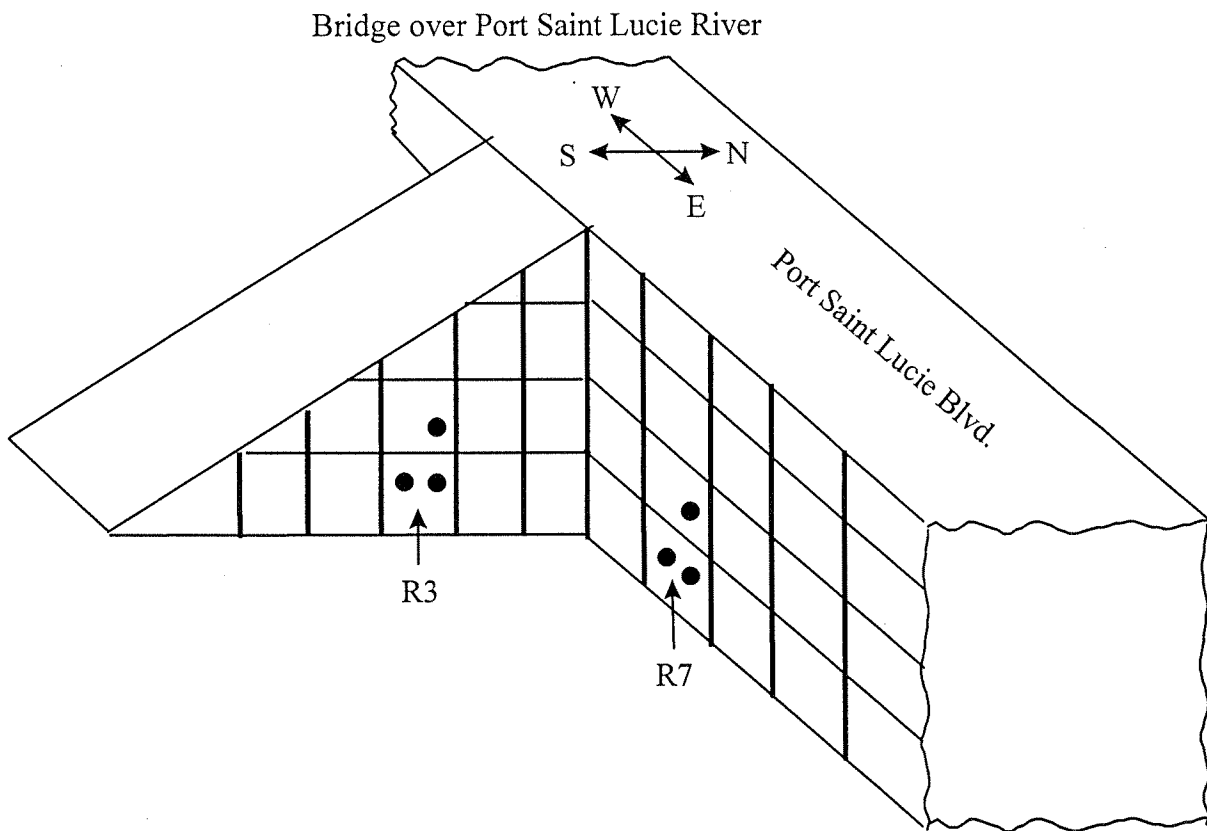


Figure 2-31. Elevation view of the Port Saint Lucie MSE wall indicating the location of instrumented panel sets R3 and R7.

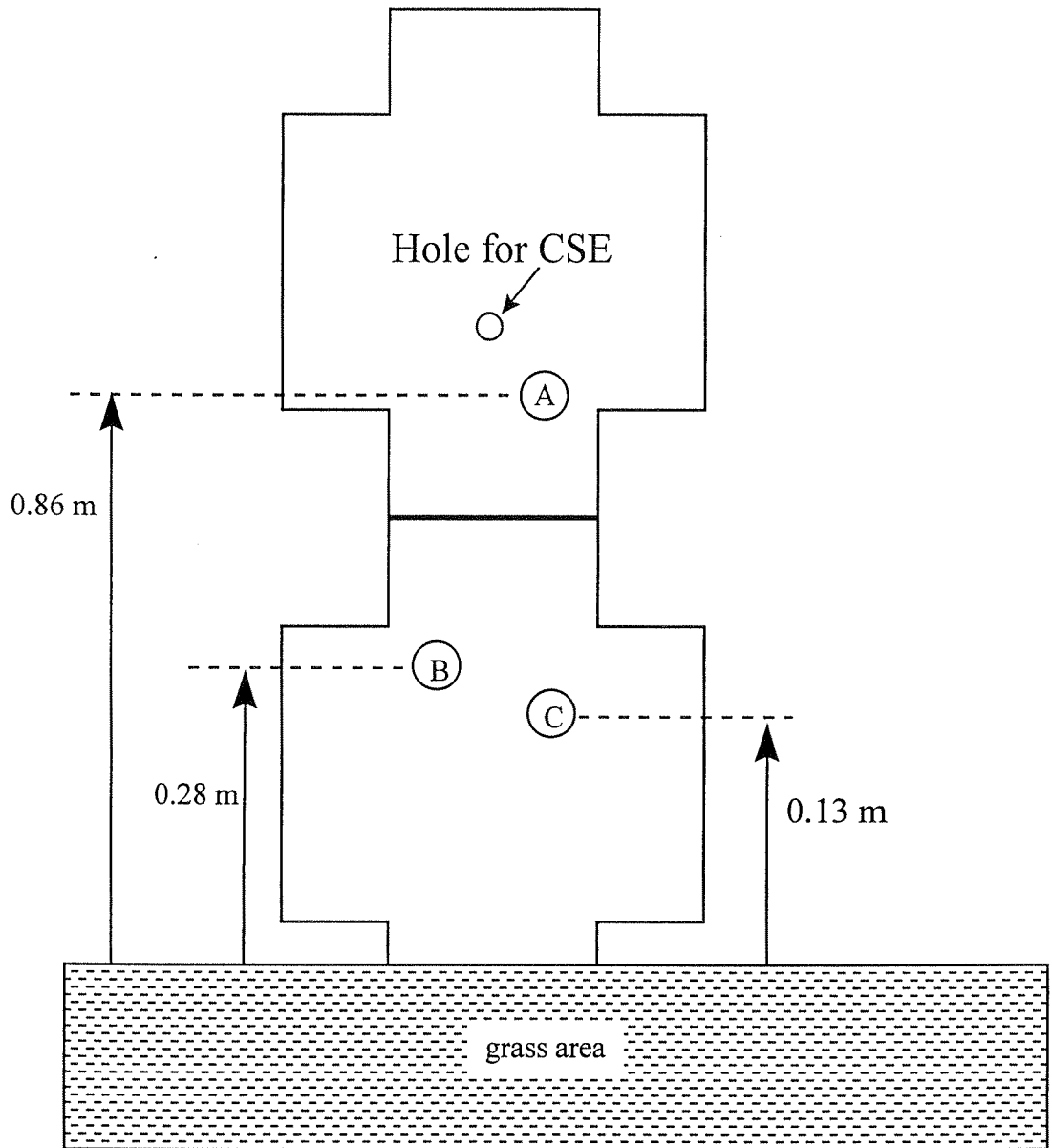


Figure 2-32. Position of the contacts for panel set R7 of the Port Saint Lucie MSE wall. See Table 2-7 for contact and electrode details.

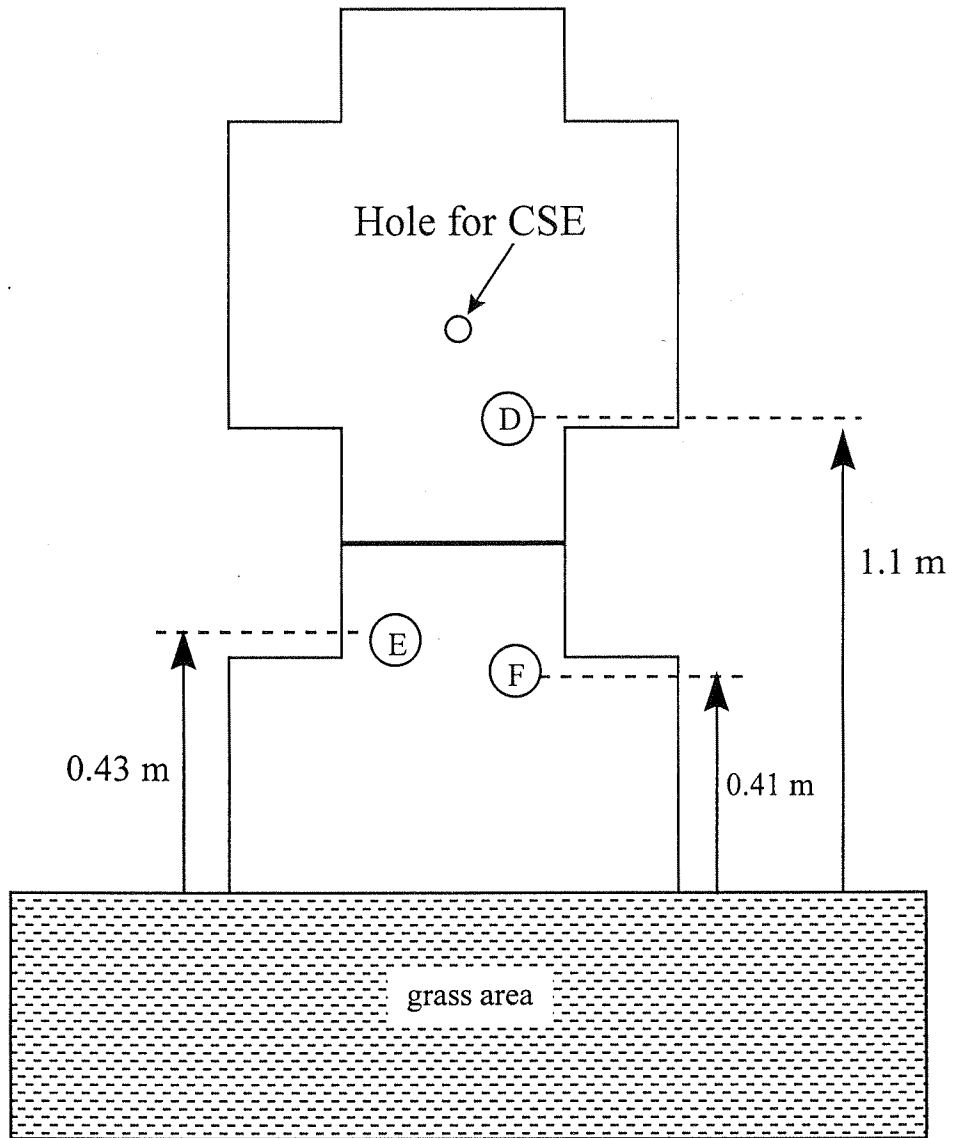


Figure 2-33. Position of the contacts for panel set R3 of the Port Saint Lucie MSE wall. See Table 2-7 for contact and electrode details.

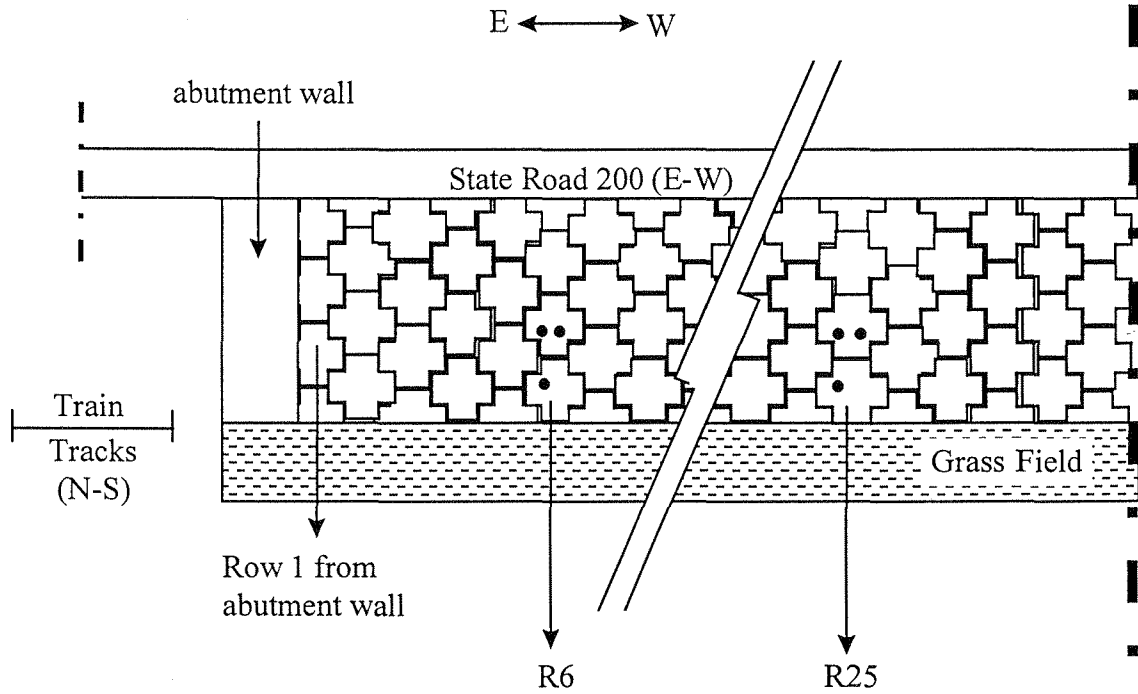


Figure 2-34. Elevation view of the Ocala MSE wall indicating the location of instrumented panel sets R3 and R25.

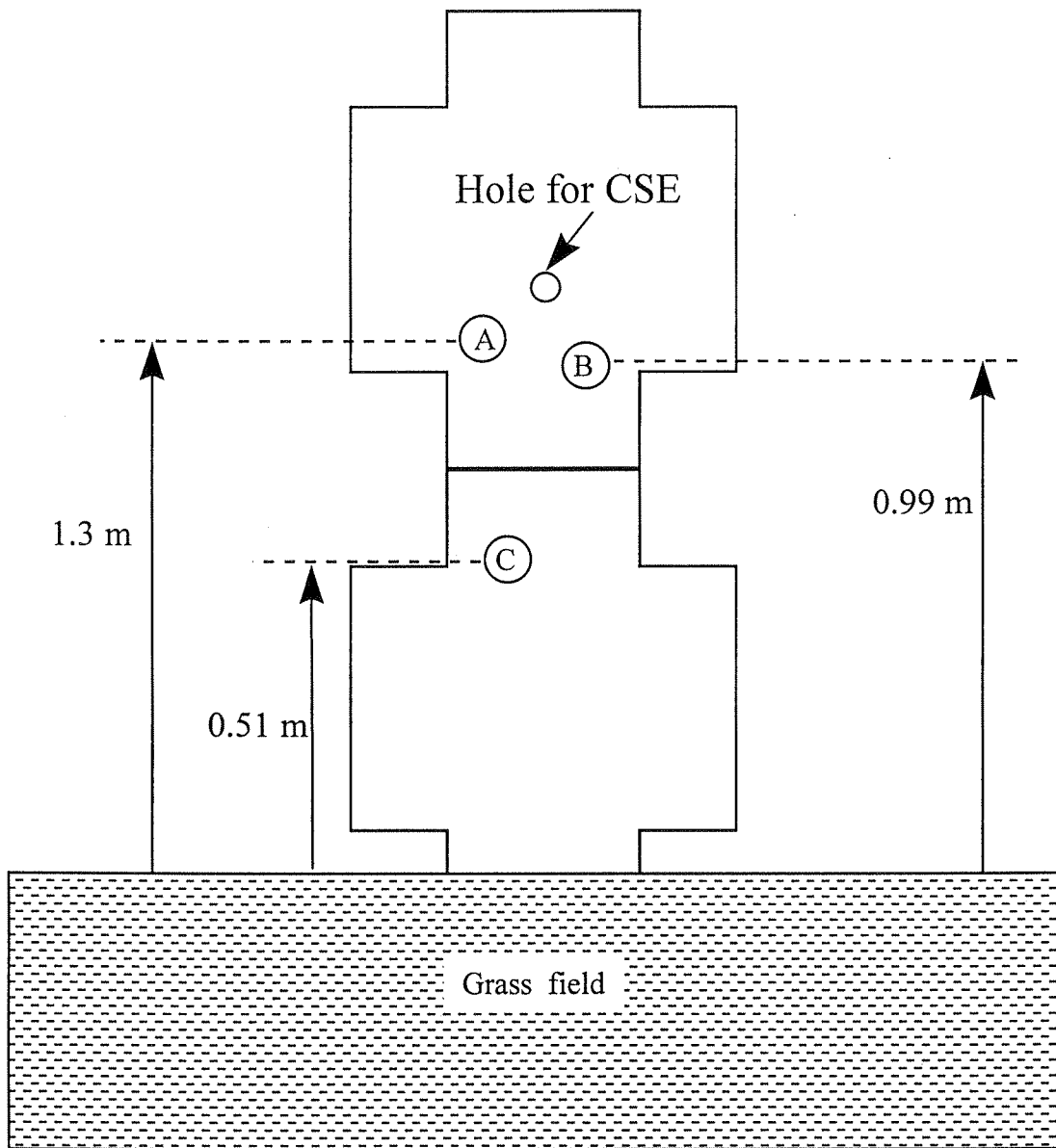


Figure 2-35. Position of the contacts for panel set R25 of the Ocala MSE wall. See Table 2-8 for contact and electrode details.

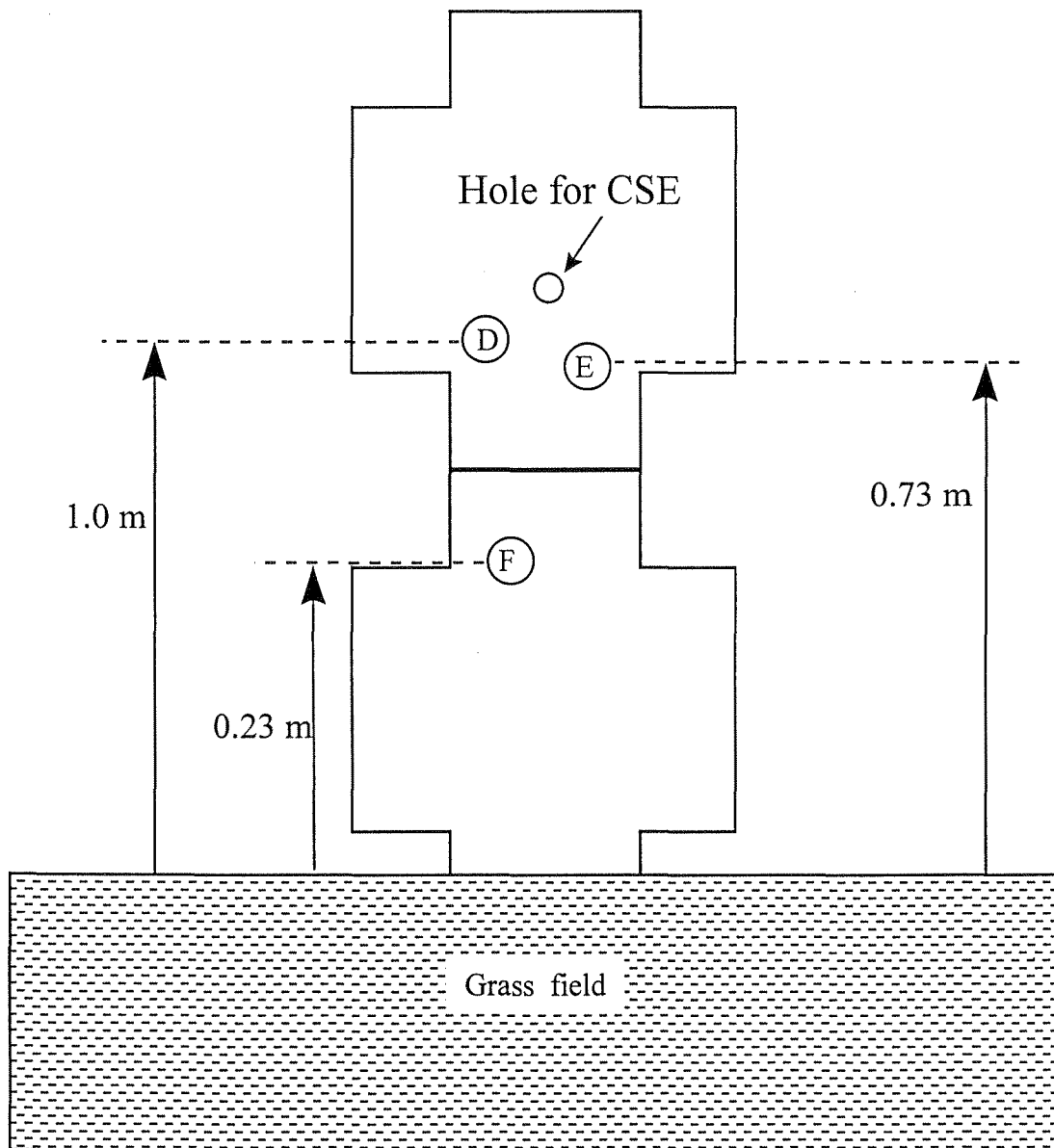


Figure 2-36. Position of the contacts for panel set R6 of the Ocala MSE wall. See Table 2-8 for contact and electrode details.

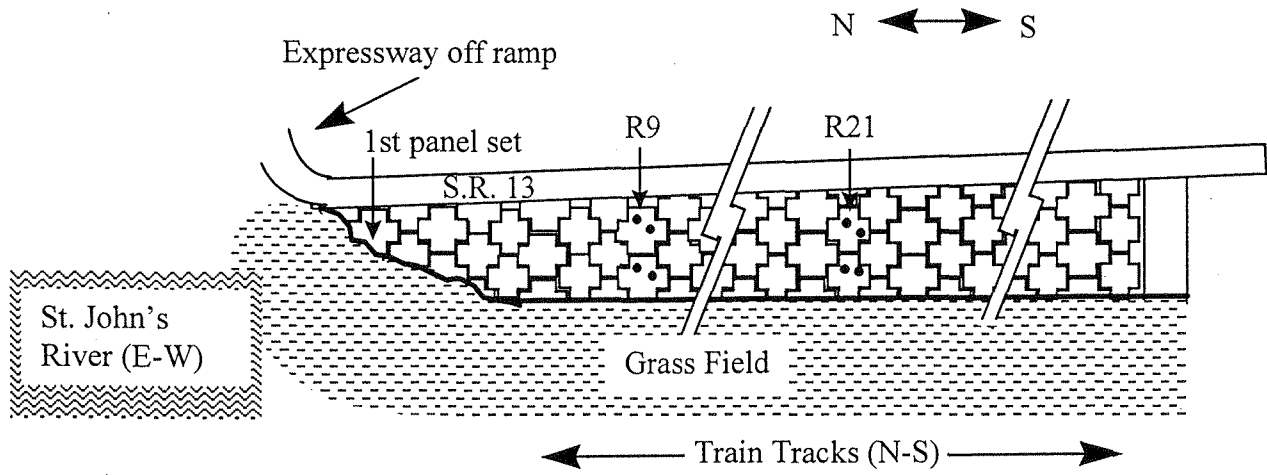


Figure 2-37. Elevation view of the Jacksonville MSE wall indicating the location of instrumented panel sets R9 and R21.

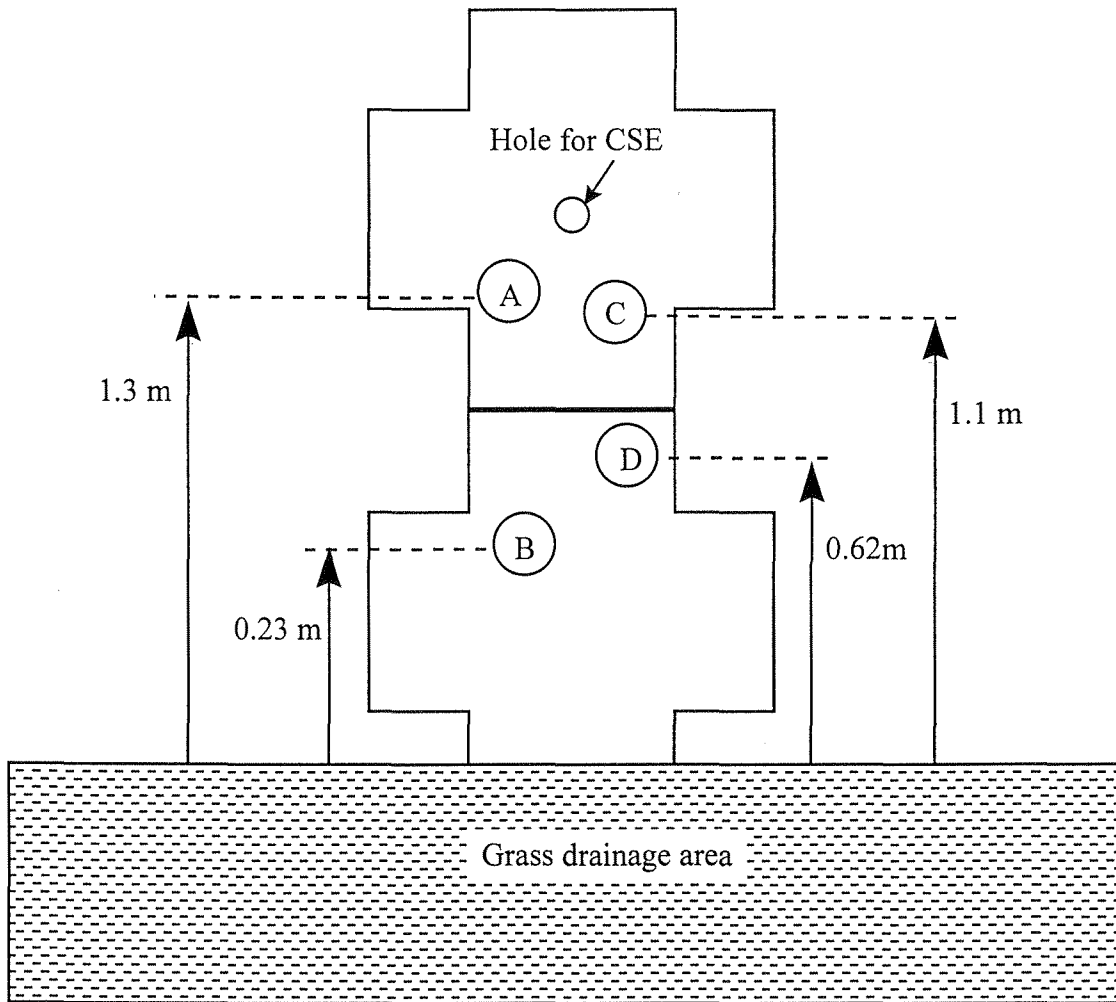


Figure 2-38. Position of the contacts for panel set R9 of the Jacksonville MSE wall. See Table 2-9 for contact and electrode details.

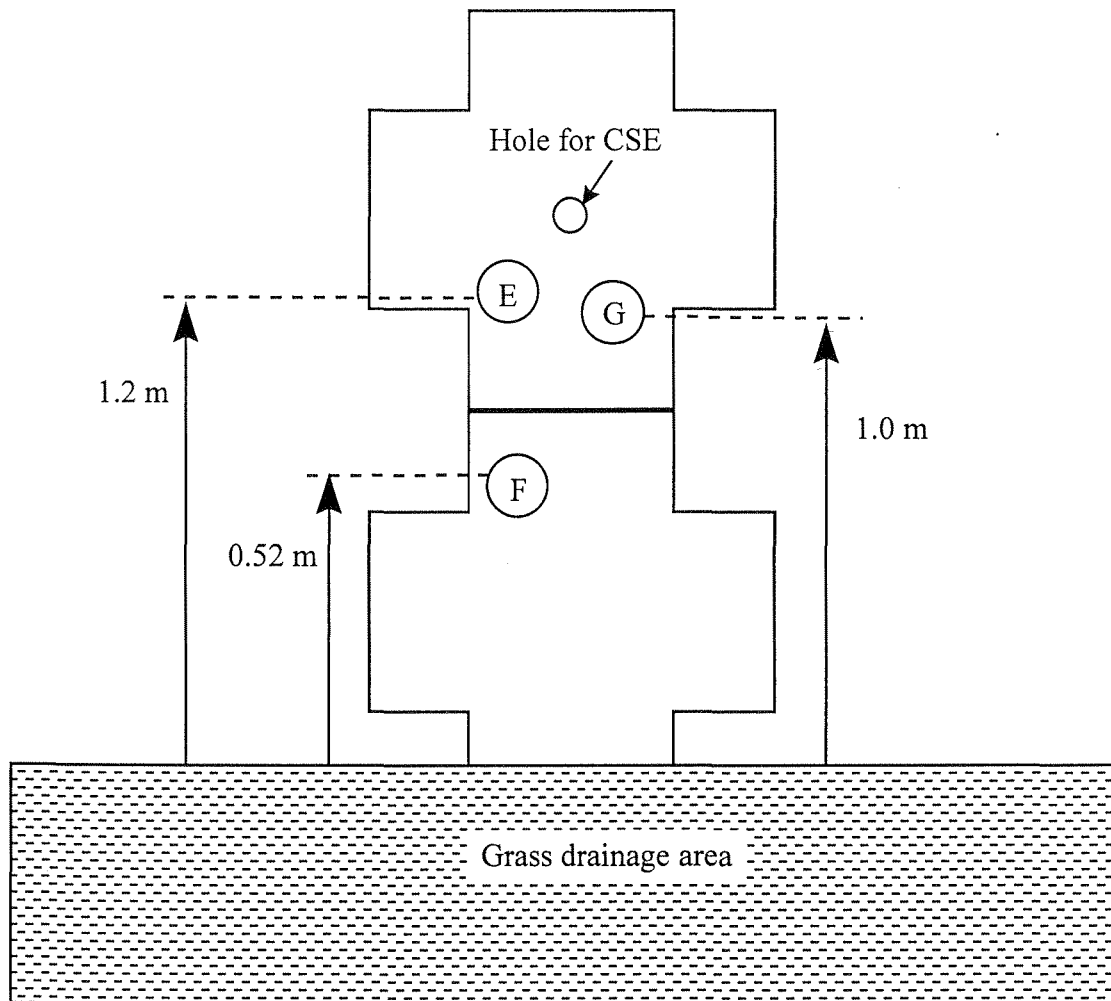


Figure 2-39. Position of the contacts for panel set R21 of the Jacksonville MSE wall. See Table 2-9 for contact and electrode details.

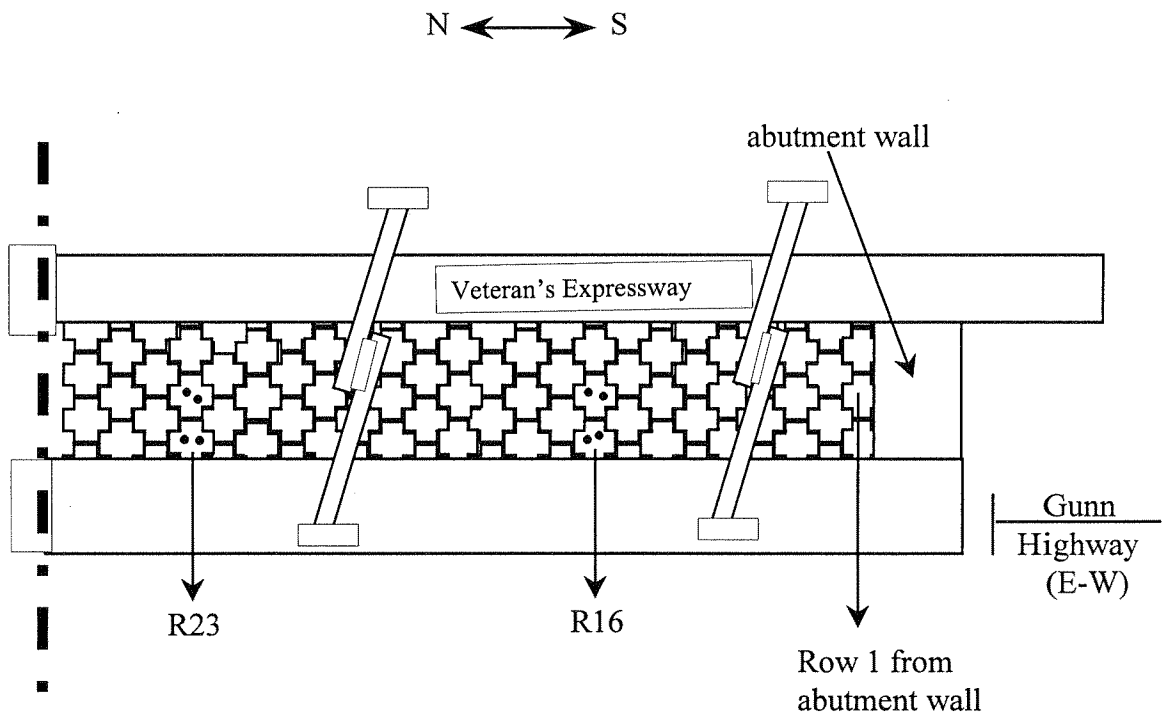


Figure 2-40. Elevation view of the Veteran's Expressway MSE wall indicating the location of instrumented panel sets R16 and R23.

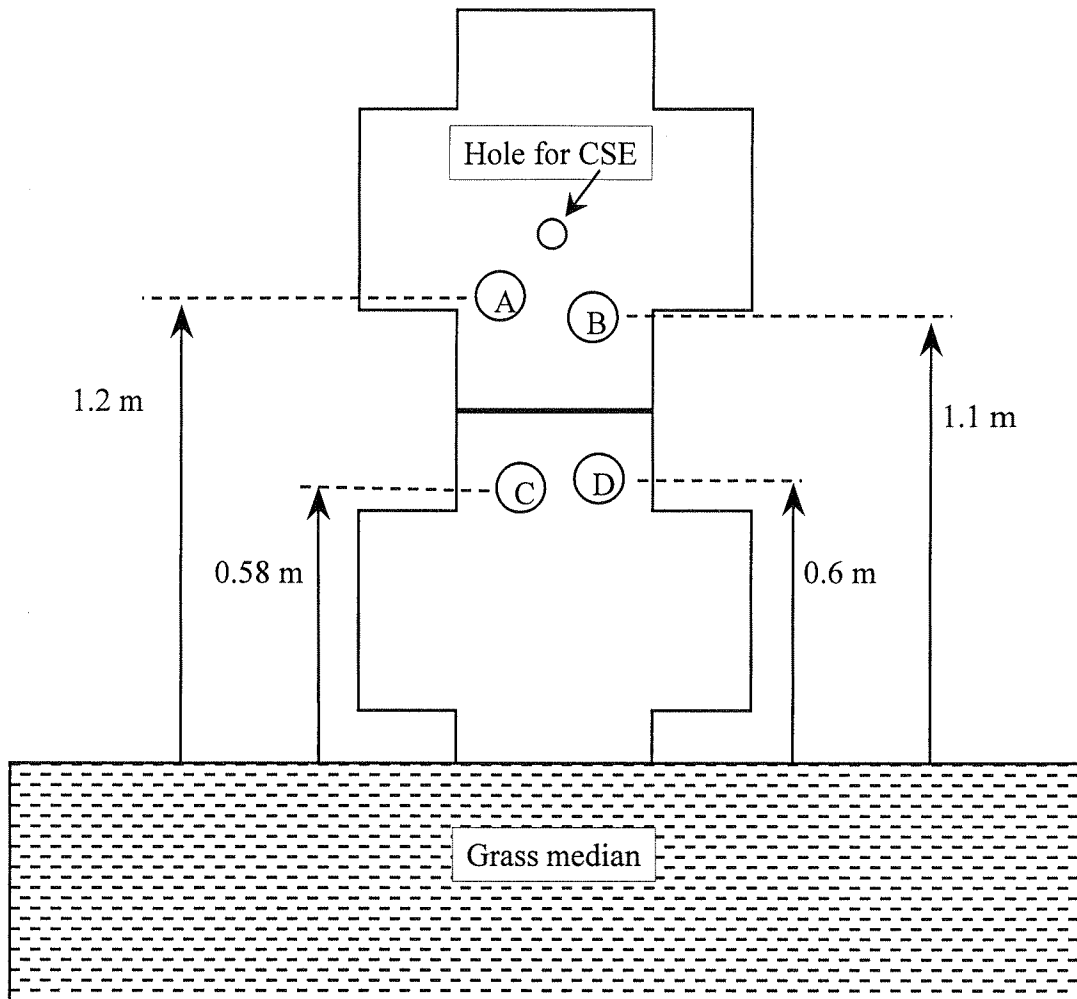


Figure 2-41. Position of the contacts for panel set R16 of the Veteran's Expressway MSE wall. See Table 2-10 for contact and electrode details.

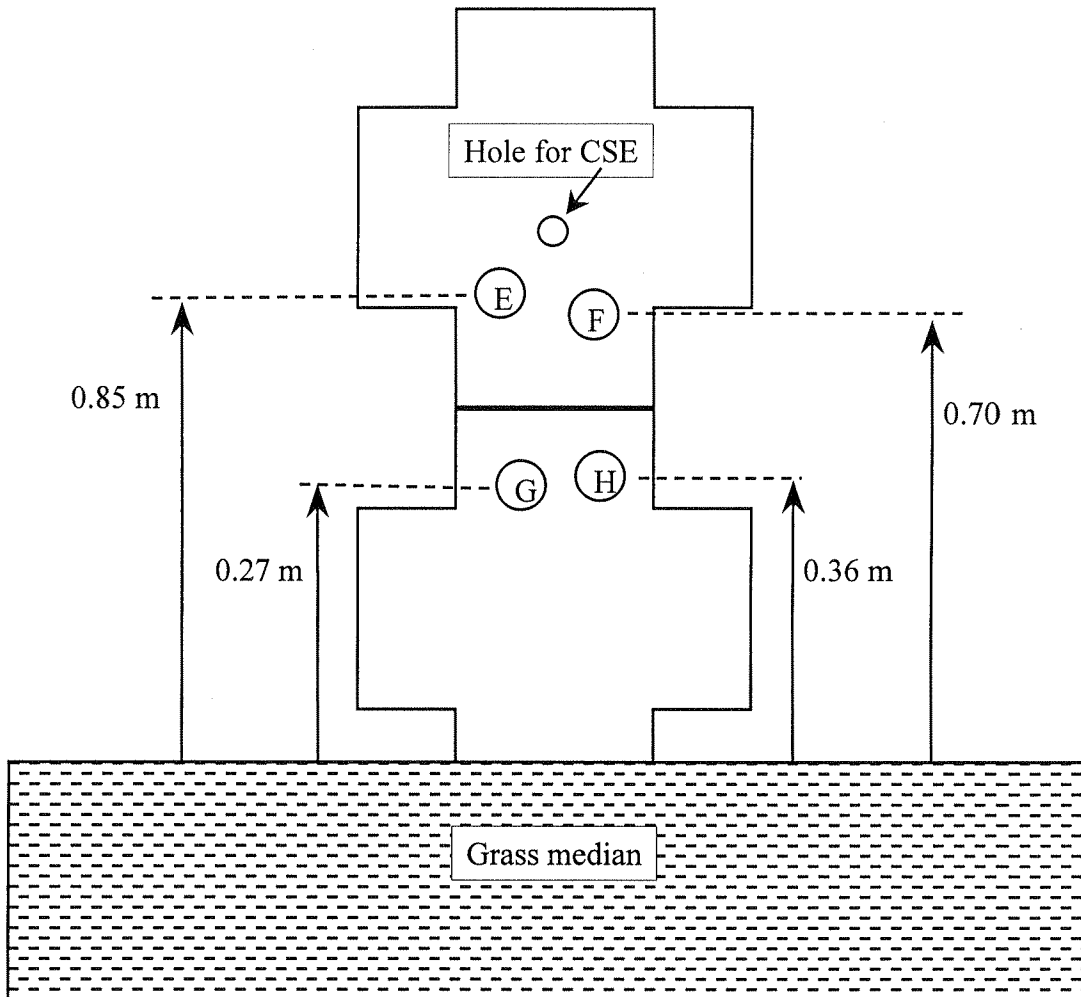


Figure 2-42. Position of the contacts for panel set R23 of the Veteran's Expressway MSE wall. See Table 2-10 for contact and electrode details.

2.2 Laboratory Investigation Arrangement

The purpose of the laboratory experiments was to characterize the effect of chloride contamination on corrosion of both galvanized and bare steel under simulated field conditions. In the MSE walls, the zone adjacent to the panel can not be fully compacted because of the reinforcement. Therefore, there may exist a sharp difference in soil density between the soil within three feet from the wall and the rest of the backfill. This difference in soil properties can be an important driving force for corrosion macrocell development. Another important issue is the effect of density of the soil on its ability to drain water and allow for washout by freshwater, thus reducing the extent of contamination as time progresses. The laboratory investigation was intended to identify the anode and the cathode regions and relate the corrosion behavior to soil density differences and chloride contamination.

Two separate laboratory test series were conducted. Series 1 was intended to reveal the extent of macrocell corrosion that may develop after chloride contamination of adjacent soils with different density. Series 2 explored the separate effect of soils of different coarseness on the development of long-term corrosion rates.

2.2.1 Experimental Setup - Series 1

To simulate differences in soil compaction that actually occur in earth wall structures between zones adjacent to the panel wall and areas far from the wall, four soil boxes were prepared with two types of soils each (Figure 2-43). To create

a difference in soil density, a fine backfill (sand) was selected to fill one half of the box and a coarse mix of sand and crushed lime rock (70 % rock + 30 % sand) was made to fill the other half. The boxes were filled to a height of 13 cm above the bottom of the box); the samples were placed on the soil, then more soil was added to a final height of 36 cm. Compaction was done by hand using a metallic cylinder and both halves of the box were separated using a temporary Plexiglas sheet to keep each type of soil from mixing with the other during assembly. The sheet was removed after the boxes were filled taking care not to move the specimens. A 0.5 in hole was drilled in the bottom of each half of the boxes and a rubber hose was placed (prior to filling the boxes with soil and placement of test specimens) to provide adequate drainage in order to keep moisture content approximately constant.

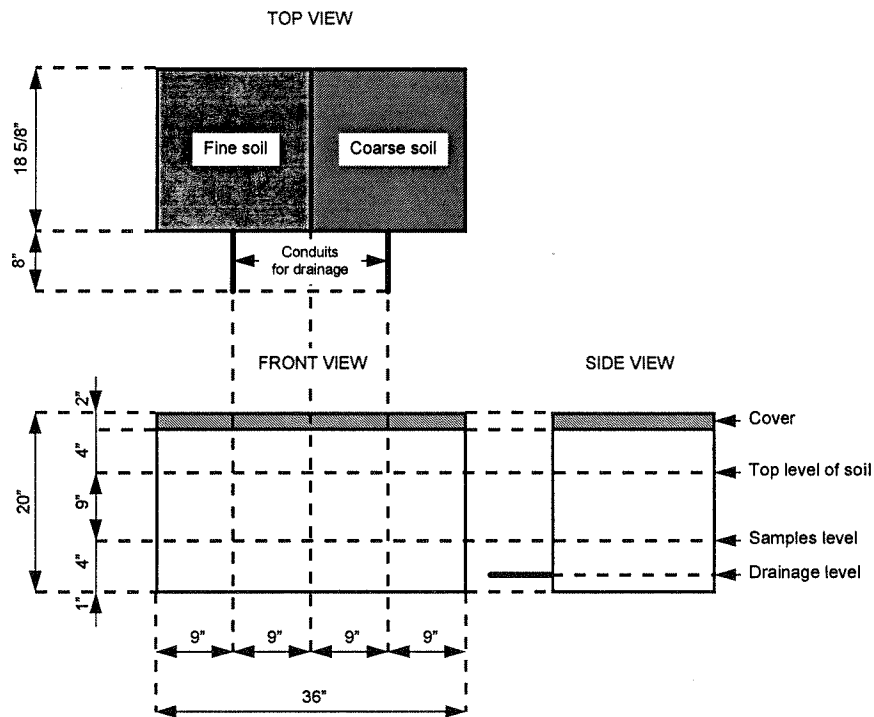


Figure 2-43. General layout (not to scale) of macrocell soil boxes.

Each box has six specimens: four galvanized strips (from the same stock as the lower reinforcement in the Brickell Ave. walls) and two plain steel rebar (No. 4) segments. Both types of specimens are detailed in Figure 2-44. In addition, four reference electrodes were buried to facilitate corrosion measurements. The layout of the position of the specimens is shown in Figure 2-45. The nomenclature used in Figure 2-45 is given Table 2-11. The galvanized layer thickness of the galvanized specimens was between 160 μm and 280 μm as determined with a magnetic caliper gage.

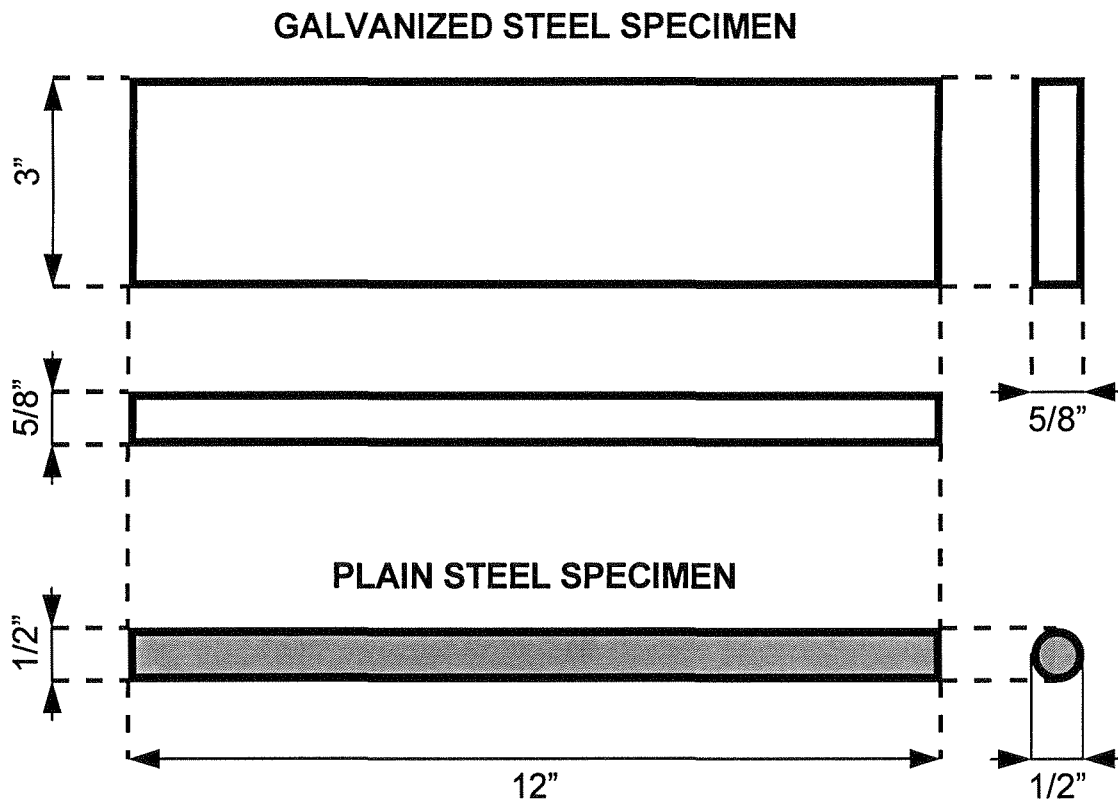


Figure 2-44. Dimensions of Laboratory Specimens (not to scale).

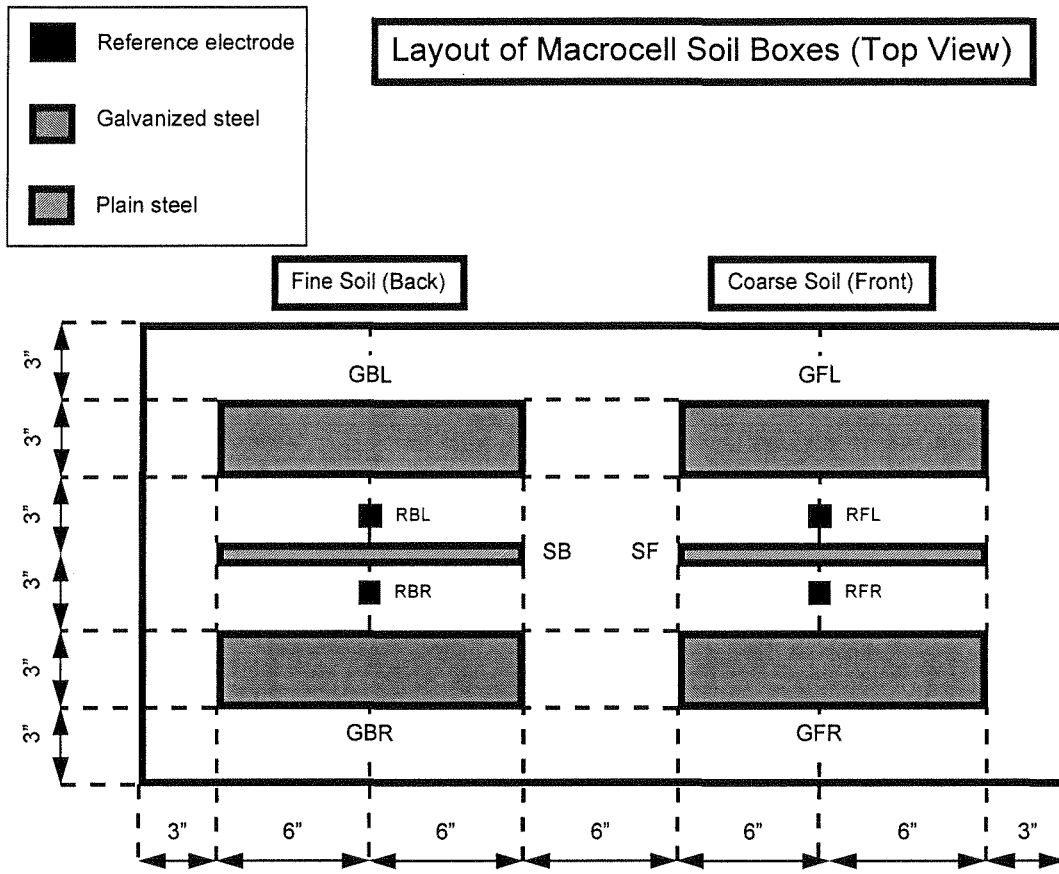


Figure 2-45. Plan view of soil boxes showing the position of the specimens. See Table 2-11 for nomenclature.

Table 2-11. Specimens position and nomenclature (titanium electrodes are reference electrodes).

Side	Position	Type	Name
Left	Front	Galvanized	GFL
Right	Front	Galvanized	GFR
Left	Back	Galvanized	GBL
Right	Back	Galvanized	GBR
Middle	Front	Steel	SF
Middle	Back	Steel	SB
Left	Front	Titanium	RFL
Right	Front	Titanium	RFR
Left	Back	Titanium	RBL
Right	Back	Titanium	RBR

2.2.2 Soil Boxes Assembly Sequence - Series 1

All boxes were assembled the same day (01/17/96) according to the following sequence:

1. The coarse soil was made with 70 % crushed lime rock and 30 % sand by weight and mixed using a cement mixer during 10 minutes. After mixing, the soil was poured into a batch without stopping the mixer rotation and carried to the laboratory where the soil boxes were ready for filling.
2. The boxes were filled to a height of 13 cm. Each half was temporarily separated from the other using a Plexiglas sheet. Compaction was done using a metallic cylinder to apply pressure over each soil layer.
3. Specimens and reference electrodes were placed and the boxes were filled to an approximate height of 36 cm. The weight of the soil (stockpile conditions) in each box was kept to 230 kg. (507 pounds), 130 kg (287 pounds) of coarse fill and 100 kg (220 pounds) of fine fill. The Plexiglas sheet was carefully removed once the boxes were filled.
4. Front and back specimens were interconnected electrically so that the macrocell would be established from the beginning.

2.2.3 Soil Boxes Saturation - Series 1

To create an environment representative of aggressive field conditions, the moisture content of the boxes was kept above 60 % of complete saturation. To determine the saturation point, a sample of each type of backfill (coarse and fine) was taken from the batch, oven dried during 24 hours at 105 °C and weighed. Then, each sample was saturated with water and weighed again. The amount of water for complete saturation from oven-dry conditions was calculated, then the amount of water for 60 % saturation was back-calculated.

2.2.4 Contamination of the Soil Boxes (simulated seawater inundation)

Boxes B and D were contaminated with artificial sea water (ASTM D1141-52,

with a chloride concentration of 19,500 ppm) 70 days after assemblage (on 03/28/96). The contamination was performed according to the following sequence:

1. The excess water in the boxes was drained by opening the drain hoses until the water ceased to drain.
2. The drain hoses were closed while contaminating the soil boxes with artificial sea water. The sea water was added until a film of water was observed on the surface of the soil indicating full saturation. The total amount of artificial sea water added to each box was 15 liters.
3. Once the boxes were contaminated, the drain hoses remained closed for a 12 hours period, after which they were opened to drain the excess liquid as in step 1.

2.2.5 Experimental Setup - Series 2

Four sets of duplicated test boxes were prepared with the dimensions and configurations shown in Figure 2-46. Each box set contained a different type of soil, ranging from fine to coarse sand. The soil properties are presented in the results section.

Only galvanized specimens were used. The specimens were made out of the same ribbed strip stock used in the actual structures. The dimensions of the specimens were 50 mm wide, 4 mm thick and 100 mm long. A total of four galvanized specimens was placed in each box; two of the specimens were wired to allow electrochemical measurements and two of them were non-wired for future retrieval.

2.2.6 Assembly, saturation and contamination - Series 2

These procedures generally replicated those used for series 1. Specimen

potentials, corrosion rates, resistivity of the soils and resistance of the solutions were monitored in each set of boxes for a period of twenty-three days before contaminating one of the boxes of each set with synthetic seawater. At day twenty-three, one box of each set was subjected to a simulated flooding event with synthetic seawater prepared according to ASTM D1141-52. The experiment extended over a period of six hundred days.

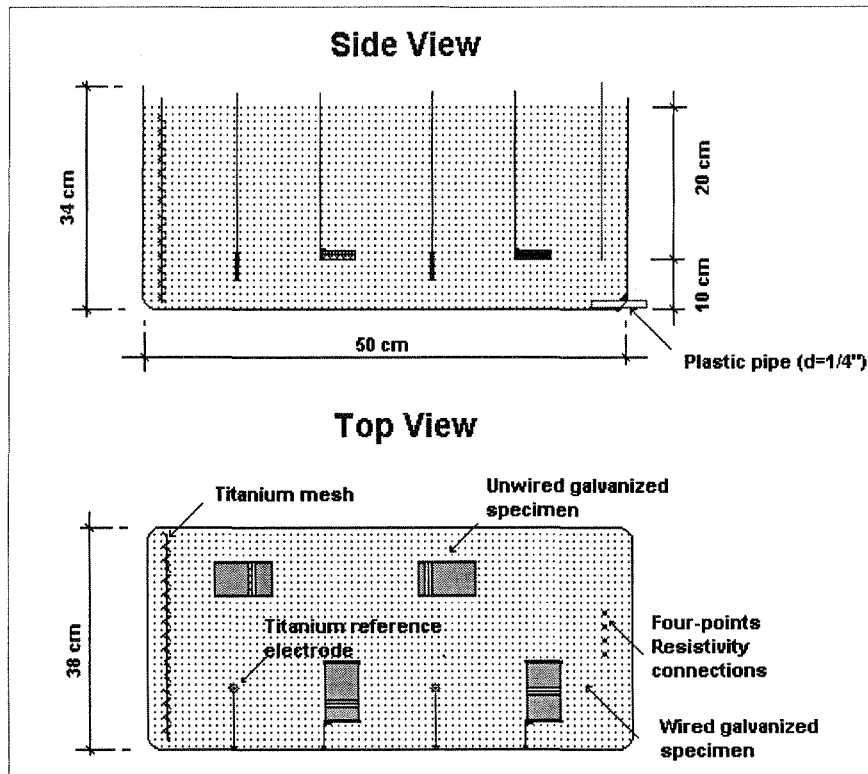


Figure 2-46. Text box layout for series 2.

2.3 Field and Laboratory Testing Methods

2.3.1 Soil Properties

Physical Properties of Soils. The physical properties considered were particle size distribution (soil grade), fineness modulus, unit weight and bulk specific gravity. Particle size distribution curves and fineness modulus were done according to ASTM C136 - 84a, the unit weight was measured as indicated in ASTM C138 - 81 and the bulk specific gravity was determined in accordance to ASTM C128 - 96. Single experiments were conducted for each site (field) and for each type of soil (soil boxes) due to limitations in the size of the soil samples.

Electrochemical Properties of Soils. Electrochemical properties measured in soil samples included pH, chloride content, sulfate content and resistivity. The pH was measured as specified in FM 5-550 (1993), chloride and sulfate analyses were done according to FM 5-552 (1994) and FM 5-553 (1994), respectively. The resistivity of the soil samples from the field and the boxes was measured using the California Soil Box described in ASTM G57 - 78 (1984) with a soil resistivity Nilsson[®] meter model 400 (operates with square-wave alternating current at 97 Hz). For each test, two samples were analyzed and the average computed.

2.3.2 Electrochemical Measurements

2.3.2.1 Corrosion Potentials

Corrosion potentials were measured using an MCM[®] voltmeter model LC-4 with an input resistance of 200 M Ω and a copper sulfate electrode (CSE).

Field Measurements. During the first year of the investigation, field measurements were taken by placing the CSE tip on the center of the concrete panel after wetting the selected spot with distilled water. Afterwards, measurements were performed by directly contacting the soil through a hole drilled in the concrete panel.

Laboratory Measurements. Laboratory measurements were taken by placing the CSE tip into the soil (approximately 1.3 cm below the surface), always in the same place (the side with fine backfill, Figure 2-47).

2.3.2.2 In Situ Resistivity Estimates

Field Measurements. Mutual resistance measurements conducted in the field were used to estimate in situ resistivity values. This field parameter differs from the resistivity measured in the laboratory since the laboratory measurements are performed with the soil completely saturated with water. Since the field measurements are taken at the prevailing moisture content, (which is typically less than saturation) the lab and field results may not agree.

Mutual resistances were measured between top and bottom reinforcing strips or grids except for Brickell Avenue where measurements were taken between left and right strips. A schematic representation is shown in Figure 2-48. Resistances were measured with the soil resistivity Nilsson meter set in a two point configuration.

In situ resistivities were estimated from mutual resistances by previous calculation of the cell constant factor. The calculation procedure is described in appendix 3 of Ref. [8].

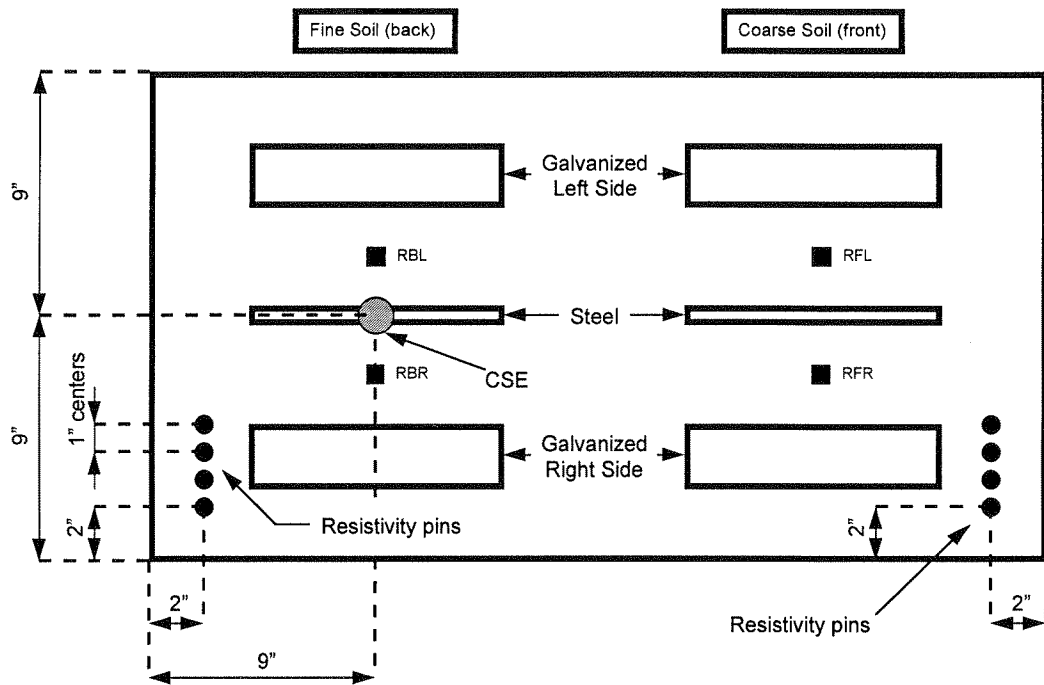


Figure 2-47. Plan view (not to scale) of the soil boxes showing positions of the CSE and the resistivity pins (4 Point Method). See Table 2-11 for nomenclature.

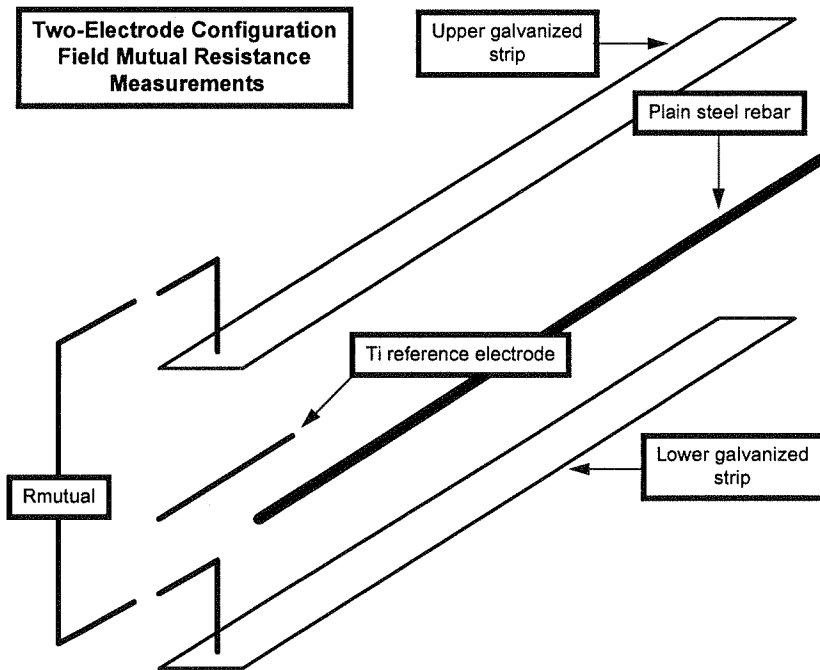


Figure 2-48. Two-Electrode configuration for field mutual resistance measurements.

Laboratory Measurements. In situ resistivity measurements were periodically performed in the soil boxes using the four point method (ASTM 136) with the Nilsson meter in the four point configuration. The resistivity was measured in both sides of each box (front, coarse fill, and back, fine fill) using four segments of solid copper wire (2.5 cm long) inserted into a Plexiglas sheet with a separation of 2.5 cm between each other (the sheet was used to keep the separation and depth of the tips constants). The tips were slightly buried into the soil. The measurements were always taken at the same place (Figure 2-47). The following expression (ASTM 136) was used to calculate the resistivity (ρ):

$$\rho = (2\pi * a * R)$$

where:

a = distance between copper segments (cm.).

R = resistance measured with the Nilsson meter (Ohm).

2.3.2.3 Polarization Resistance Measurements

Polarization resistance measurements (PR) were performed using a computer controlled Gamry[®] potentiostat, model CMS100, with IR compensation disabled. In all cases (field and laboratory specimens), a three-point array method was implemented.

Field Measurements. Field measurements were taken using the selected

specimen (galvanized reinforcement or plain steel rebar) as the working electrode (WE), the galvanized reinforcement as the counter electrode (CE) and the activated titanium electrode as the reference electrode (RE). The counter electrode was always the galvanized reinforcement to avoid current distribution effects. When using the upper galvanized strip as the WE, the lower strip was the CE (or the opposite) and when using the plain steel rebar as the WE, either the upper or the lower strips were the CE (Figure 2-49). All tests were conducted by shifting the potential (starting from the open circuit potential) in the cathodic direction, at a scan rate of 0.125 mV/s. The test was interrupted when the potential reached 10 mV below the starting potential.

The polarization resistance (RP_{PR}) was evaluated by taking the slope of the potential-current curve at 10 mV excursion and subtracting the IR ohmic drop. The ohmic drop was measured independently with the Nilsson soil resistivity meter using the same three-electrode configuration as for the PR test.

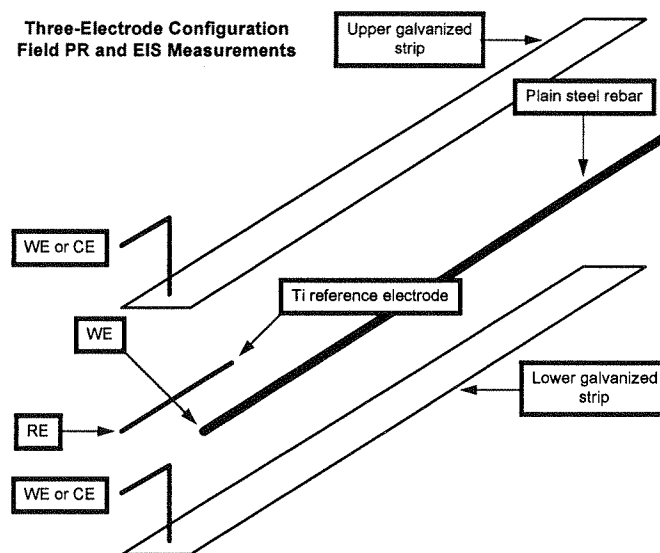


Figure 2-49. Three-Electrode configuration for field PR and EIS measurements.

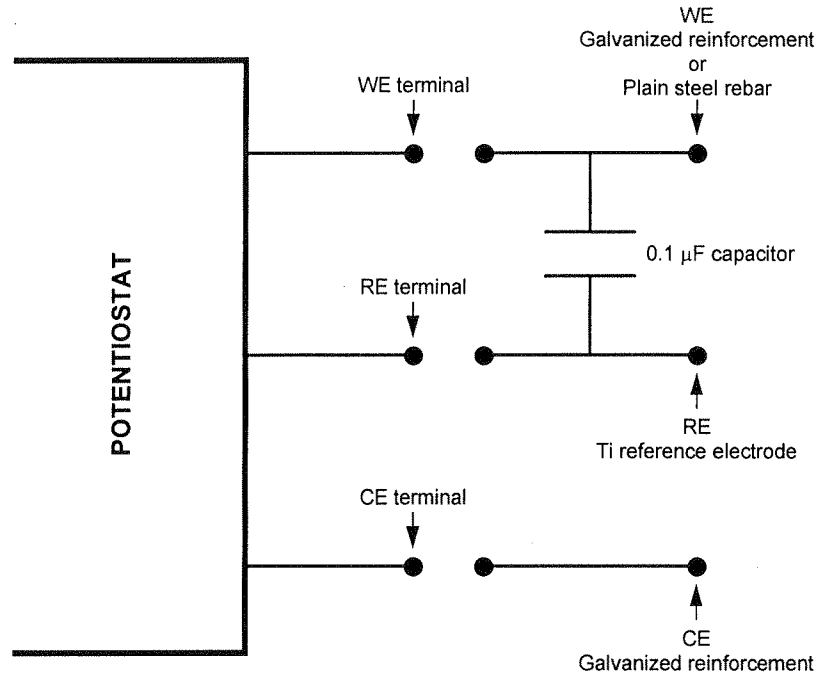


Figure 2-50. Schematic representation of the filter connection during field PR and EIS measurements.

In most field measurements, a 0.1 μF capacitor was used to filter AC noise coming from power sources. This capacitor was connected between the WE and the RE as shown in Figure 2-50.

Laboratory Measurements. Laboratory tests were conducted using the selected specimen as the WE (galvanized steel or plain steel), a galvanized specimen as the CE and an activated titanium electrode as the RE. Two types of measurements were performed (Figures 2-46, 2-51 and 2-52):

1. Coupled measurements: front and back specimens interconnected, behaving electrically as one specimen (this was the usual condition of the system).
2. Individual measurements: front and back specimens not interconnected and electrically behaving as separate specimens (but potentiostated at the normally connected potential value). The system was returned to its usual condition immediately after each test.

For series 2, only individual measurements were performed.

All tests were conducted by shifting the potential (starting from a reference potential) in the cathodic direction, at a scan rate of 0.125 mV/s. The test was interrupted when the potential reached 10 mV below the starting potential. When performing coupled measurements, the potentiostated potential was the open circuit potential. When conducting individual measurements, the potentiostated potential was the open circuit value measured before opening the electrical connection between front and back specimens.

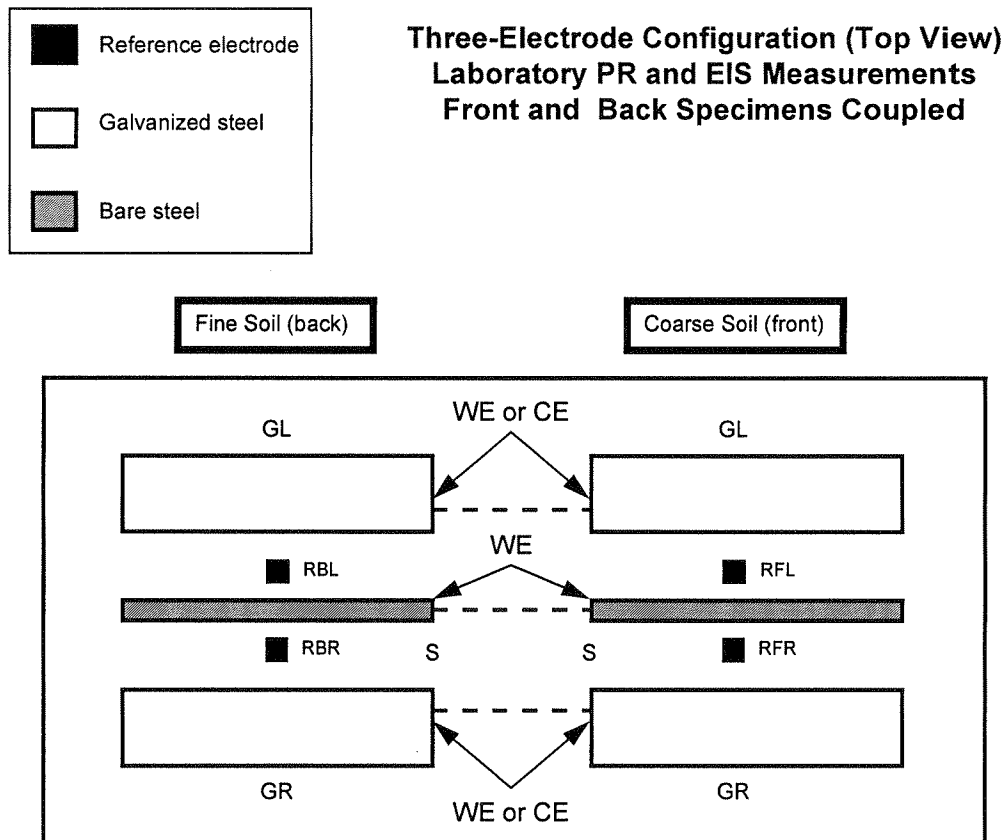


Figure 2-51. Top view of Three-Electrode configuration for lab PR measurements. Front and back specimens are coupled.

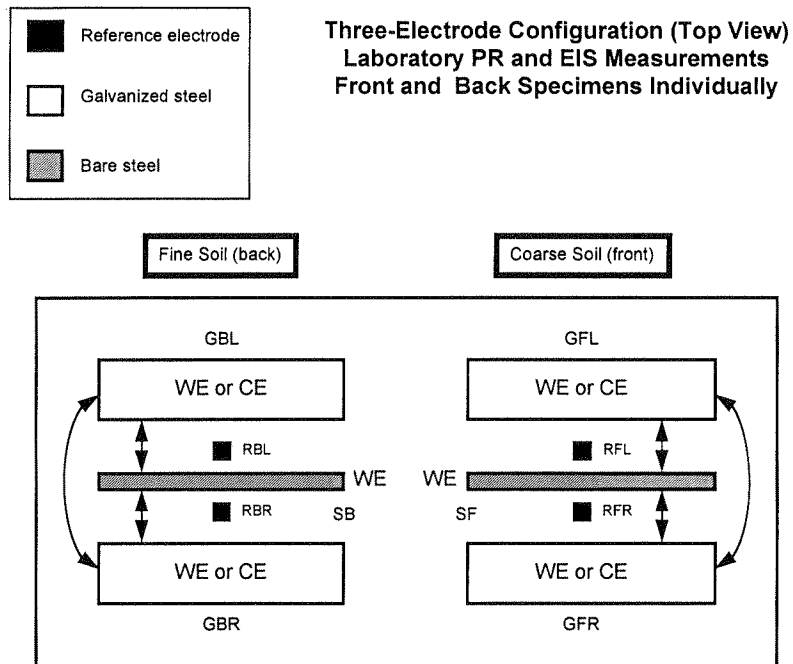


Figure 2-52. Top view of Three-Electrode configuration for lab PR measurements. Front and back specimens are uncoupled but potentiostated at the normally connected potential. Arrows indicate all possible WE-CE combinations.

2.3.2.4 Conversion to Apparent Corrosion Rates

Apparent corrosion rates were estimated from PR and EIS measurements by means of the Stearn-Geary equation and a B constant of 26 mV.

2.3.2.5 Macrocell Currents

Macrocell currents were measured in the soil boxes (laboratory) between front and back specimens. Measurements were taken with a Hewlett Packard® multimeter model HP 34401A set in the 10 mA range (input resistance of 5 Ω), allowing the system to stabilize for up to 10 minutes before recording the readings. The input resistance of the meter caused virtually no underestimation of the

macrocell current value, except in instances of relatively large currents (some of the specimens in contaminated soil).

2.3.2.6 Macrocell Resistances

Macrocell resistances were measured in the soil boxes between front and back specimens (previously uncoupled) using the Nilsson meter in the two point configuration.

2.3.3 Analysis of Metal Samples

The condition of the reinforcement in the Pensacola Street and Palm City structures was evaluated from the analysis of metal samples retrieved from both places. The assessment consisted in two parts: the analysis of the metal surface by SEM measurements and the characterization of the zinc coating by micro hardness measurements.

3. RESULTS

3.1 Field Investigation Results

Table 3-1 is a summary of all the field observations in the instrumented structures. All structures were visited at least 2 and as many as 6 times. Unless otherwise indicated, the properties indicated for the soil correspond to samples extracted during the first visit when the holes for the electrical connections were drilled. Electrochemical measurements of buried steel components were executed during the initial and subsequent visits.

3.1.1 Soil Properties

Grain Size Distribution. As indicated in Table 3-1, in all instances, the grain size distribution of the extracted soil samples fell within the limits stated in the FDOT Structures Design Manual (FDOTSDM) Section 528 [1].

Resistivity (California Method). With the exception of one structure, the soil resistivity values ranged from 5.2 k Ω -cm to 66 k Ω -cm, exceeding the minimum required value of 3 k Ω -cm stated in the FDOTSDM [1]. The exception was from samples of the bottom panels of both panel sets in Structure 4B (Palm City, NW wall), extracted at the time of the second visit. Those samples yielded values of 0.44 k Ω -cm and 0.45 k Ω -cm. Soil samples extracted from nearby holes at the same elevation in the previous visit yielded resistivity values in excess of 13 k Ω -cm.

Resistivity (In-situ Estimates). Table A-1 (Appendix) lists the mutual resistance measurements (as indicated in 2.3.2.2) obtained for all the structures investigated during the site visits, as well as the assumed cell constant values. The

table also lists the average values of the estimated in-situ resistivity which show order-of-magnitude agreement with the California-method measurements performed in the extracted soil samples.

Chloride and Sulfate Content. Sulfate content of all soil samples was below the 200 ppm limit specified in FDOTSDM [1]. Chloride content was also below the corresponding specified limit of 100 ppm, except for the same two samples that did not meet the resistivity specifications. Those samples had chloride levels of 372 ppm and 541 ppm.

pH. With the exception of the case of one marginal soil sample from Structure 8 (Veterans Expressway, pH=4.98), all samples had pH values within the range of 5 and 10 (see Table 3-1) as specified by the FDOTSDM [1].

3.1.2 Electrochemical Corrosion Assessment

Corrosion Potential. The corrosion potential of each type of buried component (galvanized and plain steel) varied over a wide range. However, the potentials for each type were distributed over two clearly differentiated populations (Figure 3-1). Table 3-2 shows the median and average potentials for the galvanized components, showing that the galvanized steel tended to be significantly more negative than the plain steel. The results for the novel 85-15% Zn-Al material are also shown for comparison in Table 3-2. No consistent trend of variation of the corrosion potential with time was identified for any of the materials examined.

Table 3-1. Summary of field observations for instrumented structures. (Continue on next two pages)

Structure #	Site and Location	Age ¹ (years)	Environment	Panel Set	Elevation ² (m)	Element ³	Internal Connection ⁴	Electrochemical Testing												Soil Properties					
								Potential vs CSE (mV)						Corrosion Rates (mpy) ⁵						Resistivity ^{6,7} (ohm-cm)	Chloride Content ⁷ (ppm)	Sulfate Content ^{7,8} (ppm)	pH	Moisture Content (%)	Grain Size ⁹
								Visit 1	Visit 2	Visit 3	Visit 4	Visit 5	Visit 6	Visit 1	Visit 2	Visit 3	Visit 4	Visit 5	Visit 6						
								2/9/95	9/26/95	1/26/96	3/18/96	8/29/97	11/26/97	2/9/95	9/26/95	1/26/96	3/18/96	8/29/97	11/26/97						
1A	Brickell Ave.; Southeast (SE) wall Miami	0	Costal	SE top	5.89	LG	GSC	-	-460	-	-	-	-	-	0.025	-	-	-	-	33750	5.25	9	9.15		x
						GSC	-	-475	-	-	-	-	-	0.025	-	-	-	-							
						F+BG	GSC	-	-455	-	-	-	-	0.029	-	-	-	-							
						FG	GSC	-	-	-	-	-	-	-	-	-	-	-							
						BG	GSC	-	-	-	-	-	-	-	-	-	-	-							
				SE bottom	2.44	LG	GSC	-504	-492	-470	-384	-656	-681	0.033	-	-	0.090	0.073	-						
						RG	GSC	-529	-577	-585	-483	-712	-710	0.027	0.046	-	0.084	0.035	-						
						F+BG	GSC	-	-517	-	-435	-696	-689	-	0.017	-	0.160	0.036	-						
						FG	GSC	-495	-	-546	-	-565	-	0.026	-	-	0.025	0.042	-						
						BG	GSC	-521	-	-546	-	-773	-	0.030	-	-	0.385	0.048	-						
1B	Brickell Ave.; Northwest (NW) wall; Miami	0	Costal	NW top	5.31	LG	GSC	-	-543	-	-	-	-	-	0.028	-	-	-	-	41750	12.65	30	9.09		x
						RG	GSC	-	-691	-	-	-	-	-	0.029	-	-	-	-						
						F+BG	GSC	-	-689	-	-	-	-	-	0.027	-	-	-	-						
						F+BS	SSR	-	-471	-	-	-	-	-	0.472	-	-	-	-						
						FG	GSC	-	-	-	-	-	-	-	-	-	-	-	-						
						BG	GSC	-	-	-	-	-	-	-	-	-	-	-	-						
						FS	SSR	-	-	-	-	-	-	-	-	-	-	-	-						
				BS	SSR	-	-	-	-	-	-	-	-	-	-	-	-								
				NW bottom	2.69	LG	GSC	-	-347	-554	-558	-716	-664	-	0.028	-	0.046	-	-						
						RG	GSC	-	-216	-368	-334	-445	-405	-	0.057	-	0.089	-	-						
						F+BG	GSC	-	-369	-	-555	-730	-686	-	0.026	-	0.047	0.020	-						
						F+BS	SSR	-	-440	-	-211	-367	-320	-	0.594	-	0.993	0.509	-						
						FG	GSC	-	-	-576	-	-753	-	-	-	-	-	0.017	-						
						BG	GSC	-	-	-585	-	-698	-	-	-	-	-	0.023	-						
FS	SSR	-	-			-247	-	-370	-	-	-	-	-	1.385	-										
BS	SSR	-	-	-252	-	-346	-	-	-	-	-	0.689	-												
2	Howard Frankland; Tampa	3	Costal	R7	12.14	top G	ZAC	11/15/95	12/13/95	2/8/96	4/22/96	7/2/96	8/20/97	11/15/95	12/13/95	2/8/96	4/22/96	7/2/96	11000	8.75	none	8.45		x	
						bot. G	ZAC	-747	-793	-786	-882	-841	-699	0.029	0.004	0.022	0.026								
				R11	12.14	top G	ZAC	-752	-797	-782	-837	-778	-644	0.025	-	0.020	0.021	-							-
						bot. G	ZAC	-	-749	-751	-929	-960	-637	-	0.027	0.042	0.020								
				11.38	top G	ZAC	-	-723	-734	-909	-882	-805	-	0.021	0.025	0.019	-	-							
					S	SSR	-	-471	-476	-585	-572	-363	-	0.019	0.204	0.085	-	-							
				R15	12.14	top G	ZAC	-766	-823	-853	-999	-	-670	0.028	-	0.027	0.017	-							-
						bot. G	ZAC	-772	-842	-837	-995	-	-645	0.023	-	0.023	0.018	-							-
				11.38	top G	ZAC	-	-661	-699	-784	-805	-599	-	-	0.012	0.021	-	-							
					bot. G	ZAC	-	-695	-707	-770	-786	-626	-	-	0.009	0.018	-	-							
				11.76	top G	ZAC	-	-414	-417	-450	-469	-346	-	-	0.030	0.107	-	-							
					S	SSR	-	-	-	-	-	-	-	-	-	-	-	-							

91

Table 3-1(con't). Summary of field observations for instrumented structures. (continue on next page)

Structure #	Site and Location	Age ¹ (years)	Environment	Panel Set	Elevation ² (m)	Element ³	Internal Connection ⁴	Electrochemical Testing												Soil Properties								
								Potential vs CSE (mV)						Corrosion Rates (mpy) ⁵						Resistivity ^{6,7} (ohm-cm)	Chloride Content ⁷ (ppm)	Sulfate Content ^{7,8} (ppm)	pH	Moisture Content (%)	Grain Size ⁹			
								Visit 1	Visit 2	Visit 3	Visit 4	Visit 5	Visit 6	Visit 1	Visit 2	Visit 3	Visit 4	Visit 5	Visit 6									
3	Pensacola St.; Tallahassee	17	Land	R17	22.63	top G	SSC	1/12/96	1/19/96	9/25/97					1/12/96	1/19/96	9/25/97					24500	4.5	25.2	7.52	x		
					22.02	bot. G	SSC	-371	-406	-553					0.036	0.119	0.056											
					22.02	S	SSR	-437	-488	-616					0.035	0.062	0.060											
					23.01	top G	SSC	-157	-252	-					0.227	0.407	-											
					22.40	bot. G	SSC	-	-367	-523					-	0.015	0.032											
					22.40	S	SSR	-	-398	-527					-	0.033	0.123											
				R23	2.21	top G	SSC	-	-348	-385					-	0.114	0.064							17000	6.85	25.8	8.72	
					22.10	bot. G	SSC	-	-320	-					-	0.012	-											
					22.10	S	SSR	-	-195	-					-	0.020	-											
					21.49	top G	SSC	-	-408	-					-	0.012	-											
					20.88	bot. G	SSC	-	-400	-					-	0.008	-											
					-	S	SSR	-	-	-					-	-	-											
4A	Palm City Northeast Wall Stuart	5	Costal	R1	1.98	top G	SSC	5/3/96	7/30/96	9/25/96	11/14/97				5/3/96	7/30/96	9/25/96	11/14/97				45000	1.35	none	9.09	x		
					1.30	bot. G	SSC	-620	-718	-579	-631				0.013	0.030	0.021	0.013										
					1.30	S	SSR	-660	-759	-633	-651				0.017	0.022	0.021	0.017										
					2.29	top G	SSC	-370	-409	-302	-386				0.287	0.121	0.103	0.059										
					1.68	bot. G	SSC	-601	-623	-	-585				0.029	0.041	-	0.025										
					1.68	S	SSR	-581	-609	-	-569				0.022	-	-	0.021										
				R5	3.51	top G	SSC	-648	-720	-	-				0.021	0.031	-	-										
					2.90	bot. G	SSC	-605	-638	-	-				0.015	0.031	-	-										
					2.90	S	SSR	-443	-372	-	-				0.092	0.093	-	-										
					3.72	top G	SSC	-	-641	-	-				0.019	0.045	-	-										
					3.11	bot. G	SSC	-	-648	-	-				0.021	0.015	-	-										
					-	S	SSR	-	-	-	-				-	-	-	-										
4B	Palm City Northwest Wall Stuart	5	Costal; Tidal saltwater	R3	0.41	top G	SSC	7/31/96	9/26/96	11/20/96	11/14/97				7/31/96	9/26/96	11/20/96	11/14/97				17000	9	none	10.13	x		
					-0.08	bot. G	SSC	-673	-812	-830	-838				-	0.039	0.010	0.026										
					0.02	S	SSR	-	-750	-874	-733				-	0.050	0.096	0.069										
					0.30	top G	SSC	-	-647	-740	-631				-	0.935	0.807	2.363										
					-0.18	bot. G	GSC	-711	-776	-814	-780				-	0.025	0.019	0.023										
					0.22	S	SSR	-	-942	-865	-749				-	0.108	-	0.084										
				R5	0.30	top G	SSC	-516	-442	-539	-464				-	0.029	0.677	0.233										
					-	bot. G	GSC	-	-	-	-				-	-	-	-										
					-	S	SSR	-	-	-	-				-	-	-	-										
					7800	6	none	13.02							7800	6	none	13.02										
					16000, [440]	4.5, [541]	none, [141]	6.17							16000, [440]	4.5, [541]	none, [141]	6.17										
					-	-	-	-							-	-	-	-										
5	Port Saint Lucie Blvd.; Port Saint Lucie	4	Costal; Tidal saltwater	R3	2.36	top G	GSC	11/19/96	11/14/97						11/19/96	11/14/97					12000	12	30	8.38	8.34	x		
					1.75	bot. G	GSC	-799	-782						0.067	0.076												
					1.75	S	SSR	-782	-781						0.095	0.074												
					2.39	top G	GSC	-631	-553						2.450	0.325												
					2.24	bot. G	GSC	-785	-765						0.110	0.049												
					2.24	S	SSR	-801	-754						0.160	0.086												
				R7	2.24	top G	GSC	-735	-621						2.000	0.087												
					-	bot. G	GSC	-	-						-	-												
					-	S	SSR	-	-						-	-												
					5700	15	none	8.46						5700	15	none	8.46											
					5200	27	none	15.82						5200	27	none	15.82											
					-	-	-	-						-	-	-	-											
6	State Rd. 200; Ocala	13	Land	R6	25.32	top G	GSC	1/15/97	4/9/97	9/26/97					1/15/97	4/9/97	9/26/97				21000	9	3	7.55	4.89	x		
					24.56	bot. G	GSC	-628	-663	-606					0.008	0.009	0.010											
					25.05	S	SSR	-638	-577	-578					0.011	0.012	0.014											
					25.26	top G	GSC	-497	-340	-293					0.387	0.177	0.131											
					24.48	bot. G	GSC	-580	-527	-591					0.022	0.025	-											
					24.99	S	SSR	-565	-522	-593					0.033	0.033	-											
				R5	25.26	top G	GSC	-558	-251	-243					0.180	0.170	-											
					24.48	bot. G	GSC	-	-	-					-	-	-											
					24.99	S	SSR	-	-	-					-	-	-											
					60000	7.5	3	7.12						60000	7.5	3	7.12											
					66000	9	3	7.65						66000	9	3	7.65											
					-	-	-	-						-	-	-	-											

Table 3-1(con't). Summary of field observations for instrumented structures.

Structure #	Site and Location	Age ¹ (years)	Environment	Panel Set	Elevation ² (m)	Element ³	Internal Connection ⁴	Electrochemical Testing												Soil Properties								
								Potential vs CSE (mV)						Corrosion Rates (mpy) ⁵						Resistivity ^{6,7} (ohm-cm)	Chloride Content ⁷ (ppm)	Sulfate Content ^{7,8} (ppm)	pH	Moisture Content (%)	Grain Size ⁹			
								Visit 1	Visit 2	Visit 3	Visit 4	Visit 5	Visit 6	Visit 1	Visit 2	Visit 3	Visit 4	Visit 5	Visit 6									
7	Acosta Bridge, Jacksonville	7	Coastal	R9	2.09	top G	GSC	4/8/97	9/25/97						4/8/97	9/25/97					28000	4.5	none	8.2	1.63	x		
					1.34	bot. G	GSC	-505	-427						0.012	0.023							29000	5.25	none		8.4	-
					1.98	Zn-Al	Zn-Al	-496	-420						0.012	0.026							-	-	-		-	-
					1.48	S	SSR	-895	-649						0.049	0.022							-	-	-		-	-
				R21	2.10	top G	GSC	-470	-403						0.414	-							37000	4.5	none		8.4	2.27
					1.35	bot. G	GSC	-610	-561						0.025	0.027							24000	4.5	3		8.64	3.83
					1.85	S	SSR	-523	-512						0.026	0.036							-	-	-		-	-
								-432	-233						0.238	0.107							-	-	-		-	-
8	Veteran's Expressway, Tampa	2	Land	R16	11.18	top G	GSC	6/4/97	1/16/98						6/4/97	1/16/98					23000	3	7	5.05	7.2	x		
					10.43	bot. G	GSC	-484	-512						0.054	0.039							21000	2.5	none		6.23	8.47
					10.55	Zn-Al	Zn-Al	-466	-480						0.058	0.040							-	-	-		-	-
					10.95	S	SSR	-840	-290						0.085	0.028							-	-	-		-	-
				R23	10.89	top G	GSC	-458	-823						0.271	0.218							19000	1.5	11		4.98	8.69
					10.14	bot. G	GSC	-578	-580						0.051	0.032							22000	2	11		5.69	7.55
					10.36	Zn-Al	Zn-Al	-572	-566						0.052	0.038							-	-	-		-	-
								-785	-869						0.166	0.030							-	-	-		-	-

93

1. Age of the structure at the time of the first visit.
2. The elevations are relative to sea level. The calculations were estimated from shop drawings.
3. L=left; R=right; F=front; B=back; bot.=bottom; S=stainless steel; G=galvanized steel, Zn-Al=85-15% Zn-Al alloy.
4. GSC=galvanized steel clamp; SSR=stainless steel rod; SSC=stainless steel clamp, ZAC=Zn alloy clamp, Zn-Al=85-15% Zn-Al strip.
5. Corrosion rates for the steel rods are an average of two measurements, using the top and bottom galvanized strips as the counter.
6. Resistivity of the soil was measured after soil was fully saturated according to ASTM G57-78.
7. The resistivity and the chloride and sulfate contents were measured twice for the Palm City NW wall. The 1st value (not in brackets) is from the first visit and the 2nd value (in brackets) is from the 2nd visit.
8. If the sulfate content was below the detection limit "none" was entered here.
9. An "x" denotes the soil meets FDOT specified values for grain size standards.

Table 3-2. Corrosion rates and potentials for the different types of buried material.

	Corrosion Rates (mpy)			Potential vs. CSE (mV)		
	Galvanized	Plain	Zn-Al*	Galvanized	Plain	Zn-Al*
Average	0.041	0.46	0.080	-630	-439	-792
Median	0.027	0.23	0.067	-631	-441	-813

* short term experiment.

Apparent Corrosion Rate. Nominal corrosion rates showed significant scatter within each type of buried material, but there was clear differentiation between the behavior of the galvanized and plain steel components (Figure 3-2). Table 3-2 shows the corresponding median and average values. No consistent trend of variation of the nominal corrosion rate of the galvanized steel with age of the structure was identified for any of the materials examined (Figure 3-3).

Macrocell Currents. Macrocell current measurements between the front and back galvanized elements are available as this writing only for Brickell Avenue SE-Bottom Panel, for the dates, Aug 29, 1997 (0.80 mA) and Nov 26, 1997 (0.90 mA). In both instances the cathode was the Front element, closest to the wall. The corresponding average current densities, obtained by dividing by the surface area of either element were $0.073 \mu\text{A}/\text{cm}^2$ and $0.082 \mu\text{A}/\text{cm}^2$ respectively. Those values correspond to 0.042 mpy and 0.047 mpy respectively.

3.1.3 Correlation between Measurements

Soil Properties. Figure 3-4 shows a composite diagram of the chloride

content versus the soil resistivity measured in every soil sample; Figure 3-5 includes the sulfate content. The results are as expected, confirming that the soil resistivity is inversely proportional to the extent of ionic contamination. Figure 3-6 shows the chloride vs. sulfate content. The two data with the lowest resistivities in Figures 3-4 to 3-7 correspond to the highly contaminated samples from structure 4B. Figure 3-6 shows that these two samples had one order of magnitude less sulfate than chloride, confirming the expectation that the contamination was due to the tidal mixing of seawater with otherwise fresh Saint Lucie River water at that location. The contamination appears to have been sporadic as it was not observed in the previous visit. Moreover, the water in the pores of the soil immediately inside the wall (where the samples were obtained) appeared to change relatively quickly with variations in the tidal water flooding the wall at that point.

Figure 3-7 shows the chloride content vs. elevation of the test point, for all the structures examined. There was no clear relationship between those variables other than the high values observed at sea level in Structure 4B.

Corrosion Behavior. Figure 3-8 shows the corrosion potential as a function of apparent corrosion rate in the manner of an E-log i plot, incorporating the entire data set for all structures. Within each material type there is no clear correlation between both variables, indicating that the corrosion potential is not a good indicator of corrosion rate.

Figures 3-9 to 3-12 show the nominal corrosion rate as a function of the soil properties (resistivity, chloride content, sulfate content and pH) for the entire data set of all structures. The data are grouped per panel set. Whenever several

measurements of a given soil property existed for a panel set, the value representing the most aggressive condition was assigned for display in the abscissa. There was no recognizable correlation between apparent corrosion rate and soil resistivity or soil pH for either the galvanized or plain steel components. The apparent corrosion rate of the galvanized components showed also no evident dependence on soil chloride content or sulfate content. However, the apparent corrosion rate of the plain steel tended to show higher values in the soils from structure 4B, which had the highest episodic chloride and sulfate contents.

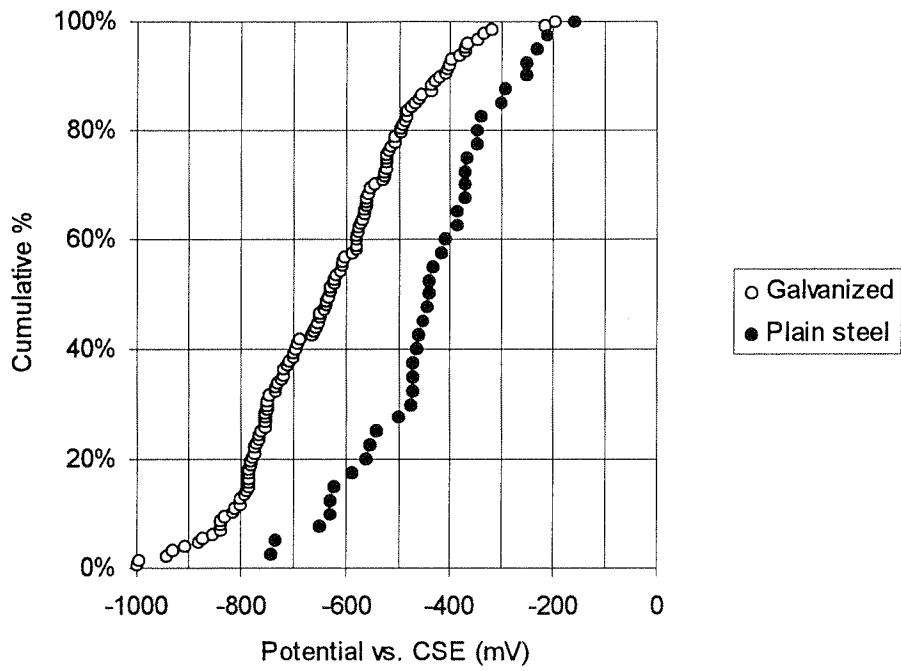


Figure 3-1. Cumulative percentage of the corrosion potentials in MSE structures.

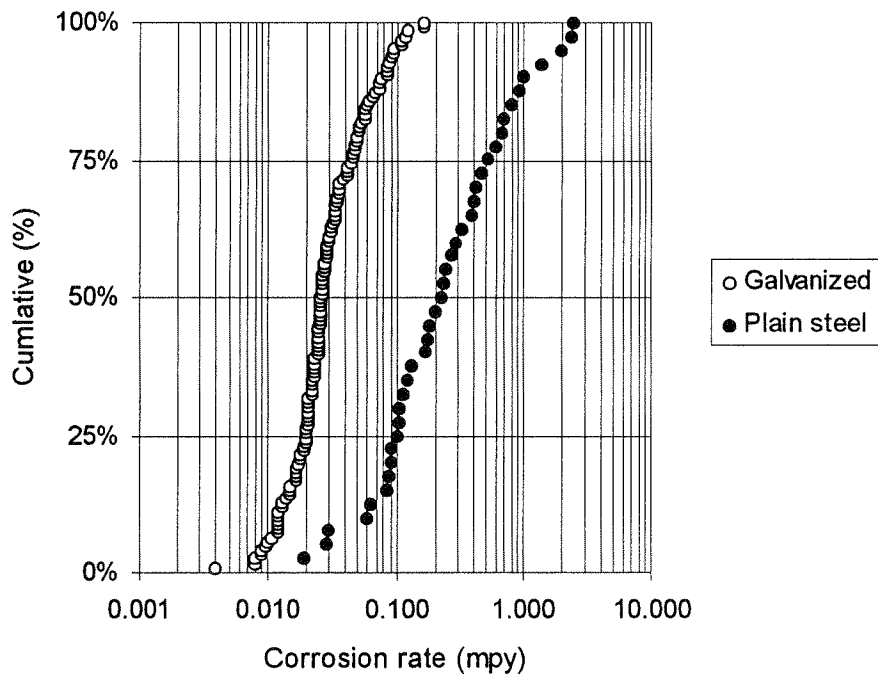


Figure 3-2. Cumulative percentage of corrosion rates in MSE structures.

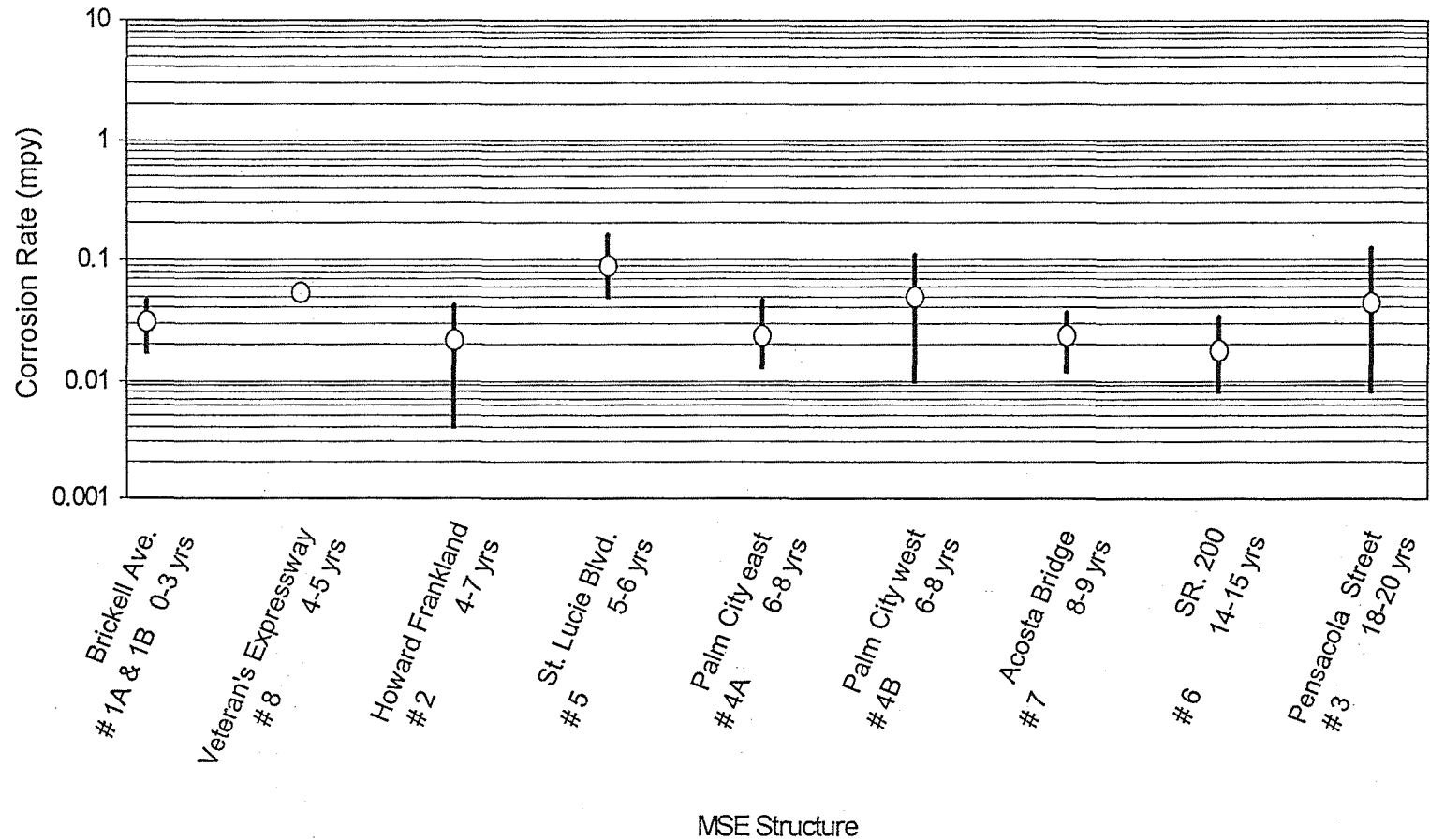


Figure 3-3. Average of galvanized Apparent Corrosion Rates (ACR) of all structures tested displayed in order of increasing structure age at the time of testing. The bars indicated the range of values obtained.

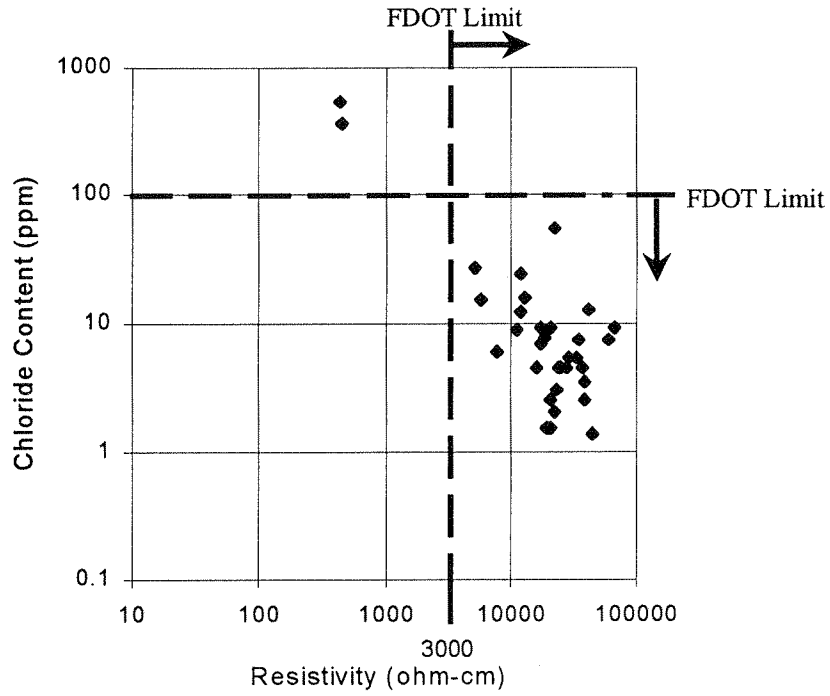


Figure 3-4. Chloride content vs. the resistivity of backfill in MSE structures.

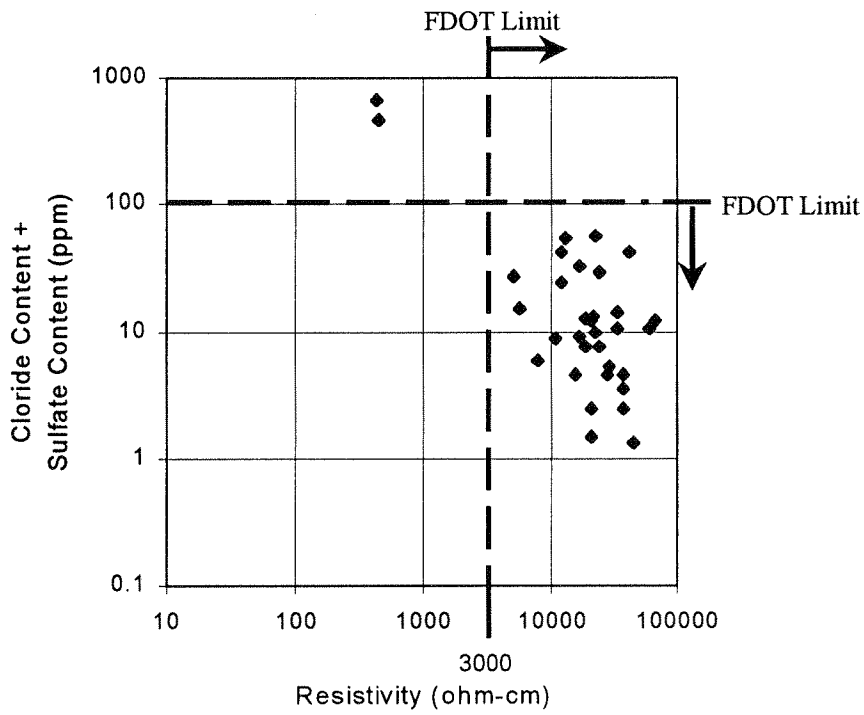


Figure 3-5. The combined content of chloride and sulfate vs. the resistivity of backfill in MSE structures.

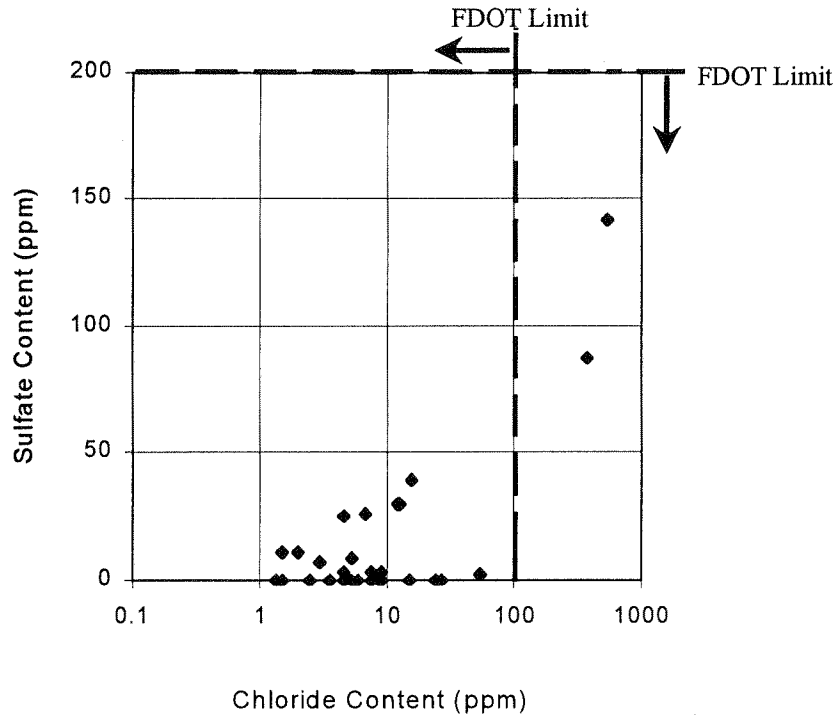


Figure 3-6. Chloride content vs. the sulfate content of backfill in MSE structures.

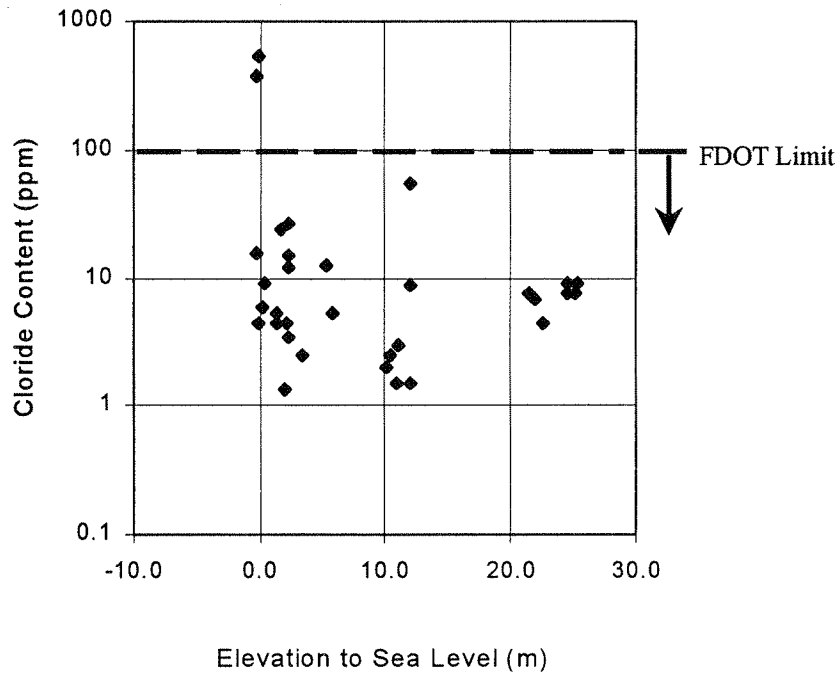


Figure 3-7. Chloride content of the soil extracted vs. the elevation of the corresponding MSE structures.

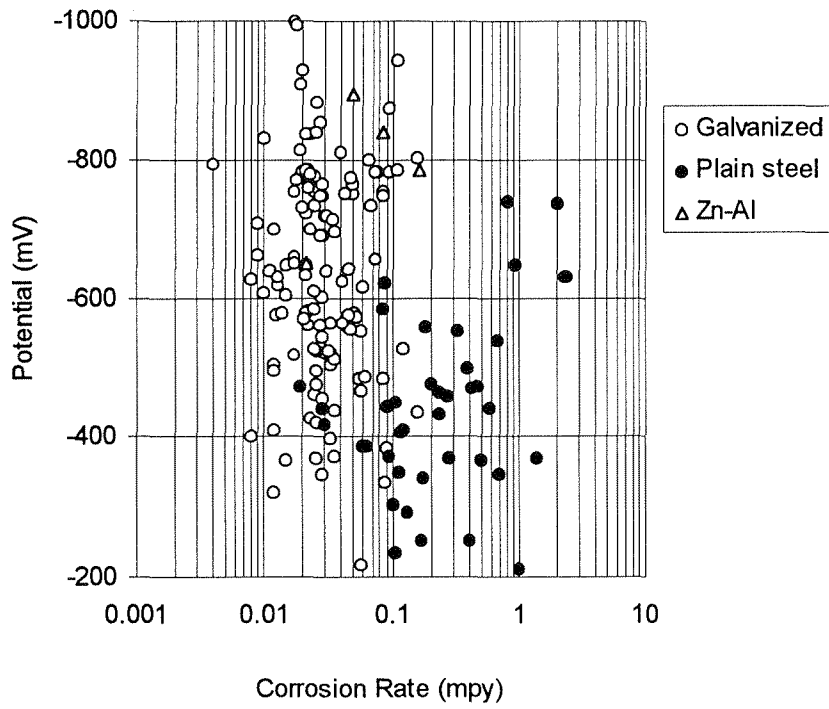


Figure 3-8. Corrosion potentials vs. the corrosion rates in MSE structures.

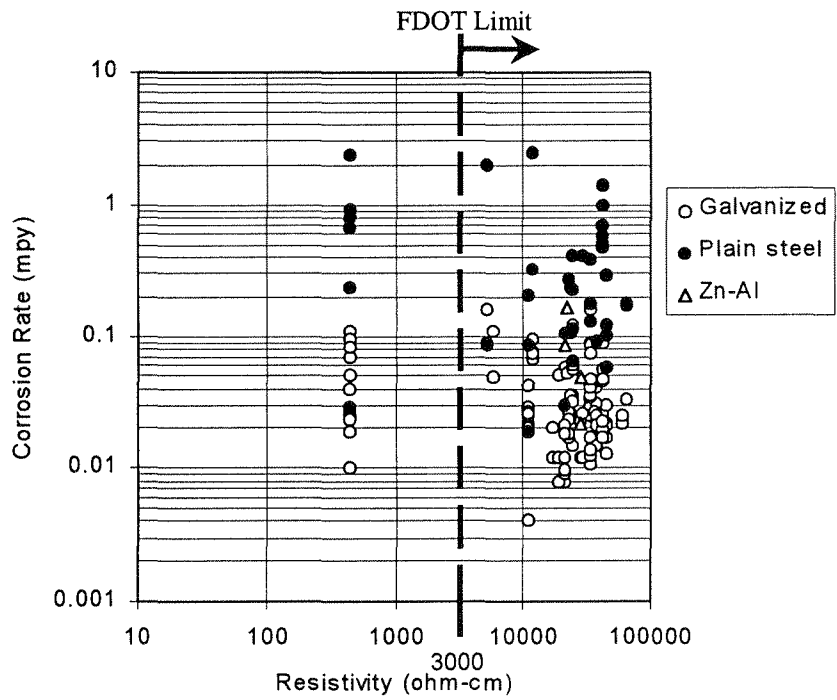


Figure 3-9. Corrosion rates vs. resistivity of the backfill at the MSE structures.

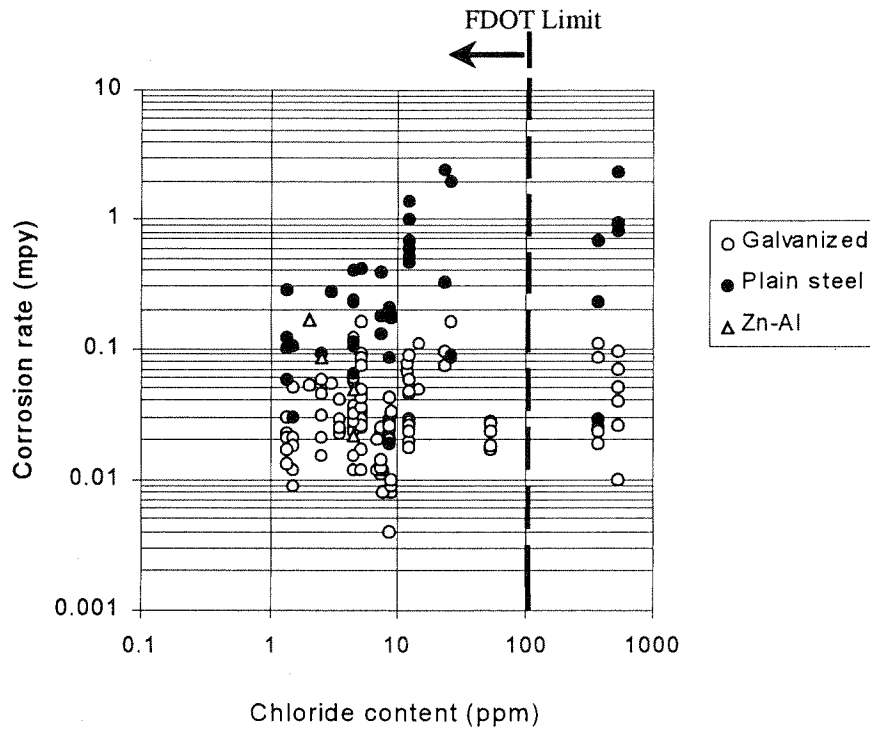


Figure 3-10. Corrosion rates vs. the chloride content of backfill in MSE structures.

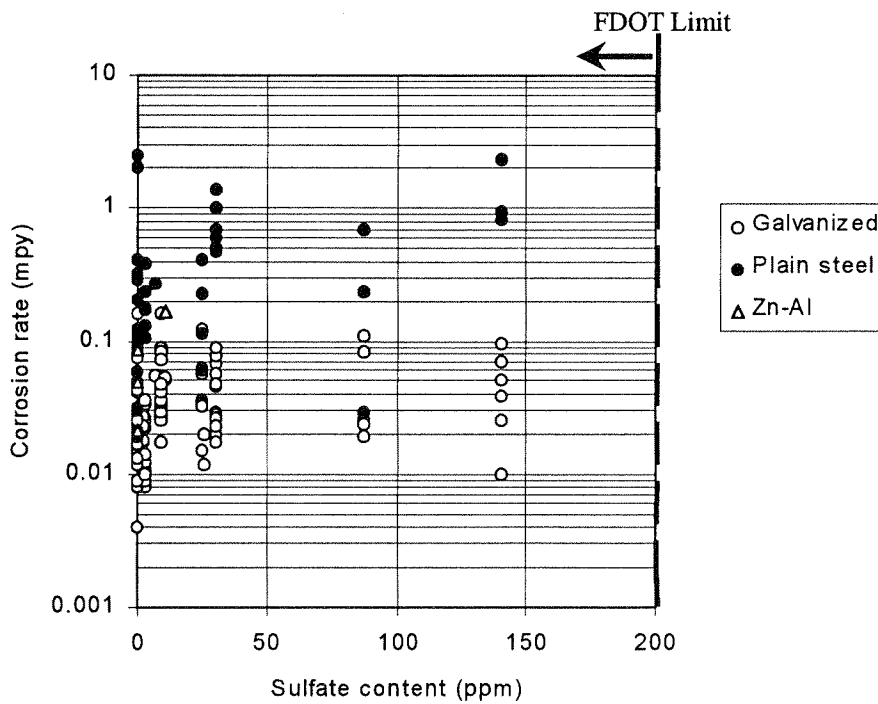


Figure 3-11. Corrosion rates vs. the sulfate content of backfill in MSE structures.

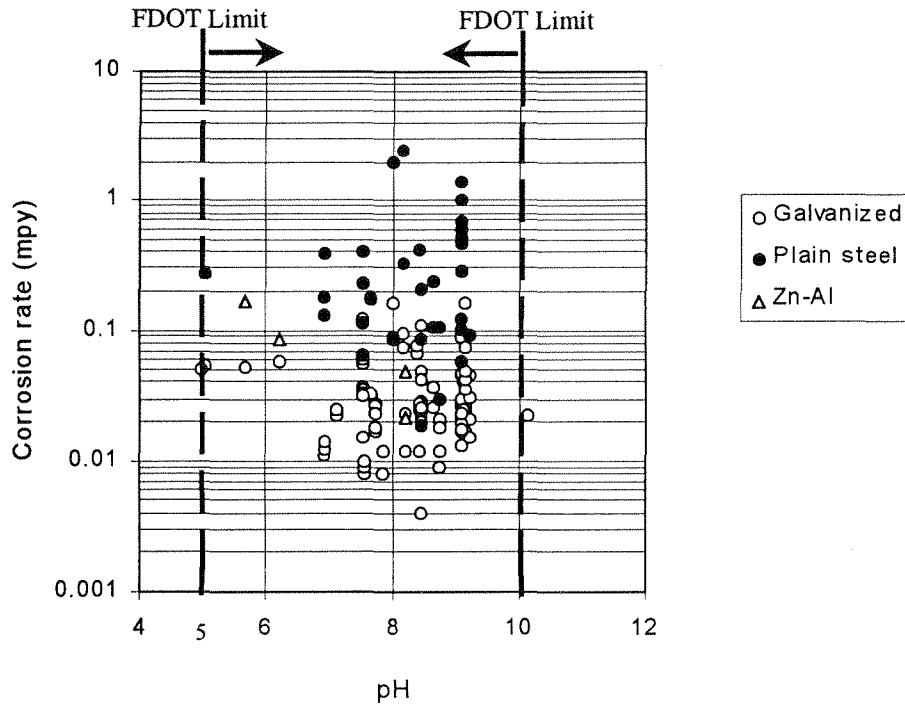


Figure 3-12. Corrosion rates vs. the pH level of backfill in MSE structures.

3.1.4 Direct Assessment

The general condition of the reinforcement in field structures that were already in service was assessed through an in situ visual inspection of the reinforcement and laboratory analyses of metal samples that were removed from the structures.

3.1.4.1 In Situ Visual Inspection

It was possible to inspect only the reinforcement that was immediately adjacent to the wall (approximately 15 cm) and that was exposed while making the contacts. This zone is hardly representative of all the metal, but it may give a rough estimate of the general condition of the reinforcement in the structure.

A summary of the in situ visual inspection is given in Table 3-2. In this table, the coating condition refers to the visual aspect of the coating. A "very good" condition implies a coating intact with no iron rust observed; a "good" condition indicates only small areas (10 % of the entire exposed surface or less) of bare steel (no zinc coating visible). A "poor" condition (observed only in two cases) denotes large areas (50 % of the entire exposed surface or more) of bare steel or iron rust. The third column, "red rust" indicates if red rust was observed and if rusted areas are "small" (10 % of the exposed area or less) or "large" (50 % or more, observed only in two cases). Finally, the apparent structural condition column refers to the physical appearance of the reinforcement, meaning possible mechanical distortions or other signs of severe strain.

3.1.4.2 Laboratory Evaluation of Hardware

Galvanized hardware (nuts, bolts and washers) was extracted from all of the structures except those in Brickell Ave. (#1a and 1b), Howard Frankland (#2),

Table 3-2. Summary of reinforcement condition from visual inspection.

Structure Number	Site	Panel Set ¹	Coating Condition ²	Red Rust ³	Apparent Structural Condition ²
2	Howard Frankland Bridge, Tampa	7	G	S	VG
		11	G	S	VG
		15	G	S	VG
		17	G	S	VG
3	Pensacola Street Bridge, Tallahassee	17	G	S	VG
		23	P	L	VG
		44	G	S	VG
		62	P	L	VP**
4A	Palm City Bridge Northeast Wall, Stuart	1	VG	NP	VG
		5	VG	NP	VG
		14	VG	NP	VG
		28	VG	NP	VG
4B	Palm City Bridge Northwest Wall, Stuart	3 (C)	VG	NP	VG
		3 (AA)	VG*	NP	VG
5	Port Saint Lucie Blvd., Port Saint Lucie	3	VG	NP	VG
		7	VG	NP	VG
6	State Road 200, Ocala	6 (A)	VG	NP	VG
		6 (C)	VG	NP	VG
		25 (F)	G	S	VG
7	Acosta Bridge, Jacksonville	21(E)	VG	NP	VG
8	Veteran's Expressway, Tampa	23 (A)	G	S	VG

1. Sampling hole designations are indicated in parenthesis for structures 4B, 6, 7 and 8.

2. VG = very good, G = good, P = poor, VP = very poor.

3. NP = not present, S = small area, L = large area

* The strip had a dull black appearance.

** The reinforcement corresponding to panel 62, Pensacola Street, was severely damaged due to previous collapse of the wall in that area.

Veteran's Expressway (#8), and Port Saint Lucie Blvd. (#5). An inventory of the extracted samples is given in Table A-2 (Appendix). All of the hardware was visually inspected in the lab to assess the condition of the galvanized layer. Furthermore, hardware from Pensacola St. and Palm City Northeast was evaluated using two complementary methods: metal surface analysis by scanning electron microscopy (SEM) and metallographic analysis of the cross section to observe the condition of the coating. The surface analysis was performed to identify corrosion products while the metallography assessed the condition of the remaining galvanized coating.

Laboratory Visual Inspection. All of the hardware was visually inspected to determine the fraction of the sample surface that was comprised of grey (dark and light) areas, black areas, white scale and red rust. The amount (%) of the surface area comprising each appearance is shown in Figure 3-13 where the age of the structure is also indicated. The presence of white scale indicates that the eta layer of the coating has been penetrated, but a good portion of the coating still exists. A black area is not necessarily bare metal, but the surface analysis (by SEM) confirmed that 15-25% of the weight of the black areas was iron, which could represent the gamma phase of the coating, indicating that only a minimal amount of the zinc coating still exists.

Figures 3-14 and 3-15 show the relationship between the fractions of red rust and grey-white appearance and the age of the structure. In general, as the structure ages, the red rust fraction increases while the grey and white scale fraction

decreases. The exception to the latter trend is predominately black appearance in structure 4B (Palm City Northwest wall) which is known to have episodic chloride contamination. However, preliminary examination revealed that a substantial fraction of the galvanized layer thickness remained on the hardware extracted from that location [19].

Microscopic Analysis. This analysis was performed on four samples: a nut (standard A 325 bolt, 3/4 in. ϕ) and a washer from panel 23 of structure 3 (Pensacola Street) and one washer (for a standard 1/2 ϕ , A325 bolt) from both panels 1 and 28 of structure 4A (Palm City, NE wall). A detailed description of the findings is given in Ref. [9].

The washer and nut from structure 3 showed white spots and red rust in some portions of their surface which were in direct contact with the soil. The rest of the surface had an undisturbed galvanized metal appearance. EDAX analysis of the rust colored spots showed a greater percentage of Fe than Zn, indicating that corrosion had penetrated through the galvanized layer. The white spots showed a greater amount of Zn than Fe, suggesting that penetration was beyond the eta layer but still not through to the base metal. Metallographic analysis confirmed these findings (Table 3-3).

Table 3-3. Approximate values of coating thickness from metallographic samples.

Structure	Sample	Fraction of the Total Section Still Coated [%]	Approximate Bottom Layer Thickness [μm]	Approximate Top Layer Thickness [μm]
Pensacola Street, Tallahassee	Washer	> 70	20 - 28	0 - 56
	Nut	< 50	15 - 33	0 - 46
Palm City Bridge, Northeast Wall, Stuart	Washer	> 90	20 - 64	18 - 69

Note: the third column refers to the fraction of the cross section perimeter where either the bottom galvanized layer (zeta + delta + gamma) alone or both the bottom and the top eta layers were present.

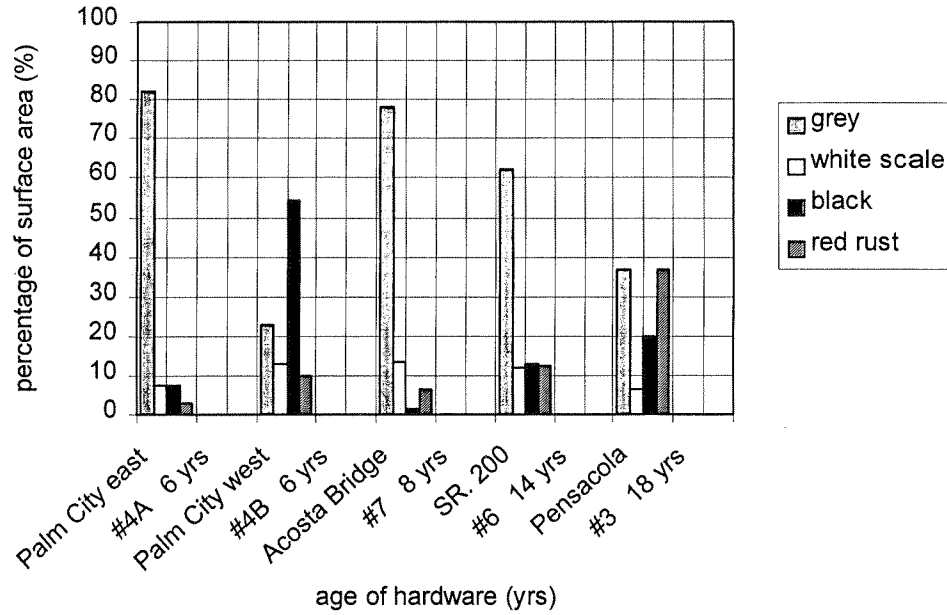


Figure 3-13. Amount of affected surface area of hardware as a function of structure age.

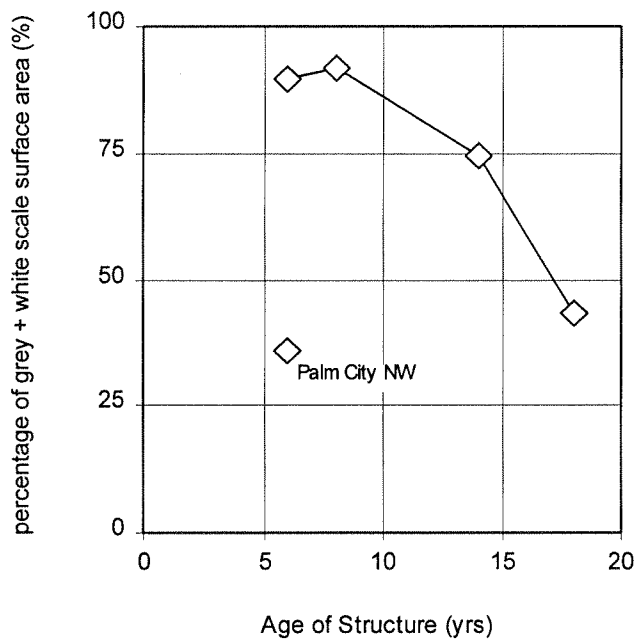


Figure 3-14. Red rust area percentage as a function of the age of the structure.

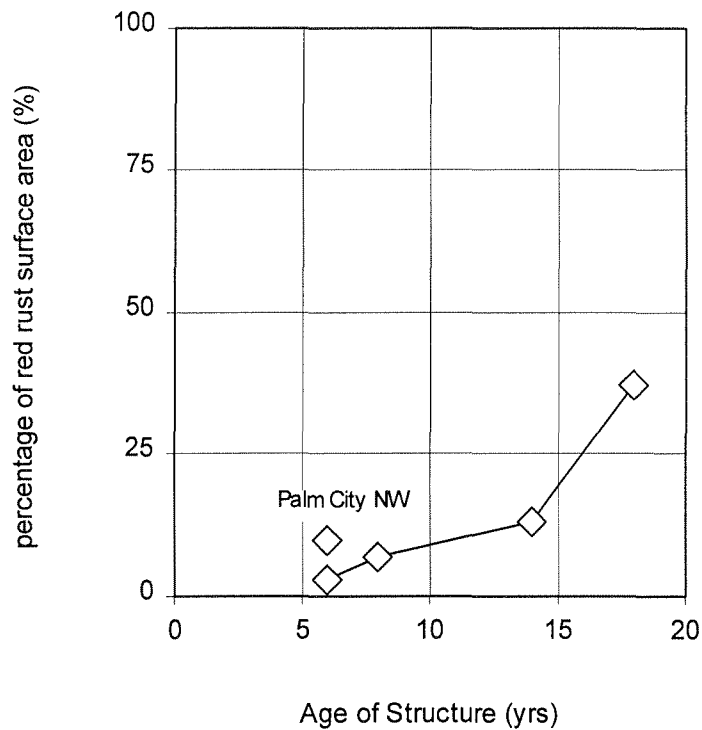


Figure 3-15. Percentage of grey and white scale as a function of the age of the hardware.

3.2 Laboratory Results - Series 1

3.2.1 Soil Physical Properties

The same physical parameters as those evaluated on field samples were measured in the soil boxes: particle size distribution curves, fineness modulus, unit weight and bulk specific gravity.

Particle Size Distribution and Fineness Modulus. Results are listed in Table 3-4 and are shown in Figure 3-16, where FDOT grading limits [1] are included for comparison purposes.

Unit Weight, Bulk Specific Gravity and Porosity. Results are summarized in Table 3-5. Porosity estimations also displayed in Figure 3-17.

Table 3-4. Grading (cumulative percent passing) and fineness modulus of soil samples from soil boxes.

Sieve Size [mm]	Fine Soil	Coarse Soil
0.075	1.4	1.0
0.15	9.6	6.4
0.30	75.4	31.2
0.45	98.1	36.7
1.18	99.8	37.4
2.36	100.0	37.8
4.75	100.0	49.9
9.50	100.0	85.4
19.05	100.0	100.0
88.90	100.0	100.0
Fineness Modulus	2.2	5.1

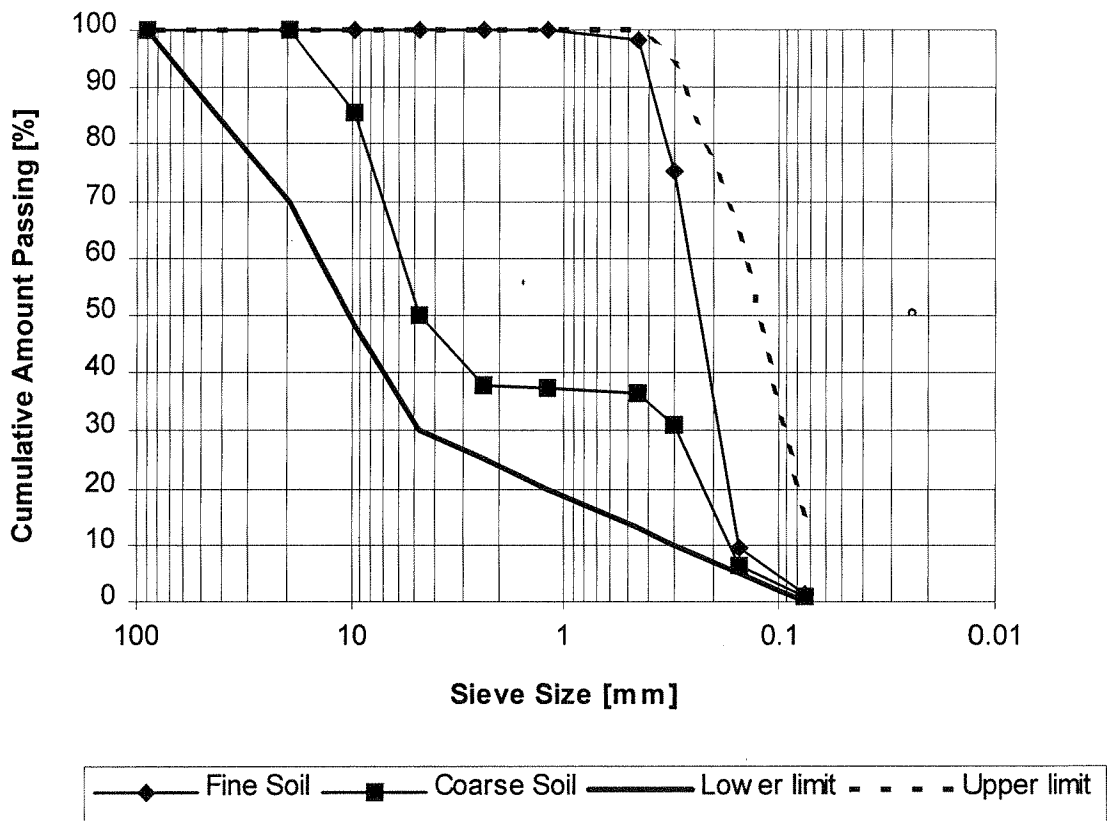


Figure 3-16. Grading curves (cumulative percent passing) of soil samples from soil boxes. The lower and upper limits indicate the coarsest and finest gradations, respectively, allowed by FDOT specifications [1].

Table 3-5. Unit weight, bulk specific gravity and porosity (percent of voids) of soil samples from soil boxes.

Parameter	Fine Soil	Coarse Soil
U. Weight [lb./ft ³]	89.15	103.78
B. S. Gravity	2.53	2.70
Porosity [%]	43.62	38.5

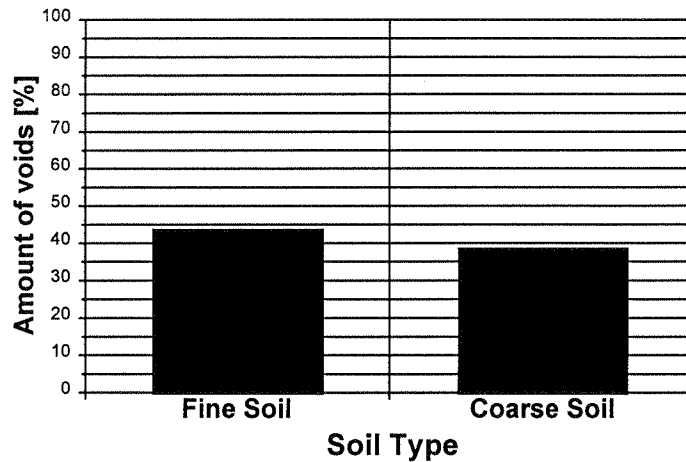


Figure 3-17. Porosity of soil samples from soil boxes.

3.2.2. Soil Electrochemical Properties

Both soil types were analyzed to determine pH, concentrations of chlorides and sulfates and resistivity (California Test Method of ASTM G57-78). Results are shown in Table 3-6.

Table 3-6. Electrochemical properties of soil samples from soil boxes.

Soil Type	pH	Cl ⁻ [ppm]	SO ₄ ²⁻ [ppm]	ρ [Ω.cm]
Fine	7.53	1.00	0.00	93000
Coarse	9.40	1.50	0.00	55000

3.2.3 Electrochemical Measurements

Electrochemical measurements including corrosion potential, resistivity, macrocell current and polarization resistance tests were performed in all boxes during a four-month period. Day 1 (first set of measurements) was 02/02/96: 1 day after the water saturation of the soil boxes was performed and 15 days after the soil boxes were assembled. A schedule indicating the dates of the different events (boxes assembly, saturation, contamination and measurements) is shown in Figure 3-18.

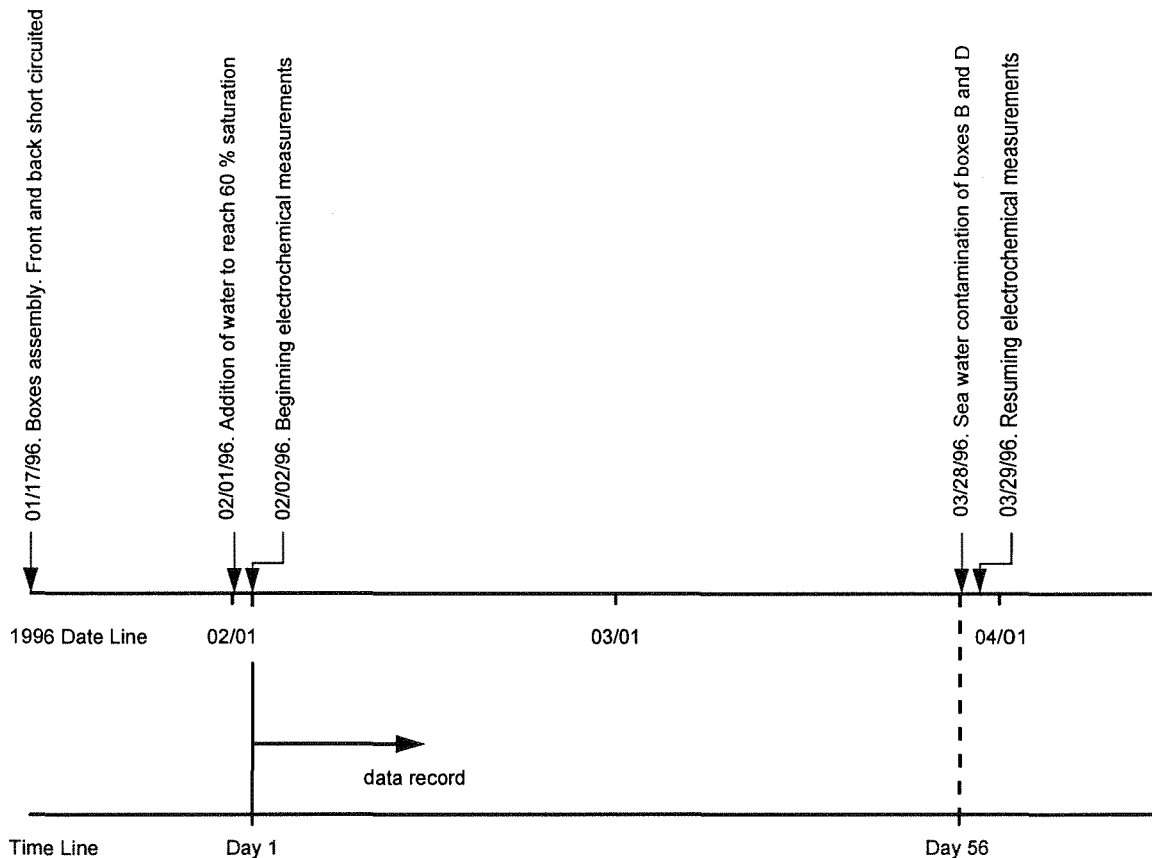


Figure 3-18. Schedule of Soil Boxes. The dates corresponding to the assembly, water saturation, beginning of electrochemical measurements and sea water contamination are indicated.

Corrosion Potentials. Corrosion potentials versus copper sulfate electrode (CSE) as a function of time are plotted in Figures 3-19 and 3-20. The front and back samples were already coupled and therefore, the nomenclature is the following: for galvanized specimens, the first letter indicates the type (galvanized), the second denotes the side (left or right) and the third indicates the box (A, B, C or D); for steel specimens, the first letter indicates the type (steel) and the second refers to the box (A, B, C or D).

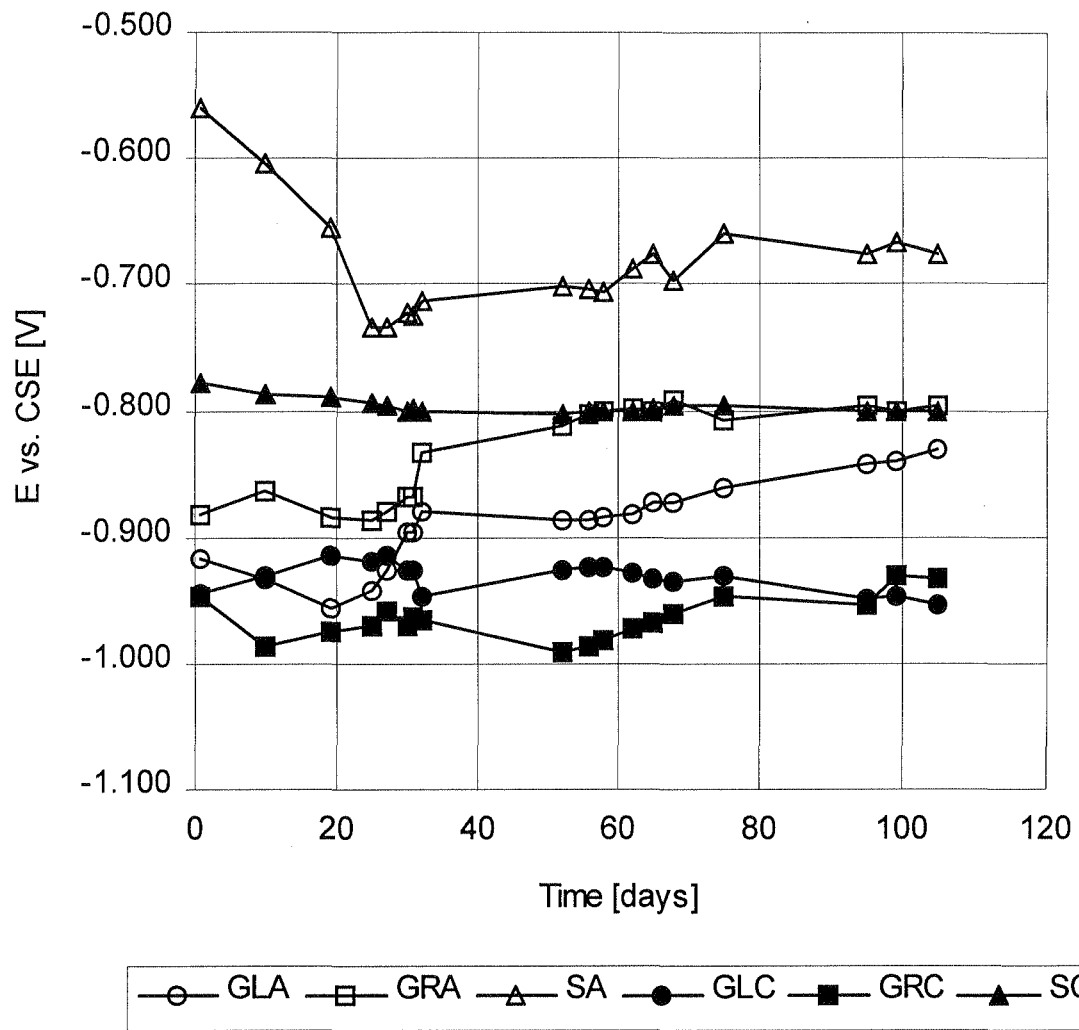


Figure 3-19. Corrosion potentials vs. CSE as a function of time, non contaminated boxes (A and C).

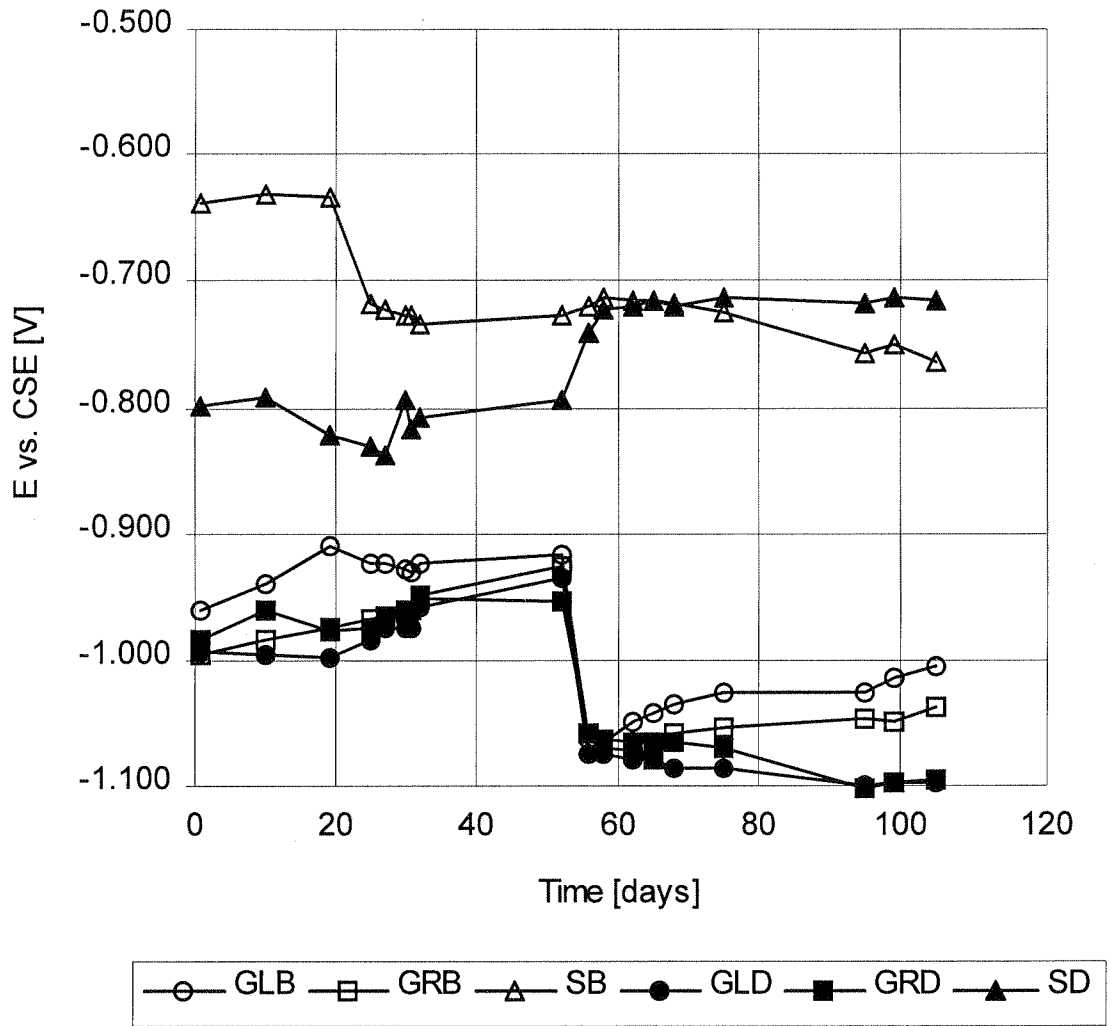


Figure 3-20. Corrosion potentials vs. CSE as a function of time, contaminated boxes (B and D).

Figures 3-21 to 3-24 are Pourbaix diagrams for zinc and iron, respectively, where potentials-pH points are shown for all boxes before contamination. The front and back specimens are located in different areas of the Pourbaix diagram (even if the corrosion potentials are the same) because there is a difference of nearly two points in pH values of both types of soil. The nomenclature for galvanized

specimens includes four letters that refer to the type, side, box and the location (front or back), in that order. For steel specimens, three letters are used indicating the type (galvanized or steel), box (A, B, C, or D) and the location (front or back), respectively.

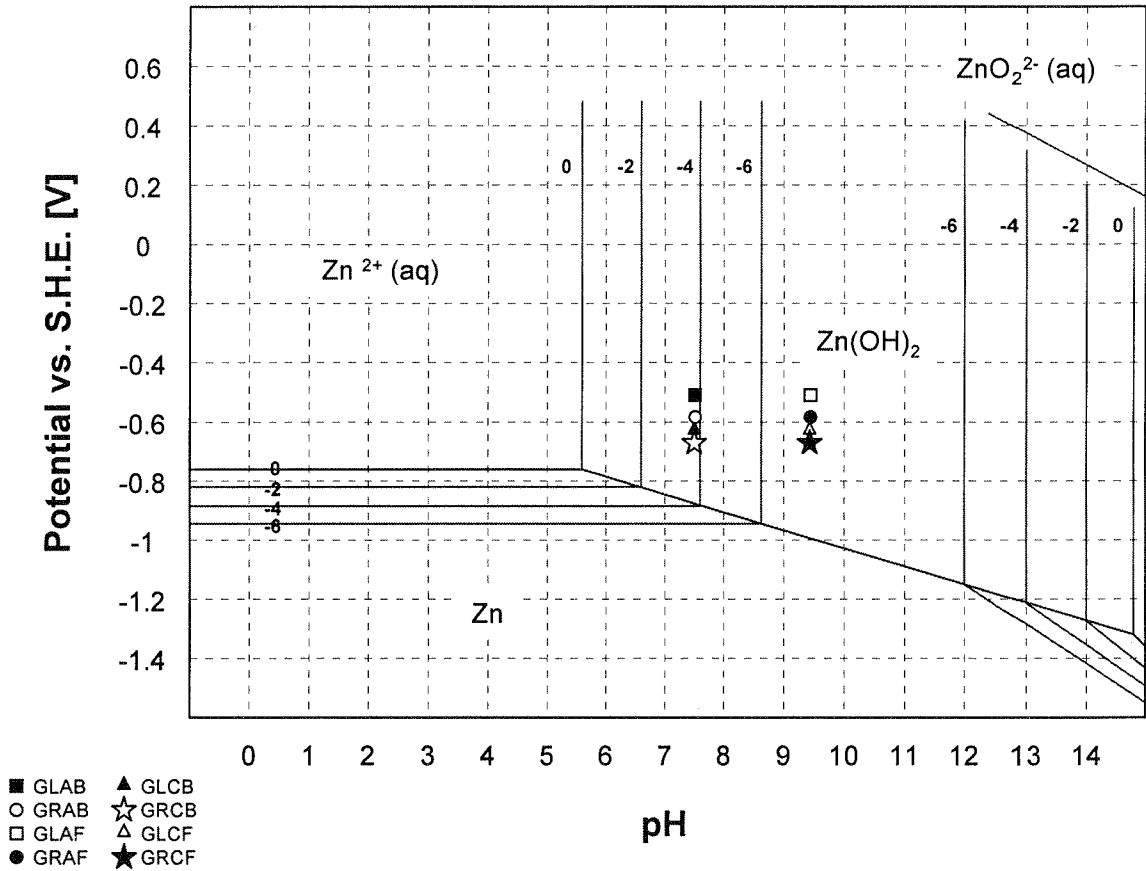


Figure 3-21. Pourbaix diagram for Zn, galvanized specimens, non contaminated boxes (A and C). Numbered lines (0, -2, -4, -6) limit zones of different activity of the Zn²⁺ ion (1, 10⁻², 10⁻⁴, 10⁻⁶).

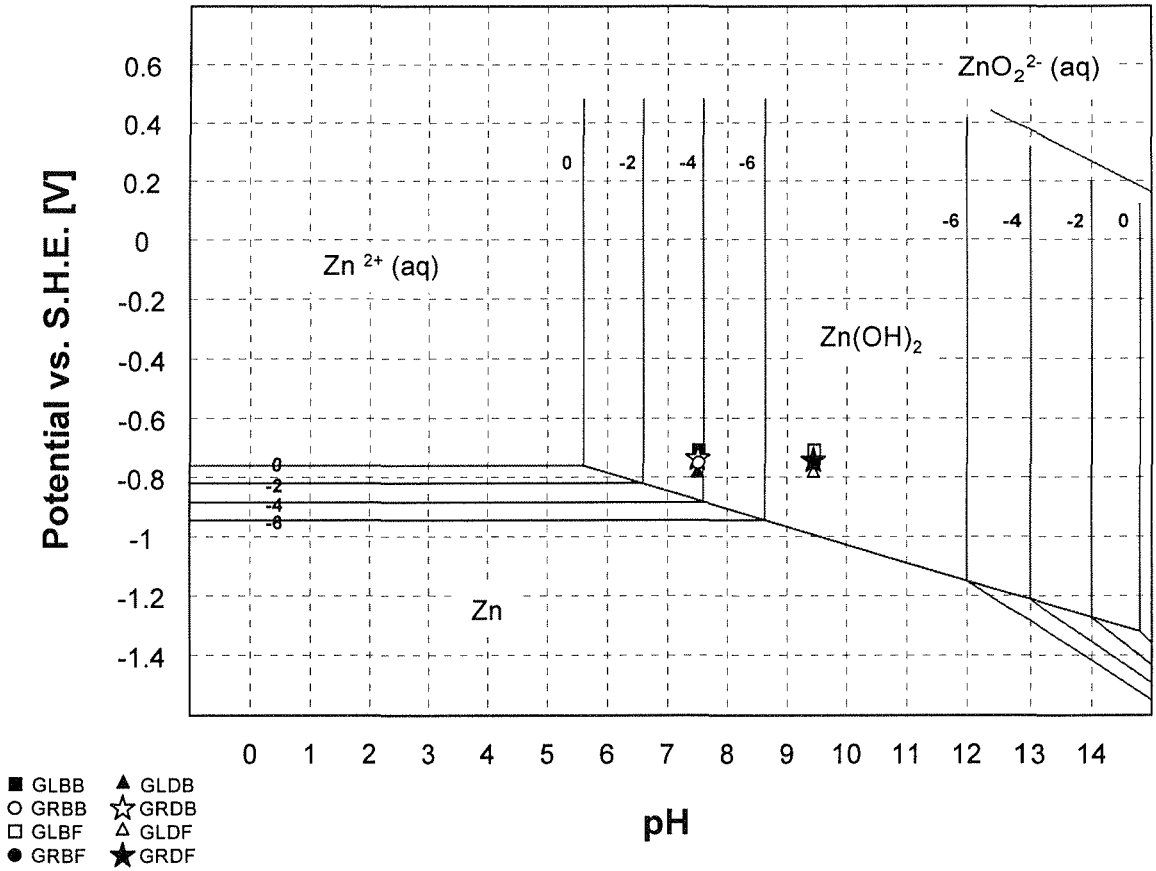


Figure 3-22. Pourbaix diagram for Zn, galvanized specimens, boxes B and D, before contamination. Numbered lines (0, -2, -4, -6) limit zones of different activity of the Zn²⁺ ion (1, 10⁻², 10⁻⁴, 10⁻⁶).

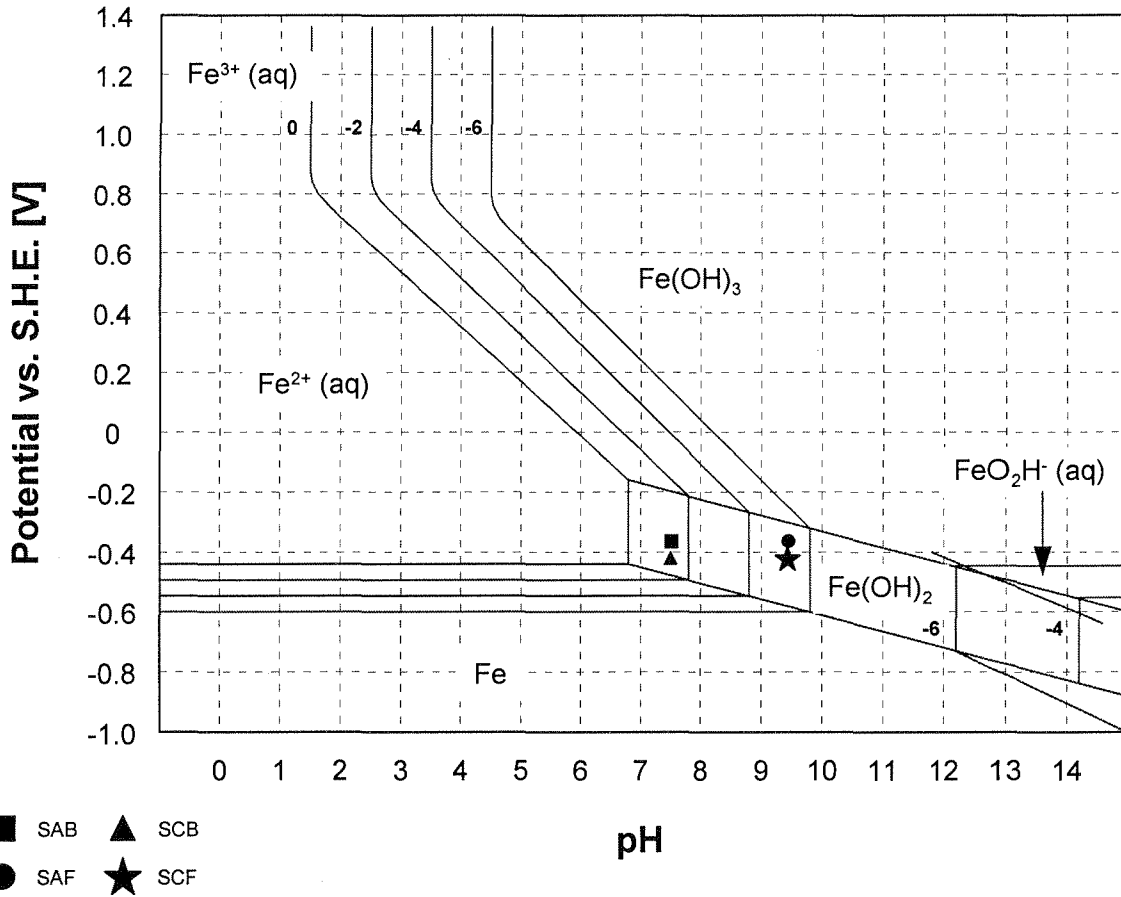


Figure 3-23. Pourbaix diagram for Fe, plain steel specimens, non contaminated boxes (A and C). Numbered lines (0, -2, -4, -6) limit zones of different activity of the Fe²⁺ and Fe³⁺ ions (1, 10⁻², 10⁻⁴, 10⁻⁶).

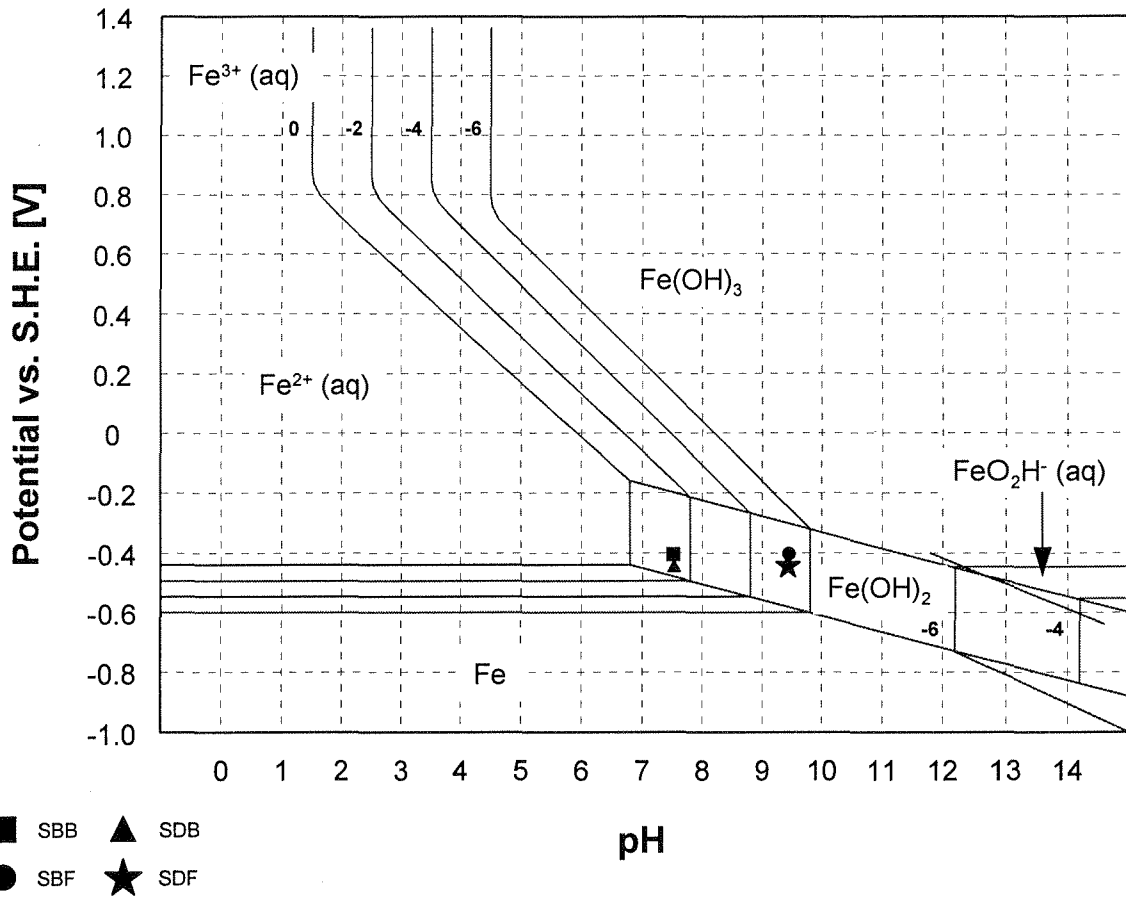


Figure 3-24. Pourbaix diagram for Fe, plain steel specimens, boxes B and D, before contamination. Numbered lines (0, -2, -4, -6) limit zones of different activity of the Fe²⁺ and Fe³⁺ ions (1, 10⁻², 10⁻⁴, 10⁻⁶).

Resistivities. Resistivity measurements using the four point method (ASTM G57-78) were performed in both halves of each box separately. Results are plotted in Figures 2-25 and 2-26. To identify both types of soils, a three letter nomenclature was used indicating fill (coarse=CS or fine=FS), and the box (A, B, C or D).

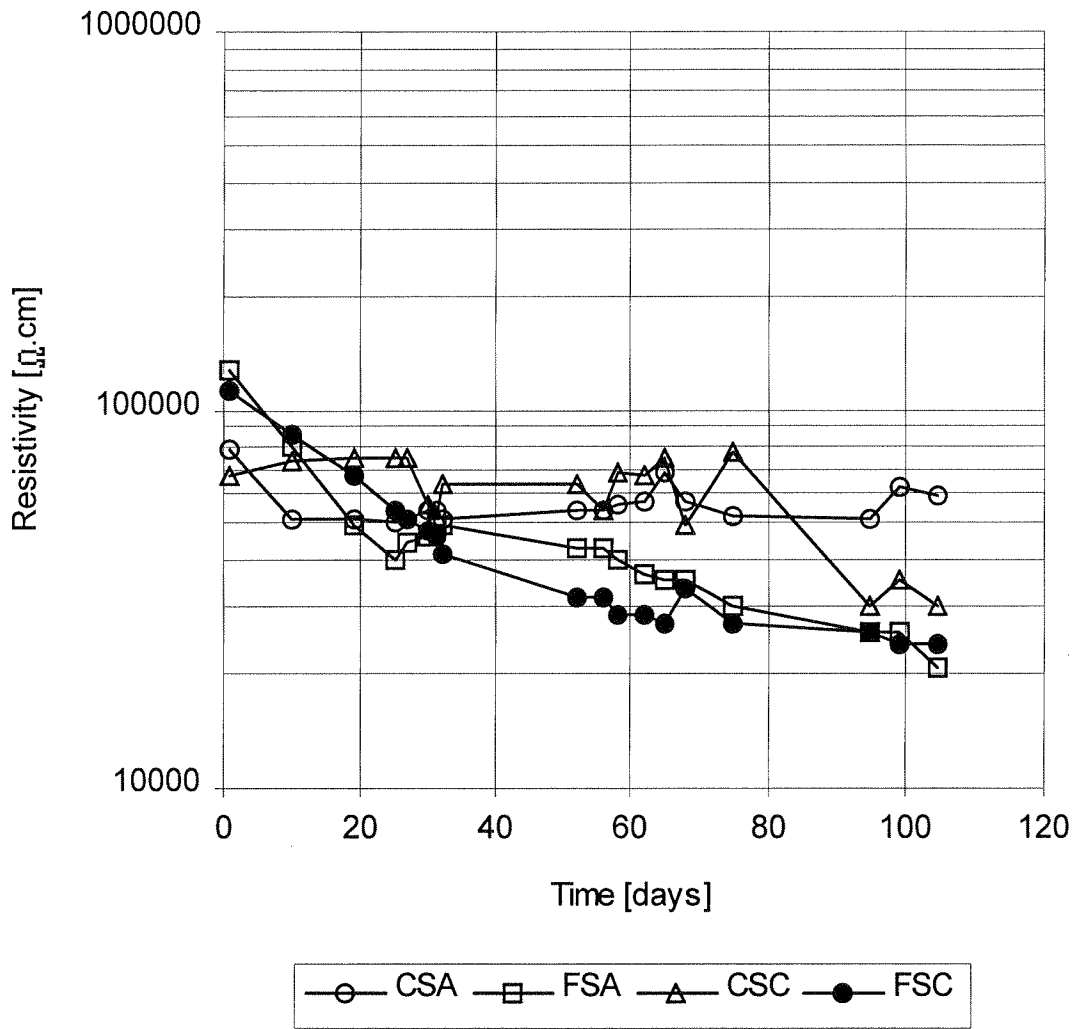


Figure 3-25. Resistivity values as a function of time, non contaminated boxes (A and C).

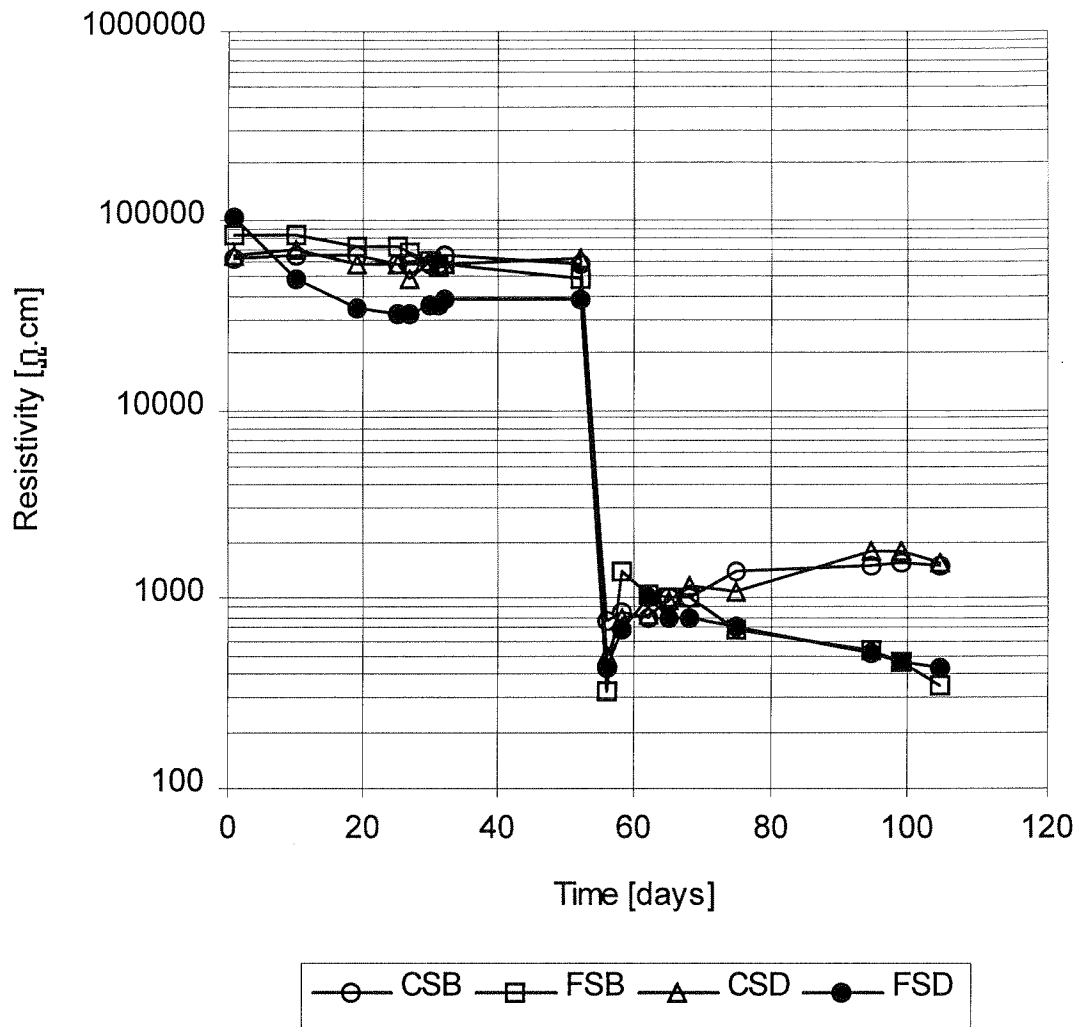


Figure 3-26. Resistivity values as a function of time, contaminated boxes (B and D).

Corrosion Rates. Corrosion rates were estimated from polarization resistance measurements with front and back specimens coupled together. Polarization resistance experiments were conducted starting from the corrosion potential.

Values of estimated corrosion currents and corrosion rates as a function of time are plotted in Figures 3-27 and 3-28. The nomenclature is the same as for

corrosion potentials except that front or back is not indicated as the specimens are coupled.

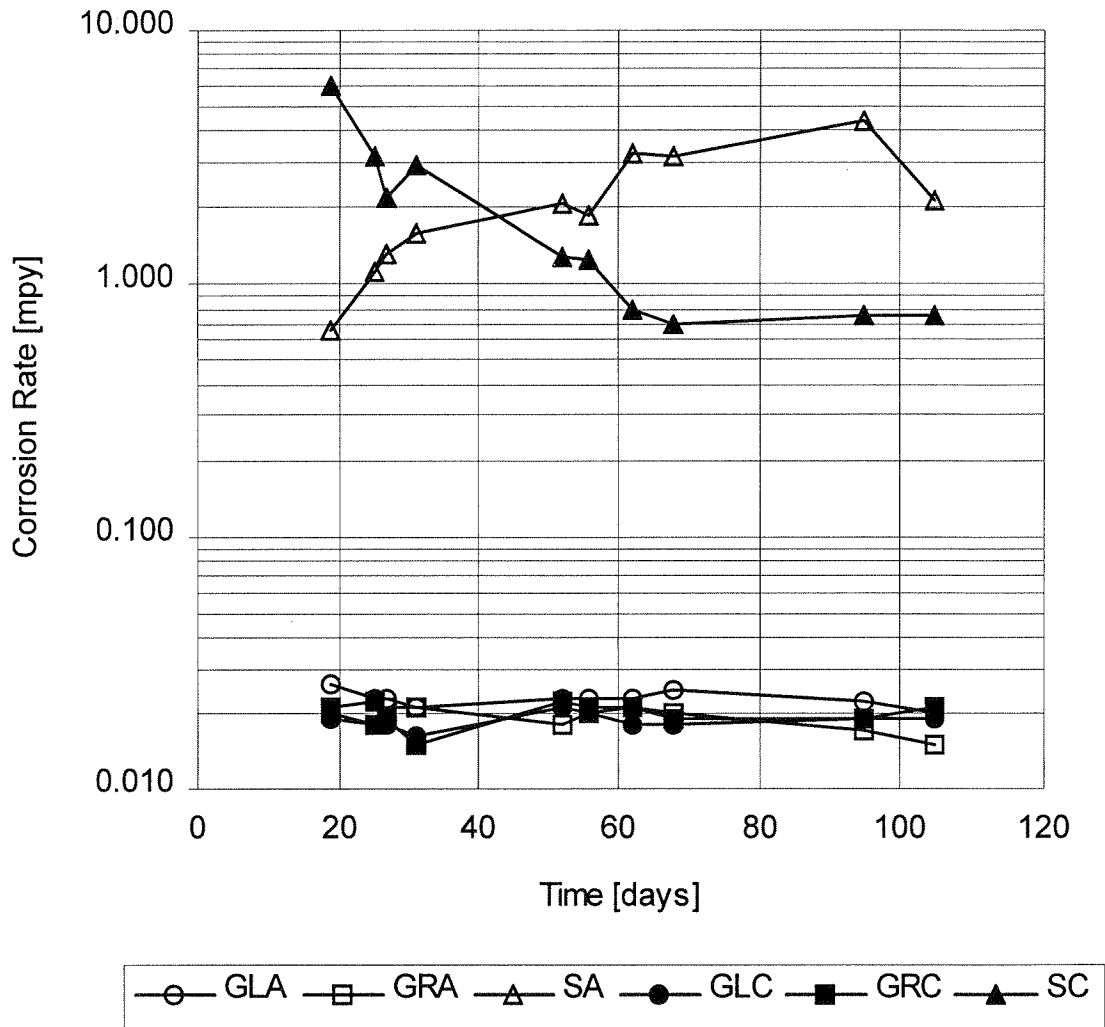


Figure 3-27. Estimated corrosion rates as a function of time, non contaminated boxes (A and C). Front and back specimens coupled.

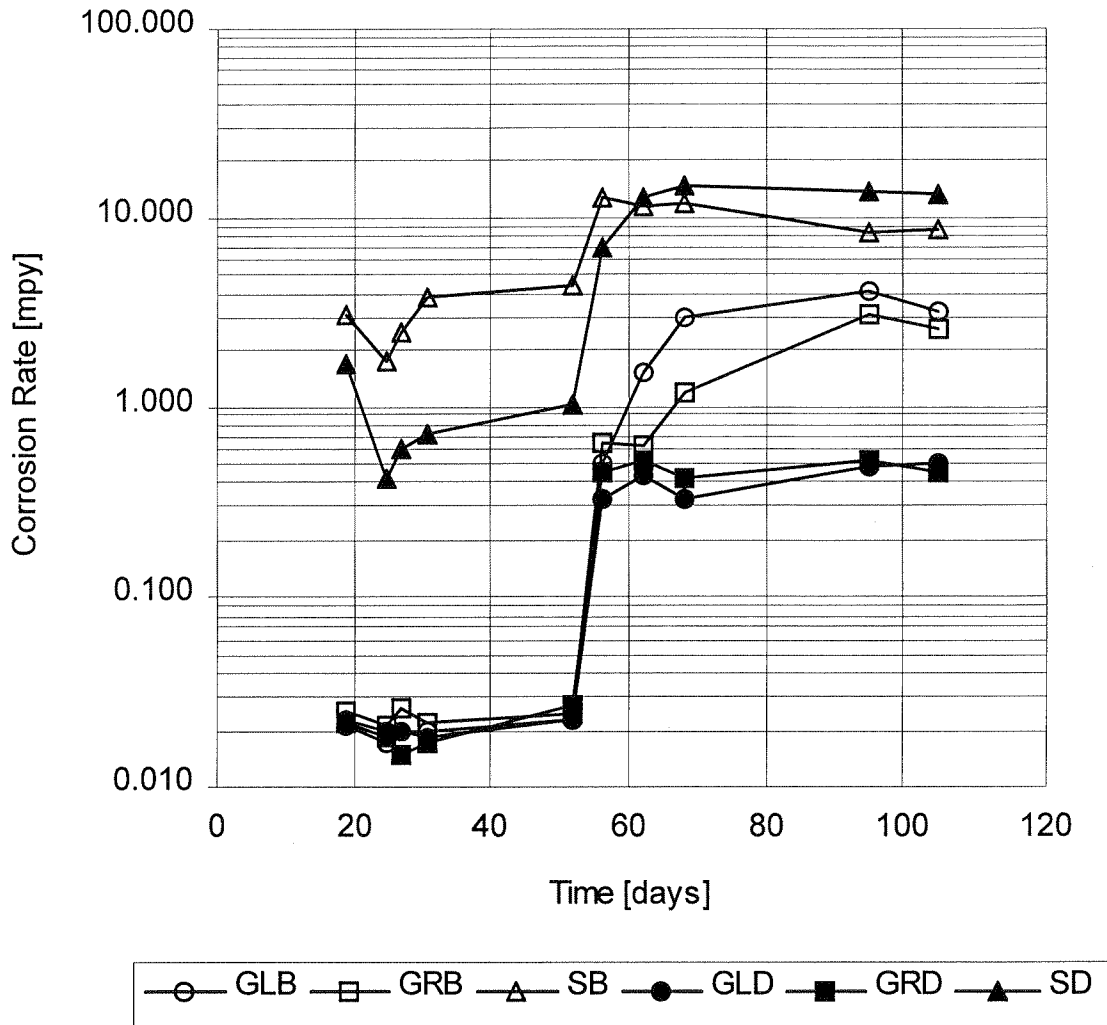


Figure 3-28. Estimated corrosion rates as a function of time, contaminated boxes (B and D). Front and back specimens coupled.

Macrocell Currents. Results from macrocell current measurements between front and back specimens for non contaminated and contaminated boxes are plotted in Figure 3-29 to 3-32. The results are shown as current densities by dividing the macrocell current by the area of one specimen. The nomenclature is the same as for the corrosion rate figures.

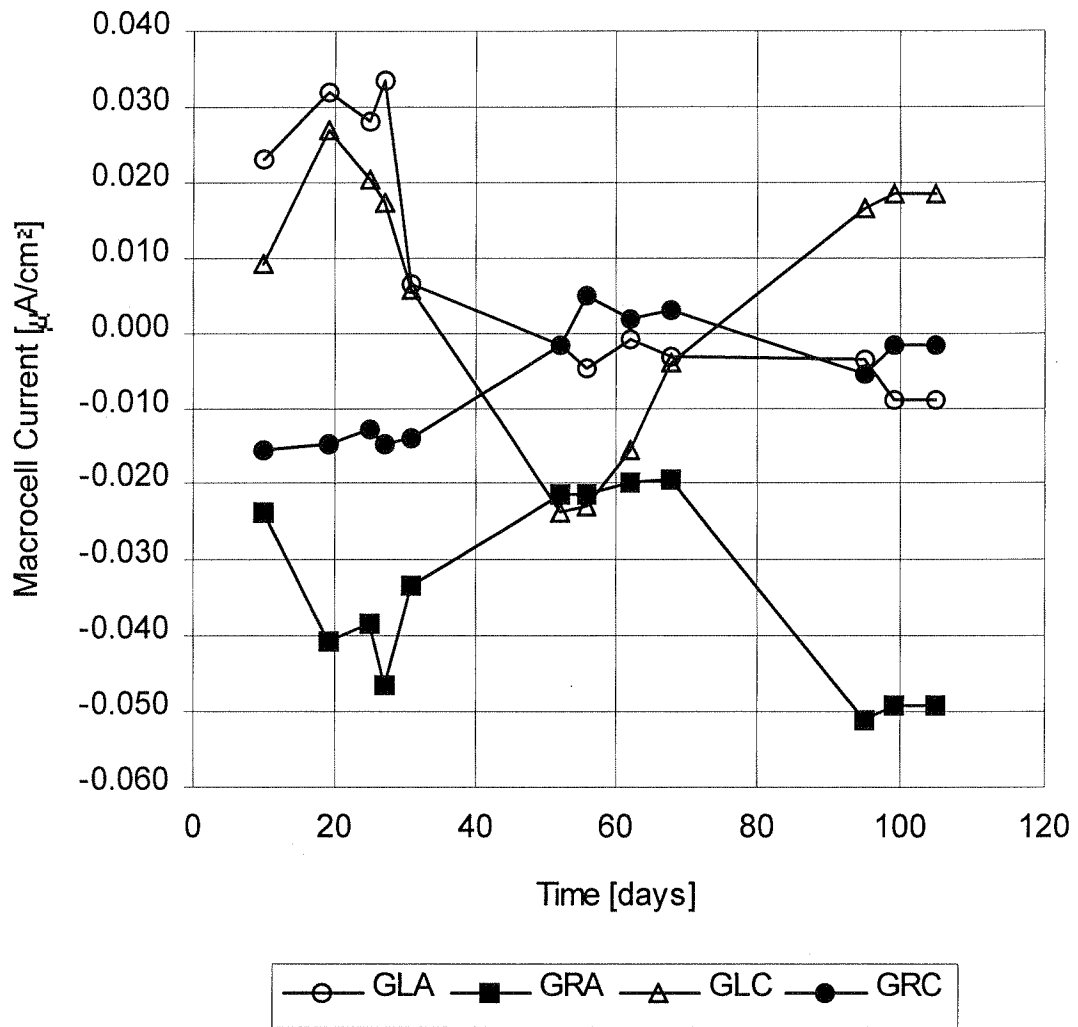


Figure 3-29. Macrocell currents (as current densities) as a function of time, galvanized specimens, non-contaminated boxes (A and C). Negative current values indicate that the cathode is the specimen buried in the side with coarse fill (front).

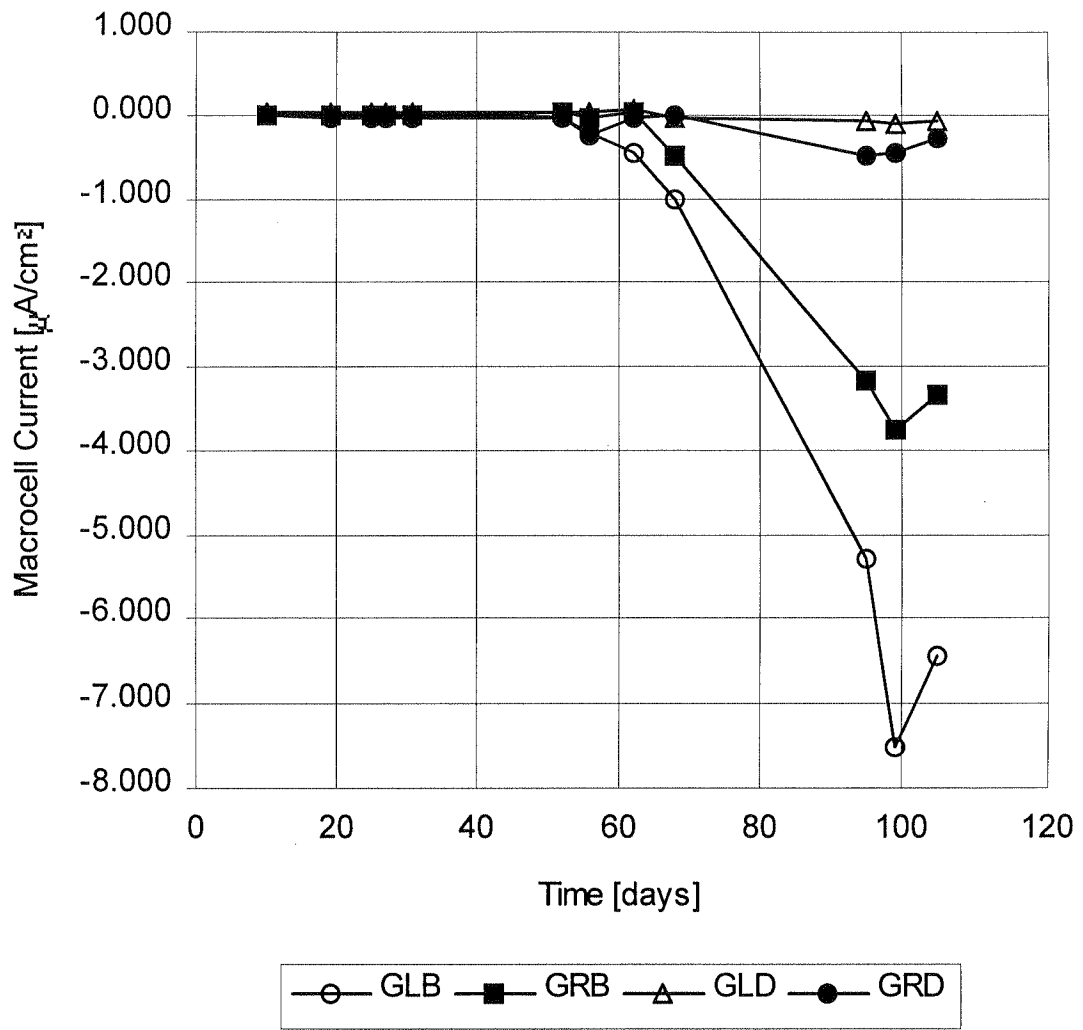


Figure 3-30. Macrocell currents (as current densities) as a function of time, galvanized specimens, contaminated boxes (B and D). Negative current values indicate that the cathode is the specimen buried in the side with coarse fill (front).

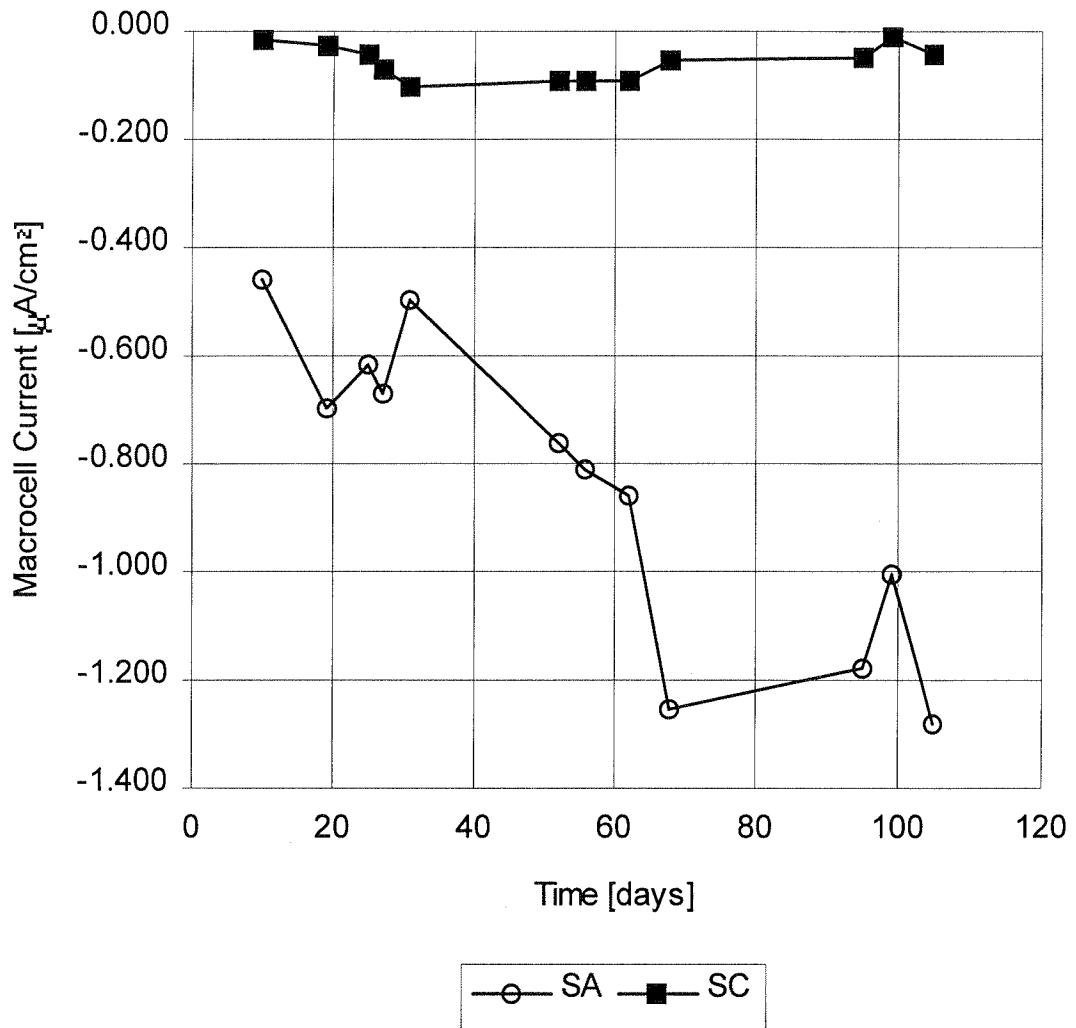


Figure 3-31. Macrocell currents (as current densities) as a function of time, plain steel specimens, non-contaminated boxes (A and C). Negative current values indicate that the cathode is the specimen buried in the side with coarse fill (front).

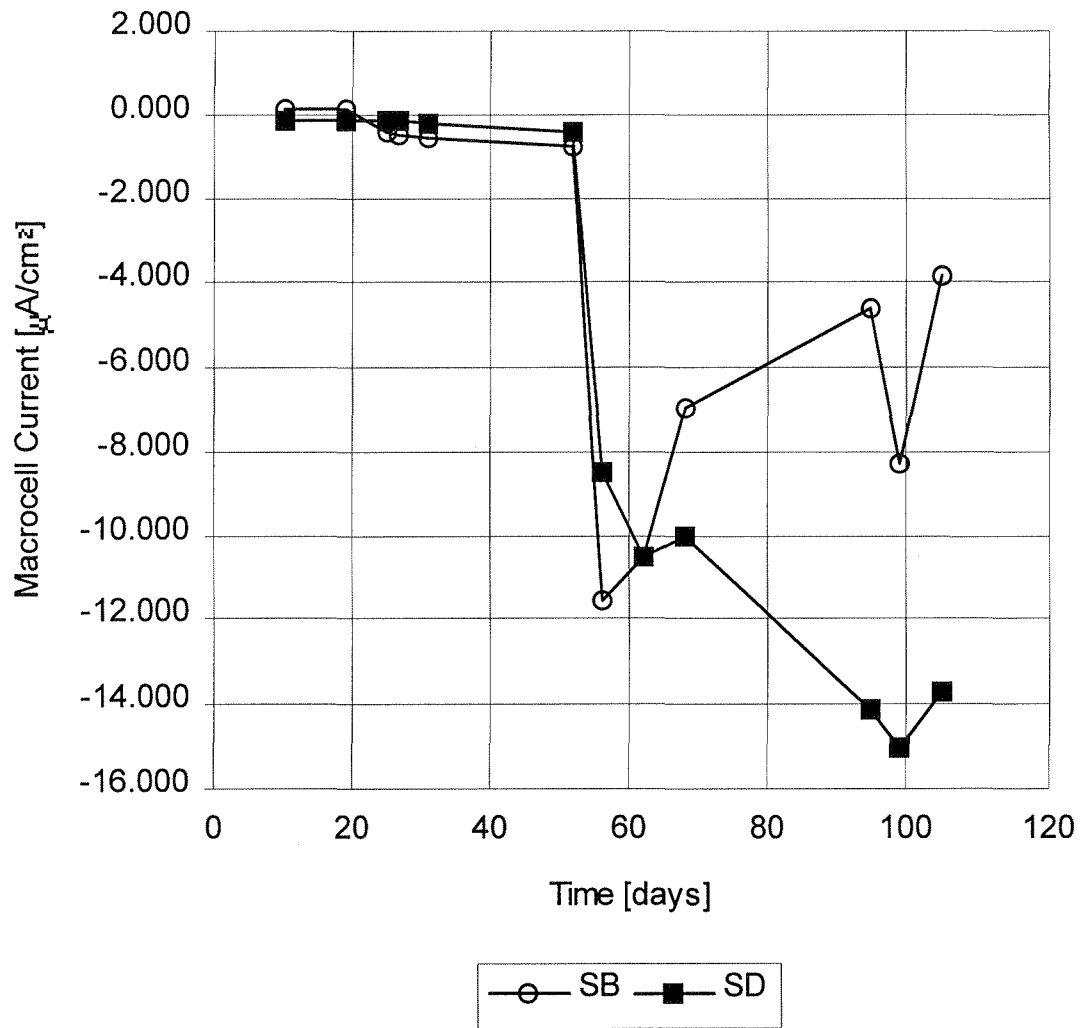


Figure 3-32. Macrocell currents (as current densities) as a function of time, plain steel specimens, contaminated boxes (B and D). Negative current values indicate that the cathode is the specimen buried in the side with coarse fill (front).

Macrocell Resistance. The mutual resistance between front and back specimens for contaminated and non contaminated boxes are plotted in Figures 3-33 and 3-34. The nomenclature is the same as for the figures for resistance and macrocell currents.

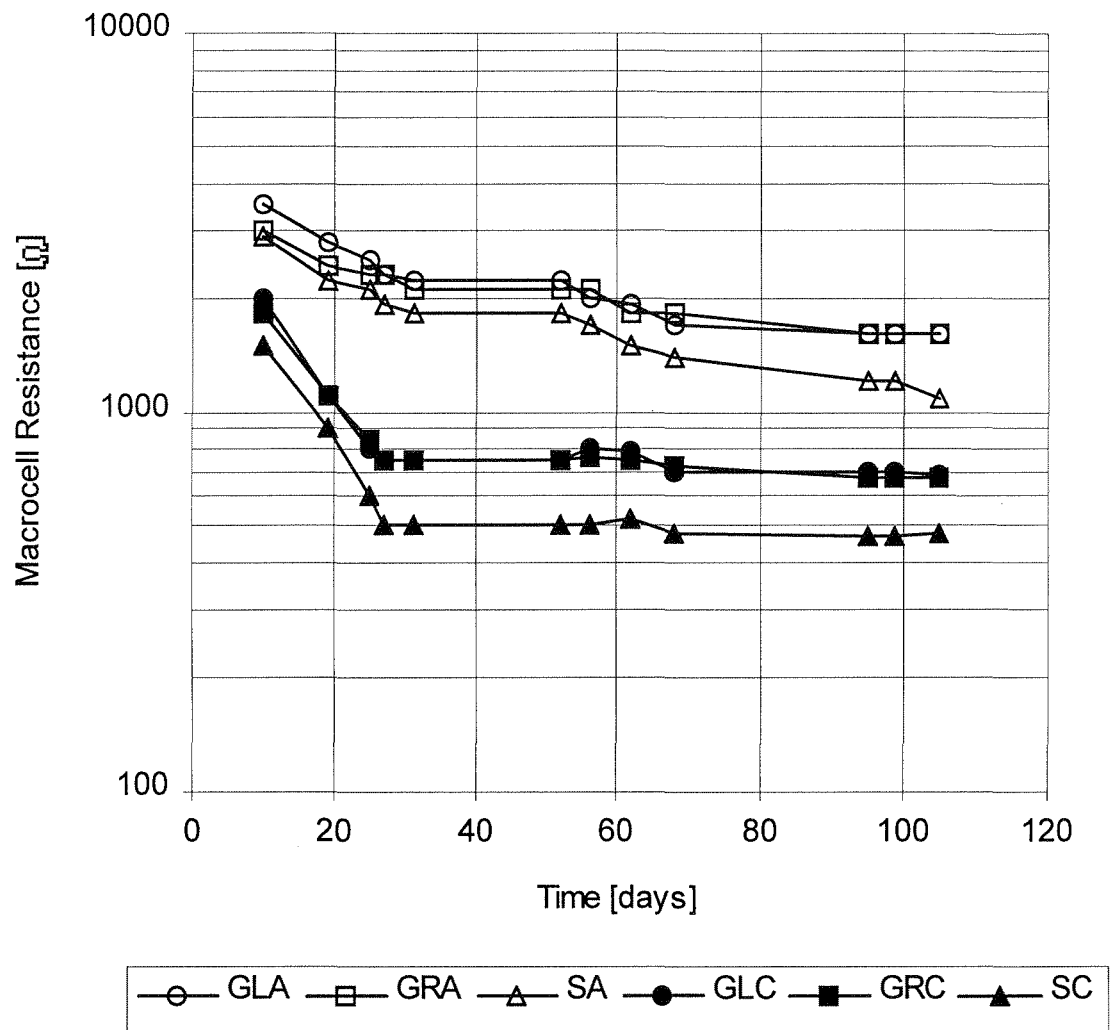


Figure 3-33. Macrocell resistance as a function of time, non contaminated boxes (A and C).

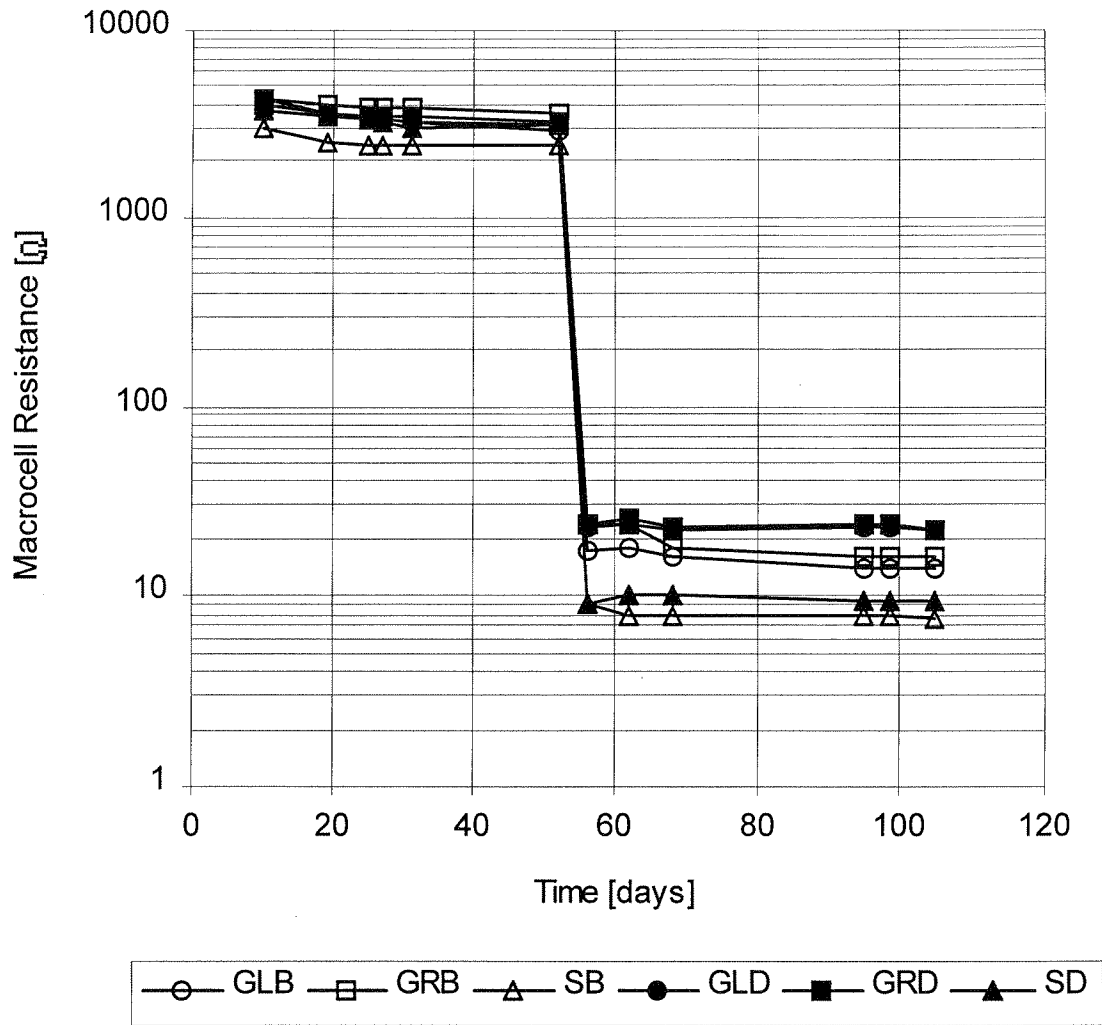


Figure 3-34. Macrocell resistance as a function of time, contaminated boxes (B and D).

3.3 Laboratory Results - Series 2

3.3.1 Soil Physical Properties

Tables 3.7 and 3.8 list the physical properties of each soil type used in this series.

Table 3.7. Specific gravity, porosity and void ratio for soils in Series 2.

Soil Type	Specific Gravity (kg/m ³)	Void ratio
Type 1	1933	0.25
Type 2	1765	0.31
Type 3	1897	0.40
Type 4	1616	0.54

Table 3.8. Particle size distribution for soils in Series 2.

Sieve	% passing Soil Type 1	% passing Soil Type 2	% passing Soil Type 3	% passing Soil Type 4
3"	100	100	100	100
1/2"	87.49	98	99.59	95.59
No. 4	66	94.53	41.99	0.6
No. 40	48.27	84.4	0.74	0
No. 100	8.16	8.56	0.3	0
No. 200	3.3	1.05	0.23	0

3.3.2. Soil Electrochemical Properties.

Analysis of chloride content, sulfate content and pH of the soil in the boxes was performed in the as received (initial) condition, one day after the simulated seawater event and after 600 days of testing. Results are shown in figures 3-35, 3-36 and 3-37.

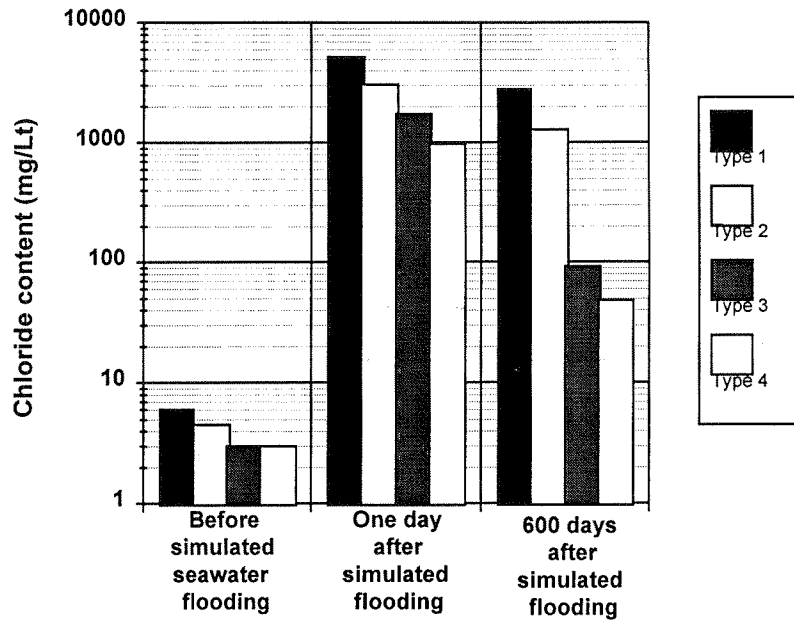


Figure 3-35. Variation in Chloride content on soils used for Series 2 during the testing period.

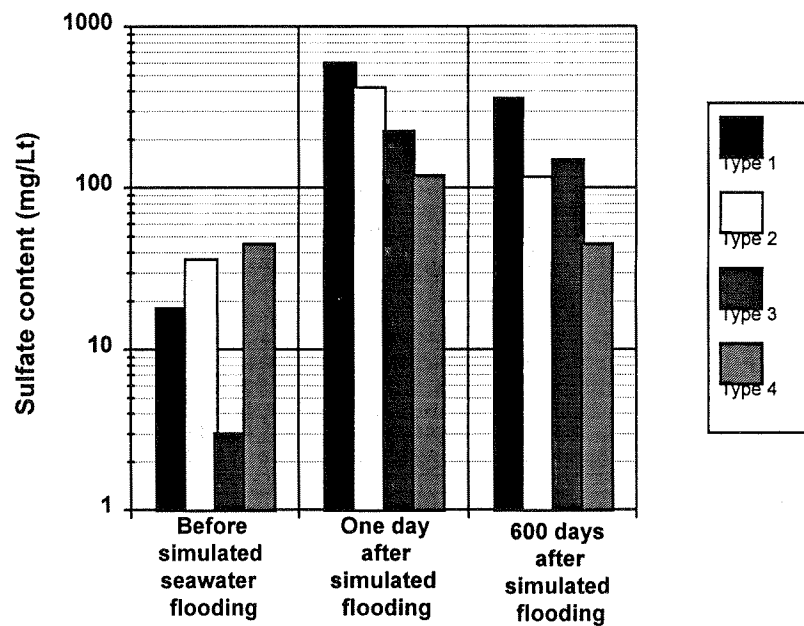


Figure 3-36. Variation in sulfate content on soils used on Series 2 during the testing period.

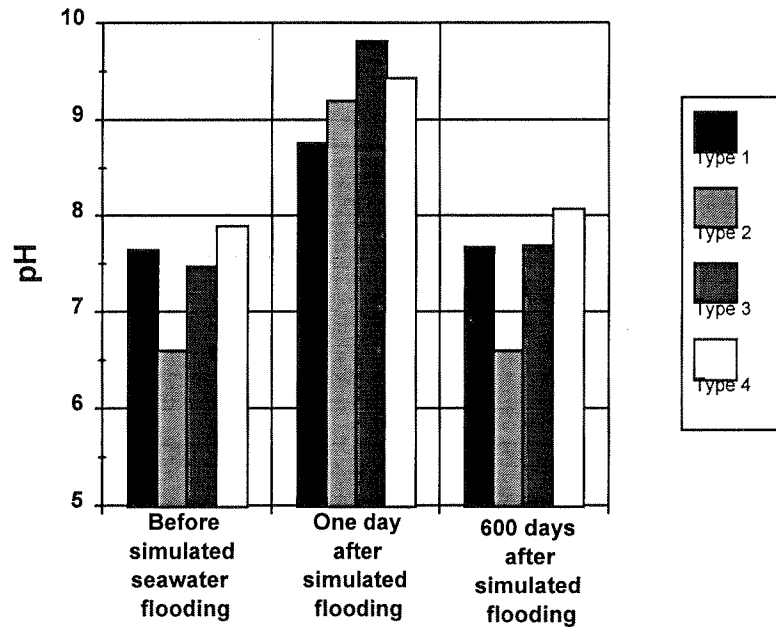


Figure 3-37. Variation in pH on soils used for Series 2 during the testing period.

3.3.3. Electrochemical Measurements.

For brevity, only the nominal estimated corrosion rates as a function of time of specimens in each test box are presented here (figures 3-38 to 3-45). A detailed description of all experimental results in Series 2 is given in Reference [18].

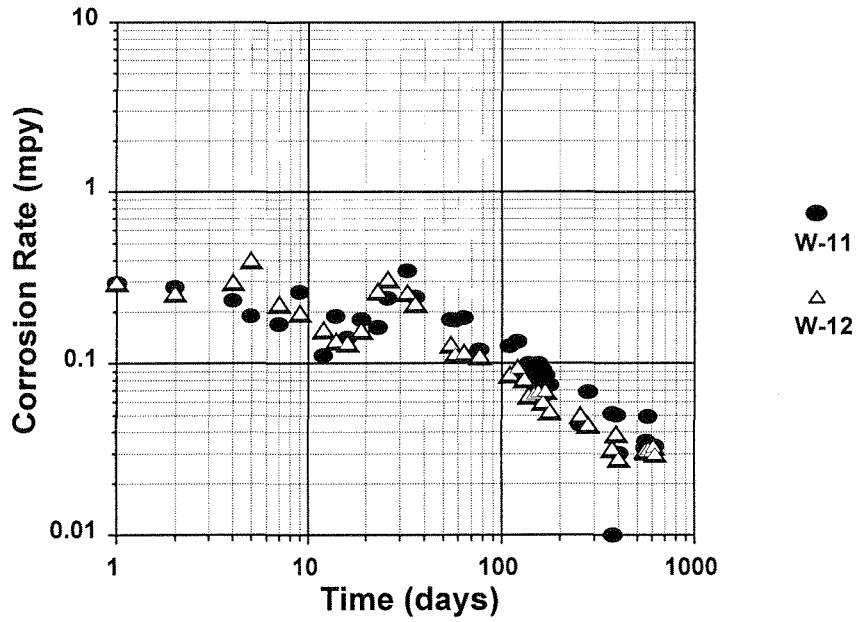


Figure 3-38. Corrosion Rate vs Time. Non contaminated Soil Type 1. W-11 and W-12 indicate duplicate specimens.

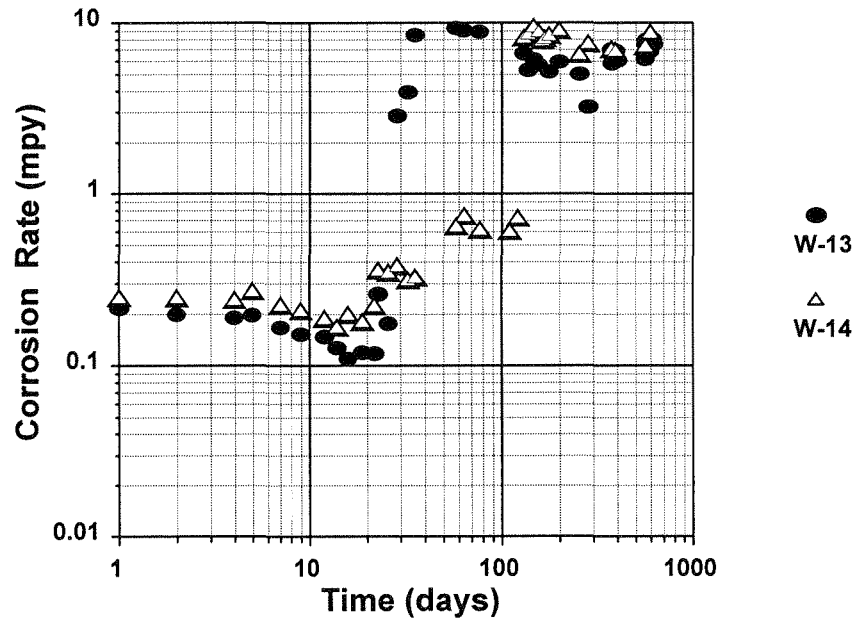


Figure 3-39. Corrosion Rate vs. Time. Contaminated Soil Type 1. W-13 and W-14 indicate duplicate specimens. Soil contamination took place at day 22.

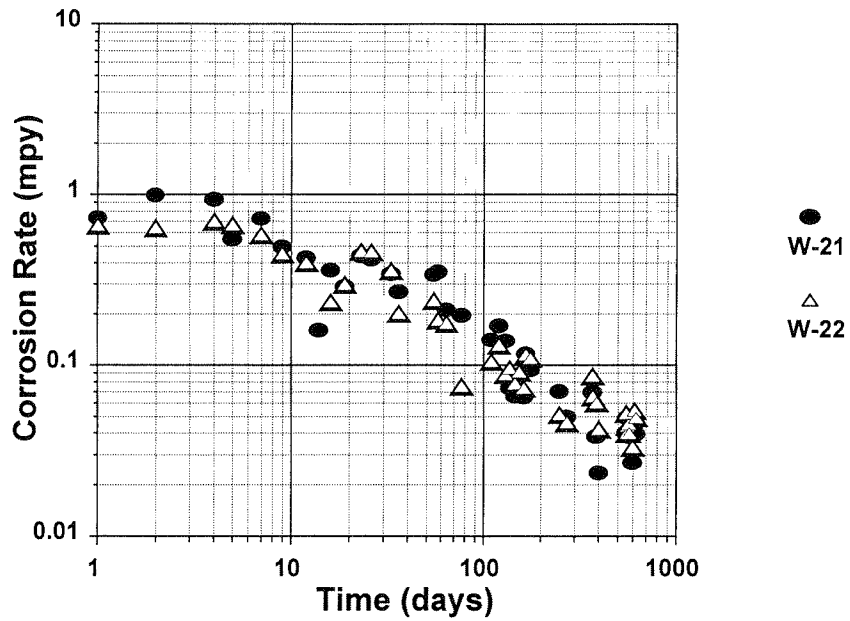


Figure 3-40. Corrosion Rate vs. Time. Non contaminated soil Type 2. W-21 and W-22 indicate duplicate specimens.

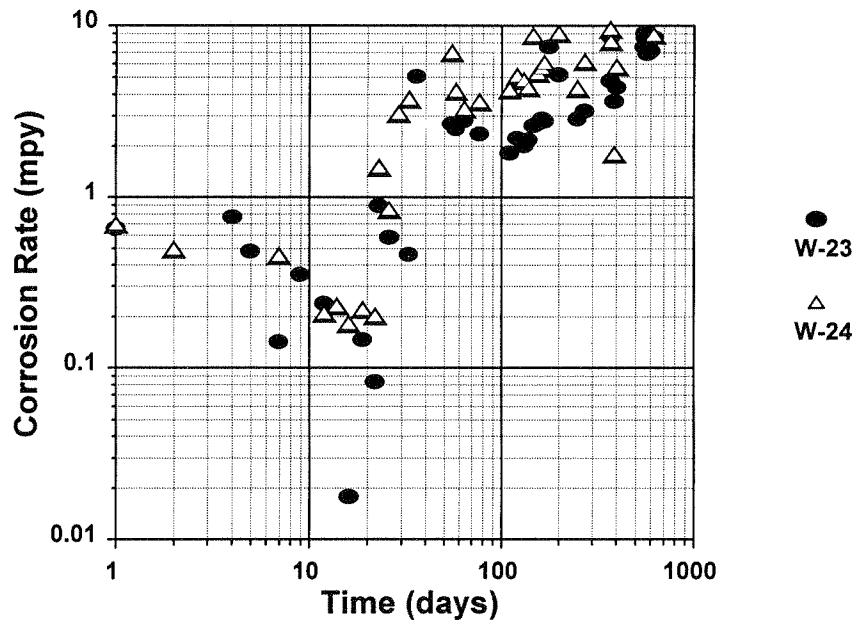


Figure 3-41. Corrosion Rate vs. Time. Contaminated Soil Type 2. W-23 and W-24 indicate duplicate specimens. Soil contamination took place at day 22.

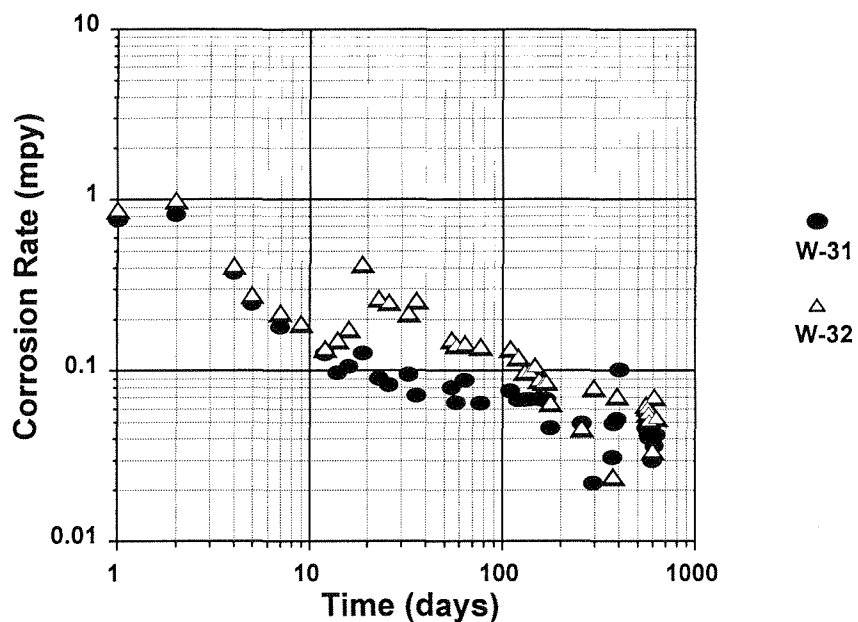


Figure 3-42. Corrosion Rate vs. Time. Non contaminated Soil Type 3. W-13 and W-14 indicate duplicate specimens.

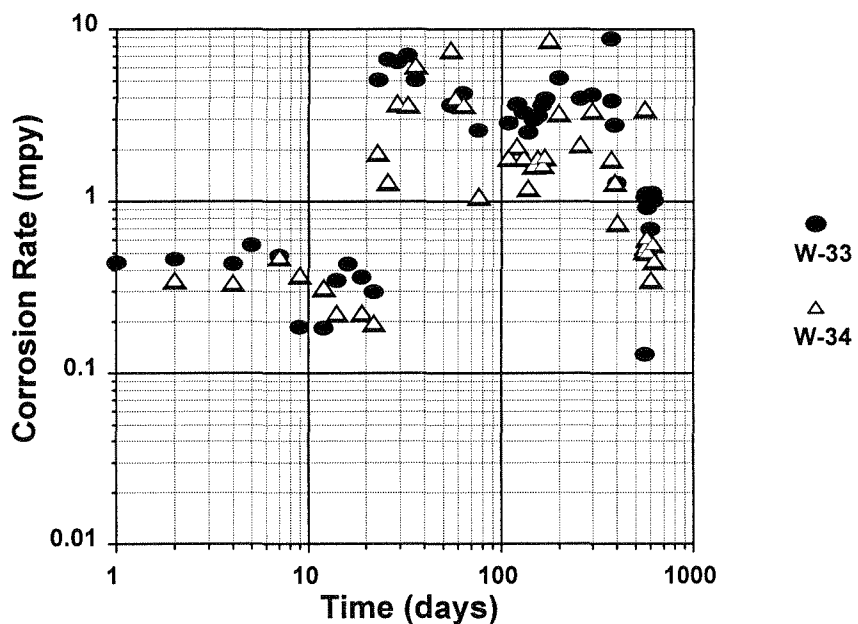


Figure 3-43. Corrosion Rate vs. Time. Contaminated Soil Type 3. W-33 and W-34 indicate duplicate specimens. Soil contamination took place at day 22.

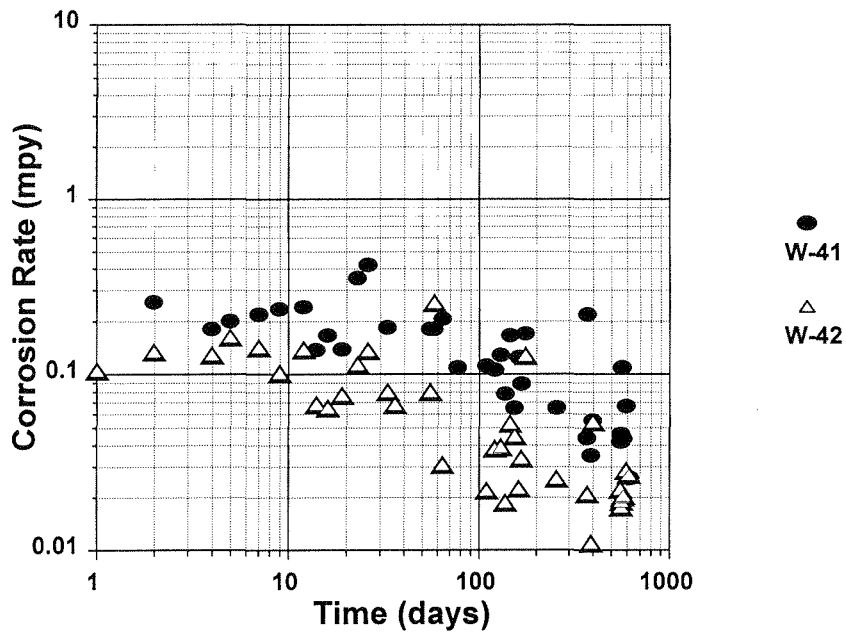


Figure 3-44. Corrosion Rate vs. Time. Non contaminated Soil Type 4. W-41 and W-42 indicate duplicate specimens.

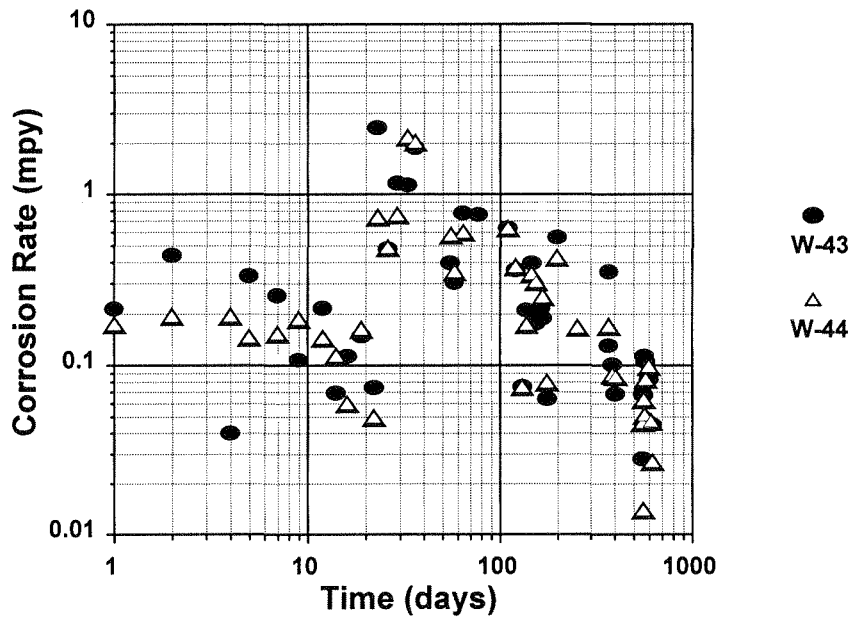


Figure 4-45. Corrosion Rate vs. Time. Contaminated Soil Type 4. W-43 and W-44 indicate duplicate specimens. Soil contamination took place at day 22.

4. DISCUSSION

4.1 Laboratory Results

4.1.1 Electrochemical Measurements

Series 1

Corrosion potentials presented sharp variations during the first 30 days of burial and then stabilized in both contaminated and non contaminated boxes. After contamination took place, a sharp drop in the potential of the galvanized specimens was observed but the potential of the steel specimens did not show any appreciable change. This difference in behavior between plain steel and galvanized specimens in boxes B and D suggest that the galvanized specimens were in the passive state before contamination occurred and became active afterwards, while the steel specimens may have been active all along [10-15]. The Pourbaix diagrams (Figures 3-21 to 3-24) may be interpreted as indicating that all zinc samples were in the passive region, and that the corrosion product present on the surface of the plain steel specimens may have been $\text{Fe}(\text{OH})_2$, which is porous and therefore, non protective [10, 11, 12, 16]. It should be noted that the estimations of the surface condition of the metal from Pourbaix diagrams are only indications since the system may be far away from thermodynamic equilibrium [10, 12].

Resistivity measurements in non contaminated boxes revealed a progressive decrease for both coarse and fine soil during the first 60 days, and a trend toward

stabilization afterwards. The difference between coarse and fine soil values became pronounced after the first 60 days, particularly in box A. As expected, there was a sharp drop in resistivity (two orders of magnitude) in boxes B and D after contamination took place. During the first 10 days after salting, the resistivity values of the coarse and fine fill were nearly identical. After 10 days, the resistivities began to gradually differ (the coarse fill having the highest value). This effect was due to the weekly addition of distilled water to keep the moisture content approximately constant and therefore, a certain amount of ions were washed out from the soil (the boxes were allowed to drain before the distilled water was added). As shown in Figure 3-26, the resistivity of the fine fill decreased 400 Ω -cm in 35 days, while the resistivity of the coarse soil increased 1000 Ω -cm in the same amount of time. Assuming that the resistivity of the coarse soil would continue to increase at the same rate with a continuous addition of fresh water, it would reach its initial value (approximately 60 k Ω -cm) a few years after contamination took place. The trend observed in resistivity values of the coarse fill suggest that *coarse fills might become less aggressive in time* due to a better drainage capacity (provided that the structure is built so that fresh water flushing is possible). The aggressiveness of the fine fill would remain approximately constant depending on the moisture content (which controls the solubility of chloride ions). It is important to observe that the resistivity values listed in this section can not be used directly to predict resistivity changes in real structures or for comparison purposes, since changes in both moisture content and chemical composition in the field can not be controlled or accurately predicted.

The nominal estimated corrosion rates computed from polarization resistance

measurements represent an average of the corrosion condition of both parts of the macrocell. The rates were similar and uniform in time for the galvanized specimens (approximately equal to 0.020 mpy for both non contaminated boxes and contaminated boxes prior contamination). Plain steel specimens in boxes A and C exhibited large variations in the first 60 days and stabilized afterwards, the specimens from box A having an average value of 3 mpy and the specimens from box C having an average value of 0.7 mpy after 60 days of exposure. In boxes B and D, an increase of approximately two orders of magnitude in the estimated corrosion rates was observed for the galvanized specimens and of approximately one order of magnitude for plain steel specimens after contamination. In addition, the estimated corrosion rates of the galvanized specimens from box B were approximately 1 order of magnitude higher than the estimated corrosion rates of the galvanized specimens from box D after 105 days, while plain steel specimens from the same boxes showed practically the same value (approximately 10 mpy).

The corrosion macrocell currents of galvanized steel and plain steel couples were generally of small magnitude in the absence of seawater contamination. Upon contamination, the macrocell currents experienced, on the average, a dramatic increase (although with significant variability from test box to test box) in both materials. The direction of the macrocell currents in contaminated soil was consistently such that the metal in the coarse, more aerated fill was the cathode. Under activation polarization conditions of the anodic reaction, the cathode, with its more noble potential, may be expected to have been experiencing the greater corrosion rate of the galvanized couple. In that case, the direction of the macrocell

current indicates that the metal in the fine fill is corroding at a faster rate than it would be in the absence of galvanic interaction. The metal in the coarse fill, that may be corroding at the fastest rate, is nevertheless experiencing a certain amount of cathodic protection.

Macrocell resistance values were nearly constant after the first 20 days for the non contaminated boxes A and C. In boxes B and D, macrocell resistance values dropped 2 orders of magnitude after contamination and remained nearly constant afterwards.

Series 2

This series afforded the opportunity of examining the corrosion behavior over a relatively long time frame of 600 days.

In the boxes not exposed to contamination the apparent corrosion rates (ACR) started at low values comparable to those obtained in Series 1. The ACR decreased further with time, t , over the entire test period, following an approximate power law $ACR = k t^n$ with $n \approx 1/2$, in agreement with the observations of previous investigations [2]. This behavior was better defined in soil types 1 and 2 and somewhat obscured by experimental scatter in soil types 3 and 4. There was little differentiation of the magnitude of the ACR at a given time for the different soil types. At the end of the 600 days, ACR values were typically $0.75 \mu\text{m/y}$ (0.03 mpy).

In the boxes exposed to saltwater contamination the ACR increased sharply immediately following the contamination event. The increase was of about one order

of magnitude in all soil types. The increased corrosion rates were sustained for the following 600 days for the specimens in boxes 1 and 2 (finer soils) but decreased in the coarser soils. The decrease was slow in soil type 3 and more rapid in soil type 4, the coarsest. The values of ACR in soil type 4 after 600 days were comparable to those in the uncontaminated soil of the same type.

The change in ACR after the contamination events replicated the behavior observed in the Series 1 experiments. For the purpose of service life estimation (Section 4.3), the increase in apparent corrosion rate that took place immediately following the simulated inundation events was treated as a discrete change and quantified in the following manner. Best-fit straight lines were calculated for the log corrosion rate - log time data for each specimen in each box. Separate calculations were made in each case for all data in the period before the simulated inundation event, and for the period for immediately after the event to 200 days after the event. Projected corrosion values CR_B (corrosion rate before) and CR_A (corrosion rate after) for the moment of the event were obtained from the before-event and after-event trend lines respectively. The Corrosion Rate Increase ratio $CRI = CR_A / CR_B$ was calculated for each case and used as an indication of the increase in corrosion severity associated with the flooding event. The values of CRI obtained from this analysis are shown in Table 4-1. The average CRI value is 9.82, in agreement with the order of magnitude increase in apparent corrosion rates observed for Series 1 under comparable circumstances.

Table 4.1. Estimated Corrosion Rate Increase Ratio (CRI). WXX indicates specimen name.

Soil Type 1		Soil Type 2		Soil Type 3		Soil Type 4	
W13	W14	W23	W24	W33	W34	W43	W44
11.4	2.8	4.5	9.5	18.5	11.6	10.1	10.2

The experience with soil types 1 and 2 indicates that increases in corrosion rates in fine particle size soils (with little fresh water makeup used) can extend over long periods of time following saltwater contamination. Conversely, washout from extended fresh water makeup for drainage of the salt water (as in soil types 3 and 4) restored the low corrosivity prevalent before the simulated inundation event. These long term reductions in ACR confirm the experience with the coarse sand side of the boxes in Series 1.

4.2 Field Investigation

4.2.1 Apparent Corrosion Rate Values

The results of the field investigation showed that apparent corrosion rates (ACR) of the galvanized reinforcement were very small in most of the elements examined. The average ACR was 1.04 $\mu\text{m}/\text{y}$ (0.041 mpy); and 95% of the elements tested had ACR <2.54 $\mu\text{m}/\text{y}$ (<0.1 mpy). These values are comparable with those obtained near the end of the 600-day tests in non-contaminated soil boxes in series

2. The results showed significant variability, which is typical of field measurements. Because of the variability, it was not possible to establish whether the ACR declined with time of service, as was suggested by long term experiments with buried test coupons reported in the literature [2], or by extrapolating the laboratory results from the non-contaminated soil boxes in Series 2. For example, the ACR values obtained for galvanized reinforcement in Structure 3 (Pensacola Ave., Tallahassee, 17 years old and oldest in the state), are on average not much different from those measured in Structure 8 (Veteran's Expressway, Tampa, 2 years old). Similar conclusions may be obtained from the other structures examined by referring to Table 3-1 and the graphic summary in Figure 3-3. The approximately constant ACR over the time period investigated may actually be the combined result of two opposite trends. The first trend is the continuing reduction of the corrosion rate of the galvanized layer that covers most of the surface of the reinforcement, following the behavior observed in the laboratory experiments with uncontaminated soils. The opposing trend is the increasing development of localized corrosion spots (as revealed by visual examination and illustrated in Figure 3-14). If the effects of these two opposing trends were roughly in balance, the measured ACR (which reflects the average behavior over the reinforcement surface) would be relatively stable with time. For the purpose of projection of service life it is convenient to treat the corrosion rate of the galvanized layer as if it were uniform and constant, at the value obtained in the field tests.

The ACR of plain steel was typically an order of magnitude higher than that of galvanized elements (average ACR 11.7 $\mu\text{m}/\text{y}$ (0.46 mpy); 95% of elements with

ACR < 25 $\mu\text{m}/\text{y}$ (1 mpy)). With the exception of episodic contamination in structure 4B, the data was not sufficient to indicate changes in ACR with time (Table 3-1). The oldest plain steel specimens tested for ACR had been exposed only for 2 years, so it is possible that over periods of a decade or more the corrosion rate may decrease following a power law as reported in the literature [2]. Nevertheless, for service life estimations it is advisable to use a conservative estimate of linear loss with time as was done for the galvanized layer.

4.2.2 Applicability of the ACR Information

Errors Inherent to the Testing Technique. The ACR values should be used with caution when attempting to project service life of new structures or remaining life of those already in service. The measurement technique itself is subject to several errors as indicated below.

The ACR values were obtained by using the Polarization Resistance technique, which is based on working assumptions of the electrochemical nature of the corrosion process at work, the distribution of excitation currents and the size of the system. Those assumptions can only be satisfied approximately.

Errors develop due to several causes, starting with the use of relatively fast potential scan rates to avoid impractical long test times. The test assumes that the metal-electrolyte interface behaves as the simple combination of a polarization resistance in parallel with an ideal interfacial capacitance, a rough approximation at best. Compensation of the effect of the soil resistance can only be done

approximately and is especially uncertain when the polarization resistance is small. Because the elements being tested are spatially distributed over several meters, the distribution of the excitation current over the entire working electrode may be significantly non-uniform, even though attempts were made whenever possible to use a counter electrode of an equally large size. The uneven excitation current distribution, combined with the practical compromise of using a single reference electrode placed at one of the ends of the assembly, creates additional sources of error in determining R_p . The values of the B constant for galvanized steel and plain steel to convert from R_p to i_{corr} (Section 2) were selected from reports in the literature based mostly on approximate empirical observations. The accuracy of the estimated corrosion rate is directly affected by uncertainty in the total amount of metal area in contact with soil. In strip-reinforced walls this has been addressed by conservatively assuming that the area of the element under testing corresponds always to a single strip, thus tending to overestimate the average corrosion rate. The combination of the factors described above results typically in errors of a factor of 2 (that is, +100%, -50%) or more on the estimate of average corrosion rates.

ACR and Localized Corrosion:

Measurement uncertainty. The values of ACR reported in Table 3-1 are affected by the errors indicated above and include the working assumption that corrosion is uniformly distributed over the entire surface of the structural element being tested. If corrosion is nearly uniformly distributed, then the ACR represents

an estimate of the average corrosion rate over the element surface. If the localization of corrosion is severe, the result deviates from the average to an extent that depends on the morphology of the corrosion distribution [8]. The additional uncertainty thus introduced in the estimation of the *average* corrosion rate is of a value comparable to that discussed in the previous paragraph. The value of the actual *local* corrosion rate at every point of the structural element surface cannot be assessed solely from the value of the average corrosion rate.

Magnitude and position of corrosion localization. Localized corrosion is more important if it causes loss of reinforcement cross-section at regions of high stress. These regions develop at some distance from the wall (typically 0.5 m). The field evidence from the Brickell Avenue test panels (soil without chloride contamination) shows some moderate macrocell current between the front and back galvanized elements; the current is on the order of the estimated corrosion current within either element. The point of separation between both elements is at about 3 m from the wall. The laboratory tests (Section 3) showed that under chloride contamination conditions macrocell currents could develop between steel in regions of different soil porosity. Because of the chloride contamination, the corrosion rates were much greater than those in the Brickell Avenue structures, but the observed macrocell currents were also on the order of the individual corrosion currents of each element. The laboratory macrocells developed over a characteristic distance on the order of 0.3 m.

The results suggest that macrocell current densities comparable to the average corrosion densities can develop over a spacial range consistent with the

development of the highest stresses in the reinforcement.

Temporal Variations. In light of the previous discussion, the ACR values listed in Table 3-1 may be considered as indicators of the instantaneous spatially averaged corrosion rate of the element tested. In the absence of soil contamination episodes, this corrosion rate can be expected to vary with seasonal changes in temperature and soil humidity. The long-term time averaged corrosion rate determines metal loss over the service life of the structure.

4.3 Working Estimate of Service Life

The approach described in the following is an attempt at forecasting the length of the service life of reinforcement or existing structures in Florida. Two cases will be considered, corresponding to structures without and with episodic chloride contamination.

4.3.1 Structures Not Subject to Episodic Chloride Contamination

A generic structure will be assumed to consist of reinforcing elements of dimensions and corrosion histories representative of those examined in the field investigation. The distribution of corrosion loss over all elements in the structure will be assumed to mirror the overall distribution of corrosion measured in the field, as in Figure 3-2. It should be noted that the data distribution in that figure represents not only spatial distribution, but also distribution over the different times the measurements were made. However, the distribution was nearly the same when

time-averaged ACR values were used instead. It will also be assumed that during the early life of the structure the corrosion rate distribution reflects that of the galvanized elements. After corrosion has consumed the galvanized layer the corrosion distribution will be assumed to switch to that of the plain steel elements.

The corrosion rates assumed for durability estimation will consist of the ACR values in Figure 3-2, but multiplied by a factor of two to reflect the discussion in Section 4.2.2 and excluding data from possibly contaminated sites. The discussion indicated that corrosion macrocell action was on the order of the average rate of corrosion (thus approximately doubling the local rate), and that the highest rate of metal loss would be expected to take place in the region of maximum reinforcement stress. It will also be assumed that the service life of a given element reaches its end when the reinforcement cross section in the highest stress region is half-consumed.

Corrosion of the underlying steel will be also conservatively assumed to proceed after the galvanized layer is first breached, at a rate equal to that of the all-plain steel elements tested in the field investigation. The rate will be assumed to be equal to the plain steel ACR rate multiplied by a factor of two to account for macrocell corrosion. The estimate will be made further conservative by not taking credit for galvanic protection from the residual galvanization in the reinforcing element. The corrosion rate of the steel will be assumed to be uncorrelated with the corrosion rate that the galvanized layer experienced before the base steel was exposed. This assumption reflects the apparent lack of correlation between plain steel and galvanized ACR values in Table 3-1.

Corrosion rates will be assumed to be constant with time (per Section 4.2). The ACR values for galvanized and plain steel will be designated by ACR_g and ACR_s respectively. For durability estimation purposes, the corrosion rates assumed to incorporate the macrocell multiplier will be designated by $v_g = 2 ACR_g$ and $v_s = 2 ACR_s$. The generic structure will be considered to contain reinforcing strips of base steel thickness, $s = 4 \text{ mm}$ (.16 inch) and galvanized layer thickness, $g = 150 \text{ } \mu\text{m}$ (0.006 inch). Therefore, a given reinforcing element reaches the end of its service life (loses half of the steel strip thickness) at a time t_f such that:

$$t_f = g / v_g + (s/4) / v_s \quad (1)$$

Eq.(1) reflects the assumptions indicated earlier and neglects corrosion from the strip edges.

The distributions of ACR_g and ACR_s values in Figure 3-2 (as well as those of v_g and v_s) can be closely approximated by cumulative lognormal distributions $C_g(x)$ and $C_s(x)$ such that

$$\%R_g = 100 C_g(x) \quad (2)$$

$$\%R_s = 100 C_s(x) \quad (3)$$

where $\%R_g$ and $\%R_s$ represents the percentage of elements having $v_g < x$ or $v_s < x$ respectively. The cumulative lognormal distribution $C(x)$ (subscripted g or s)

is by definition:

$$C(x) = [(2\pi)^{1/2}\sigma x]^{-1} \exp[-(\ln x - \mu)^2 / 2 \sigma^2] dx \quad (4)$$

where σ is the standard deviation of $\ln(x)$ and μ is the average of $\ln(x)$. The corresponding probability function is given by $P(x) = d C(x) / dx$ (subscripted g or v).

At a time t , the fraction of reinforcing elements that has lost the galvanized layer is given by:

$$F_{lg} = 1 - C_g (g/t) \quad (5)$$

The fraction of elements with galvanized-layer corrosion rates between v_g and $v_g + dv_g$ is given by:

$$d F_{lg} = P_g (v_g) dv_g \quad (6)$$

Of that fraction, a subfraction with $v_s > s / 4 (t-g/v_g)$ has already lost half of the steel thickness (end of service life). That subfraction is given by $1 - C_s[s / 4 (t- g/v_g)]$, so that the fraction $dF_f(t)$ of elements with galvanized layer corrosion rates between v_g and $v_g + dv_g$ and loss of half of the steel cross section by time t is given by

$$dFf(t) = P_g (v_g) (1 - C_s [s / 4 (t - g/v_g)]) dv_g \quad (7)$$

Integrating over all v_g values greater than g/t gives the total fraction of elements failed, F_f by time, t :

$$F_f(t) = \int_{g/t}^{\infty} P_g (v_g) (1 - C_s [s / 4 (t - g/v_g)]) dv_g \quad (8)$$

Eq.(8) was used to calculate the percentage of elements $\%R_f(t) = 100 F_f(t)$ that have ended their service life by time t in a generic MSE wall not subject to episodic contamination. The values of μ and σ used for the calculation were obtained by analysis of the distribution of ARC values over all structures except for 4B and 5 (which are subject to or may have in the past experienced corrosive inundation). The result of the analysis yielded the results listed in Table 4-2.

Table 4-2. Corrosion rate distribution parameters; all structures except 4B and 5.

Distribution Parameters	Galvanized	Plain Steel
μ (v_g , vs expressed in mpy)	-2.95109	-0.90934
σ	0.61113	1.01815

The results of the model calculations are shown in Figure 4-1 . The calculations project that virtually no elements in the generic MSE wall reach the end of the service life after 50 years, but that $\approx 5\%$ of the reinforcing elements fail after 100 years with the trend afterwards as shown.

4.3.2 Structures Subject to Episodic Chloride Contamination

In the field, only Structure 4B has showed indications of episodic contamination but the level of soil contamination appears to follow seasonal variations so that the chloride content may not stay at a high level permanently. This interpretation appears to be supported by the good appearance (although with some dark discoloration) of the exposed reinforcement in that wall (Table 3-2). Therefore, performance projections for a structure inundated with salt water will rely on the laboratory evidence from Series 1 and 2, which shows a dramatic increase in apparent corrosion rate (Table 4.1) and macrocell currents upon simulated inundation. For the purposes of this analysis, it will be assumed that inundation results in a ten-fold increase in the long term rate of corrosion of both the galvanized layer or the bare steel. To make the projection more conservative, it will be furthermore assumed that the soil retains the salt after contamination, taking no credit for possible rainwater washout (which may be further facilitated by the use of a coarse fill as indicated in Section 4.1.1) The remaining assumptions stated in Section 4.1 for non-contaminated structures will be used here as well.

The effect of a ten-fold increase in v_g and v_s as a result of corrosive inundation at year zero (Figure 4-2) is to accelerate the time scale in Figure 4-1 by a factor of 10. Thus, the projected percentage of failed elements is negligible only during the 5 years following the inundation, but reaches $\approx 5\%$ after 10 years and continues to grow fast in subsequent years. If the inundation were to affect only the lower portions of the wall, the projection in Figure 4-2 could still be used, but interpreting it as the percentage of failing elements at elevations below the flood line.

4.3.3 Applicability of Projections

The validity of the projections made in Sections 4.3.1 and 4.3.2 is contingent upon the qualifications of uncertainty and variability discussed in Section 4.2.2 and should always be contrasted with available evidence of the actual behavior of structures. The present condition of the reinforcement in the structures examined has been generally good. The oldest wall examined (Structure 2, Pensacola Street, 17 years at time of testing) showed some localized reinforcement deterioration with partial penetration of the galvanized layer. The overall reinforcement appearance was nevertheless still good (except for mechanical damage not related to corrosion) and the ACR values were on average quite low, similar to those of the newer structures. Thus, the present day field observations fit well with the projections for structures not subject to episodic corrosive floods during the first 50 years of service life. The field evidence and the projections made with the available data support also the soil chemistry and size specifications used in the present FDOT guidelines for service not subject to contamination.

The projection made for the case of an MSE wall subject to a corrosive flooding event cannot be contrasted with any of the structures examined, but is in keeping with the observed behavior in the laboratory. The trend of increasing resistivity with time after contamination of the coarse fill, ascribed to fresh water washout, was not modeled in the conservative projection used. The use of coarse fill may provide a potential resistance to the effects of salt water inundation, but the information available to date is not enough to quantitatively assess the possible extent of washout and its effect on long term corrosion rate.

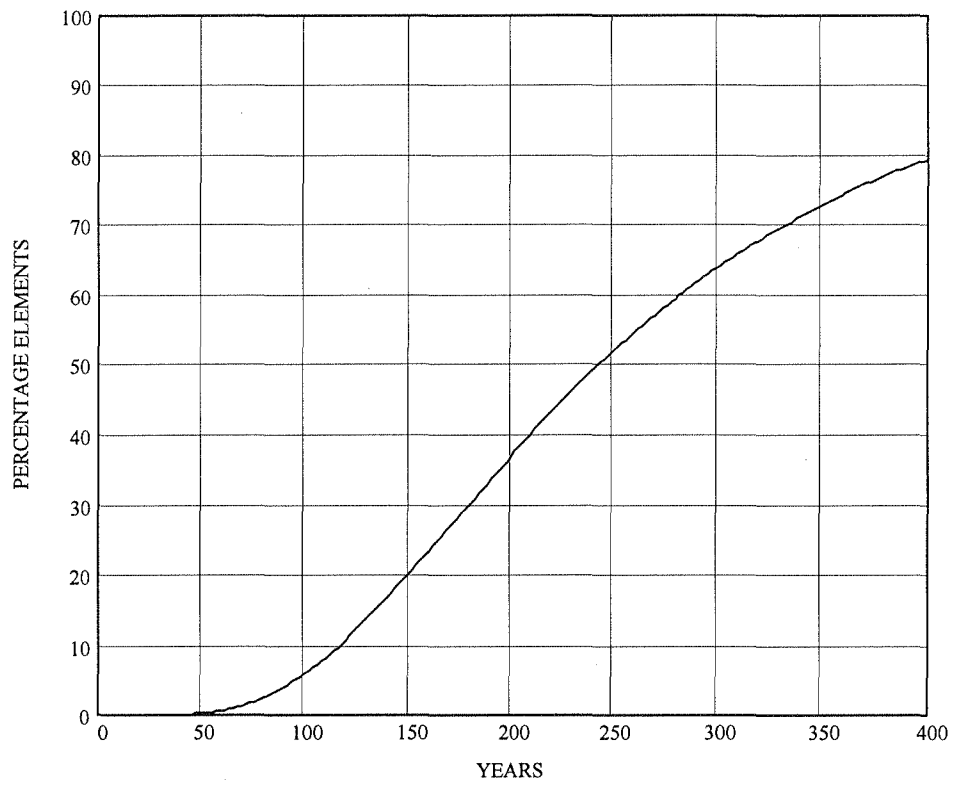


Figure 4-1. Projection of the percentage of elements that reached the end of service life as a function of time of service for the generic MSE wall not subject to episodic chloride contamination.

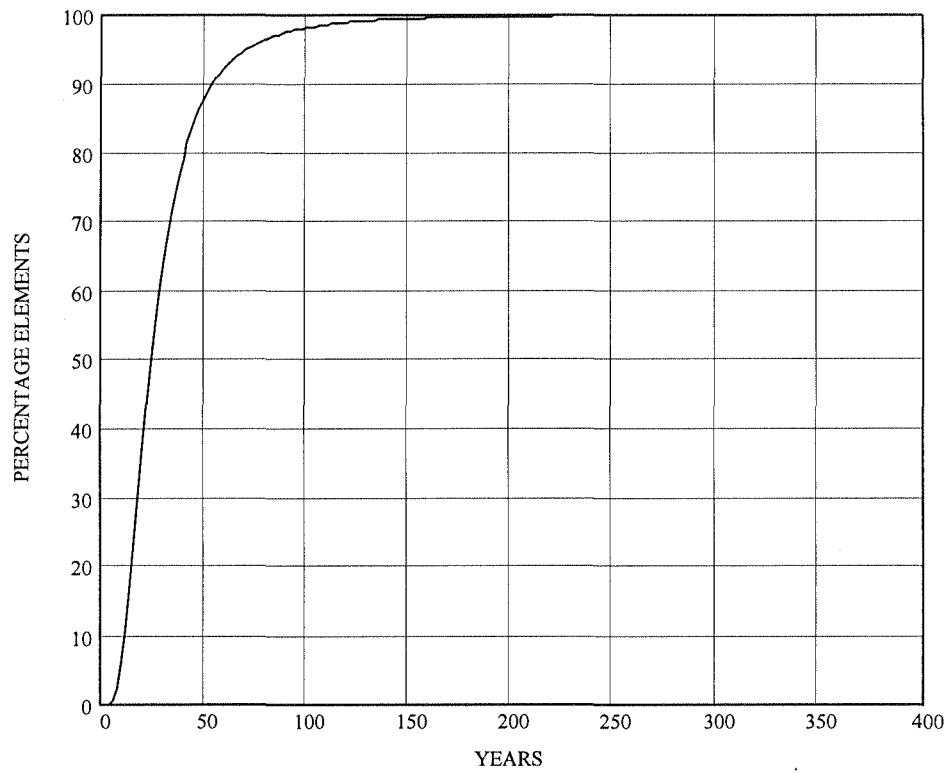


Figure 4-2. Projection of the percentage of elements that reached the end of service life as a function of time of service for the generic MSE wall subject to corrosive inundation at year zero.

5. CONCLUSIONS

1. The FDOT design limits for soil pH, resistivity, chloride content, sulfate content and size distribution were met in virtually all the test locations of the structures tested. Chloride and resistivity limits were not met at only one instance in one test point (in the Palm City North West Wall) during episodic direct contact of the wall with brackish water.

2. Direct visual examination of the reinforcement exposed at all the structures investigated revealed generally good to very good appearance of the galvanized surfaces. Microscopic examination of galvanized hardware extracted from the oldest wall in the State (Pensacola St.) showed only localized or partial loss of the galvanized layer and negligible corrosion of the plain steel substrate. Detailed examination of a newer wall showed negligible damage of the galvanized layer.

3. Field measurements of apparent corrosion rates (ACR) of galvanized reinforcement showed typically very low values, with an average of $\approx 1 \mu\text{m/y}$ (≈ 0.04 mpy). The ACR of galvanized reinforcement did not vary significantly with age of the structure tested. The ACR of recently introduced plain steel rods had an average of $\approx 12 \mu\text{m/y}$ (≈ 0.5 mpy). There was little correlation observed between the ACR of either material and the electrochemical properties of the soil in the low aggressivity range explored.

4. The corrosion potential of galvanized reinforcement in all structures tested ranged between ≈ -1000 mV and -100 mV CSE. The corrosion potential of plain steel ranged from ≈ -750 mV to -200 mV CSE. There was little correlation between the corrosion potential and the ACR for either galvanized reinforcement or plain steel.

5. Laboratory experiments indicated that saltwater contamination of the backfill increased the ACR of galvanized specimens and plain steel by about one order of magnitude. The contamination also resulted in the formation of a strong corrosion macrocell between galvanized reinforcement or plain steel joining regions of coarse and fine fill, as it may exist near the concrete panels. The intensity of the macrocell action was on the order of the average corrosion rate of the reinforcement. The polarity of the macrocell aggravated the corrosion of the metal in the denser soil side of the macrocell.

6. Resistivity measurements in the laboratory suggest that the aggressiveness of contaminated coarse backfills can decrease with time due to their drainage capacity, if fresh water is periodically added. Therefore, coarse soils may be beneficial in mitigating reinforcement corrosion after corrosion occurs if fresh water flushing (as due to rainfall) takes place.

7. A conservative durability model was formulated to project the percentage of elements that reach the end of their service life after a given service time of a generic MSE wall. The model input incorporated conservatively all the field evidence representative of Florida conditions obtained in this investigation. For walls not subject to episodic saltwater flooding and typical of those examined in the field the model projects a period of ≈ 50 years with negligible reinforcement failure, and $\approx 5\%$ failure after 100 years. For a wall with a saltwater flood at year zero the model projects failure development 10 times earlier.

REFERENCES

- [1] FDOT Structures Design Manual, Section 528, Reinforced Earth Walls, Revised 4-29-92, FDOT, 1992.
- [2] Elias, V., "Durability/Corrosion of Soil Reinforced Structures," Report No. FHWA-RD-89-186, NTIS, Springfield, VA, December, 1990.
- [3] Kessler, R. to Keenan, D., FDOT Memorandum, August 7, 1992 "Tie and reinforcing strips for reinforced earth walls."
- [4] Herman, S., Editor, Transportation Research Record 1001 "Symposium on Durability of Culverts and Storm Drains," National Research Council, Washington, 1984.
- [5] Chaker, V., and Palmer, J., Eds., "Effect of Soil Characteristics on Corrosion," ASTM STP 1013, American Society of Testing and Materials, Philadelphia, 1989.
- [6] Romanoff, M., "Underground Corrosion," NBS Circular 579, U.S. Dept. of Commerce, Washington, 1957.
- [7] Potter, J. to District Secretaries, FDOT Memorandum, August 25, 1992 "Mechanically stabilized earth (MSE) retaining walls."
- [8] Castro, P., Sagüés, A., Moreno, E., Maldonado, L., and Genesca, J., "Characterization of Activated Titanium Solid Reference Electrodes for Corrosion Testing of Steel in Concrete," Corrosion, Vol. 52, P. 609, 1996.
- [9] Rossi, J., "The Corrosion Behavior of Galvanized Steel in Mechanical Stabilized Earth Wall Structures," M.S. Thesis, University of South Florida, August 1996.
- [10] Shreir, L. L., Corrosion, Vol. 1, Newnes-Butterworths, London, (1994).
- [11] Engell, H. J., "Stability and Breakdown Phenomena of Passivating Films," Electrochimica Acta, Vol. 22, (1977), p. 987.
- [12] Pourbaix, M., "Atlas of Electrochemical Equilibria in Aqueous Solutions," Pergamon Press, Oxford, (1965).
- [13] Feitknecht, W., "Influence of Adherent Corrosion Products on Corrosion Behavior," Werkst. Korrosion, Vol. 6, (1955), p. 15.

- [14] Craig, B. D., "Fundamental Aspects of Corrosion Films in Corrosion Science," Plenum Press, New York, (1991).
- [15] Alvarez, M. G. and Galvele, J. R., "Pitting of High Purity Zinc and Pitting Potential Significance," Corrosion, Vol. 32, No. 7, (1976), p. 285.
- [16] Galvele, J. R. and Alvarez, M. G., "The Mechanism of Pitting of High Purity Iron in NaCl Solutions," Corrosion Science, Vol. 24, No. 1, (1984), p. 27.
- [17] Sagüés, A., Kranc, S., p. 58 in "Techniques to Assess the Corrosion Activity of Steel Reinforced Structures," ASTM STP 1276, N. Berke, E. Escalante, C. Nmai and D. Whiting, Eds., American Society for Testing and Materials, West Conshohoken, PA, 1996.
- [18] Peña, J. A., " Seawater contamination and soil gradation affect on corrosion of galvanized steel strips in reinforced earth walls", M.S. Thesis, University of South Florida, 1998.
- [19] Scott, R. J. "Corrosion Rate of Reinforcing Strips in Mechanically Stabilized Earth Wall", M.S. Thesis, University of South Florida, 1998.

APPENDIX

A.1. Estimated In-Situ Soil Resistivity

In-situ soil resistivities were estimated using the mutual resistances between top and bottom (or side to side) of galvanized members, measured during field visits. To estimate the soil resistivities the following calculations were made:

1) Mutual resistances (field measurements) were converted to estimated resistivities using a given cell constant [9].

2) The resistivities were converted to conductivities by taking the inverse of the values.

3) The conductivities were grouped by site visit (ie. each site location and date of field visit). All the element combinations (ie. top and bottom galvanized member), were averaged for each site visit.

4) The conductivity averages of each site visit were then averaged for all visit dates at each location.

5) The average conductivities for each location were then inverted to achieve the “estimated in-situ resistivities” for each MSEW.

Estimated resistivities for each site from mutual resistance measurements are listed in Table A-1 which also includes the averages of soil box test field results (using the California method) listed in Table 3.1. The percent difference between both results was defined as:

$$((R1 - R2) / R1) \times 100$$

where:

R1 = In-situ resistivity (from mutual resistance field measurement) [$k\Omega$ -cm]

R2 = In-situ resistivity (California soil box) [$k\Omega$ -cm]

Table A-1. Estimated in-situ resistivities for soil backfill at MSEW.

Structure Name / #	Panel Set #	Mutual Resistance (Ω)				Assumed Cell Constant (10^{-3} cm^{-1})	Average Resistivity (mutual resistance) ($\text{k}\Omega\text{-cm}$)*	Average Resistivity (California Soil Box) ($\text{k}\Omega\text{-cm}$)**	Percent Difference (%)
		2/9/95	1/31/96	8/7/96	11/26/97				
Brickell Ave. / #1a & b	NW top					1.94	20.4	36.3	-78
	NW bot.		47	47	51				
	SE top								
	SE bot.	47	31	29	33				
Howard Frankland / #2		12/15/95	2/10/96	4/22/96	7/2/96	1.65	19.6	16.1	18
	7	31	37	31	28				
	11	27	34	29	27				
	15	30	37	32					
	17	36	49	39	33				
Pensacola St. / #3		1/12/96	1/19/96	9/25/97		1.91	37.6	20.8	45
	17	73	68	50					
	23		72	54					
	44		240						
Palm City East / #4A		5/3/96	7/30/96	9/25/96	11/14/97	1.88	38.6	39.6	-3
	1	65	64	72	92				
	5	61	54		61				
	14	102	87						
	28		110						
Palm City West / 4B		7/31/96	9/26/96	11/20/96	11/14/97	1.9	14.3	12.3	14
	3		25	23	28				
	5		29	27	33				
Port St. Lucie Blvd. / #5		11/19/96	11/14/97			1.9	8.4	7.5	11
	3	19	20						
	7	13	14						
Ocala, SR. 200 / #6		1/15/97	4/9/97	9/26/97		1.9	77.9	36.7	53
	6	125	140	130					
Acosta Bridge / #7	25	200	200			1.9	42.1	28.8	32
		4/8/97	9/25/97						
	9	98	80						
Veteran's Expressway / #8	21	77	70			1.9	37.7	21.1	44
		6/10/97	1/16/98						
	16	69	69						
	23	75	74						

* The soil resistivities were calculated using the mutual resistances measured in-situ.

** The soil resistivities were measured in the laboratory using the California Soil Box method.

A.2. Hardware Inventory

Table A-2 Inventory of hardware extracted from MSE structures in service.

Structure Name / #	Panel Set / Location	Hardware Extracted
Pensacola St. / #3	23	Bolt
		Nut
		Washer
Palm City East / #4A	1	Nut
	28 / top	Washer
		Nut
		Washer
Palm City West / 4B	W3 / hole C	Stirrup*
	W3 / hole H	Bolt
		Nut
		Washer
	W5 / hole D	Bolt
	Nut	
Ocala, SR. 200 / #6	6 / hole C	Nut
	6 / hole A	Bolt
		Nut
		Washer
	25 / hole F	Stirrup*
		Bolt
Nut		
Acosta Bridge / #7	9 / hole A	Nut
	9 / hole B	Bolt
		Nut
	21 / hole E	Nut
	21 / hole F	Bolt
		Nut
Washer		

* A portion of the stirrup used to fasten a galvanized strip to the concrete panel.